ABSTRACT

YONEMOTO, DANIEL THOMAS. Modulating Excited State Dynamics with Quantum-Dot/Molecule Composite Materials. (Under the direction of Prof. Felix N. Castellano).

The following is a compilation of research efforts focused in merging quantum confined materials and surface bound molecular acceptors. The first two chapters discuss broadly the necessary background information to understand the research works in the following chapters. The third chapter and the subsequent chapters that follow discuss the findings of this work starting with understanding the effects of chromophore surface number on the observed photophysics of a series of thermally activated delayed photoluminescent cadmium(II) selenide (CdSe) quantum dots with varied surface concentrations of 1-pyrenecarboxylic acid in Chapter 3. Chapter 4 specifically discusses preliminary attempts to extend the principles found in Chapter 3 to different morphologies of CdSe and the initial findings therein. Lastly, Chapter 5 attempts to discuss the potential of these materials in a more informal manner and details some initial findings and potential avenues of new research efforts.

Modulating Excited State Dynamics with Quantum-Dot/Molecule Composite Materials

by
Daniel Thomas Yonemoto

A dissertation submitted to the Graduate Faculty of
North Carolina State University
in partial fulfillment of the
requirements for the degree of
Doctor of Philosophy

Chemistry

Raleigh, North Carolina
2021

APPROVED BY:

_____	_____
Felix N. Castellano Committee Chair	Christopher B. Gorman
_____	_____
Thomas Theis	David A. Shultz

DEDICATION

To you the reader, without you this is meaningless.

BIOGRAPHY

Daniel T. Yonemoto is the son of John Yonemoto and Peggy Thomas. He is privileged to have two brothers, one older (Bryan) and one younger (Sean) and a tremendous network of extended family and good friends. Born and raised in Albuquerque, New Mexico, Daniel spent most of his time outside soaking up shortwave photons while he partook in various sports, time with friends and thinking about the universe. During his junior year of high school, Daniel began to work at Sandia National Laboratories (SNL) under the direction of Timothy J. Boyle. There he studied novel metal alkoxides and their utility as nanomaterial precursors. In the Boyle lab, he quickly became fascinated unveiling nature's mysteries through science and decided to make a career out of it. In 2016, he graduated from the University of New Mexico (UNM) and bid farewell to the state that raised him to join the Department of Chemistry at North Carolina State University (NCSU). Under the direction of Felix N. Castellano, Daniel has grown accustomed to viewing the world with a photophysical lens while studying interfacial light matter interactions in quantum-dot composite materials. After obtaining his Doctor of Philosophy in 2021, he will be joining the scientific industrial complex where he hopes to apply his photophysical knowledge to solve the problems of tomorrow.

ACKNOWLEDGMENTS

There are so many people that really need to be mentioned here to fully convey the amount of help and support that I have received during my Ph.D. program. Realistically, there is no possible way to do that without missing someone so instead I will simply say thank you to all who have helped along the way and highlight the most entertaining acknowledgements instead. First and foremost, I need to acknowledge Bose, they make the absolute best in noise cancelling/sound generating equipment bar none. Many of the deep focus sessions that I needed to go through to get this work done wouldn't have happened without Bose equipment and I hope that someone who works there reads this and decides to give me some free stuff. Next, I want to thank the admissions committee at the University of Santa Barbara for denying me admission to their program. With the wonderful beaches and sunshine there, I indubitably wouldn't have been productive enough to complete my degree. That said, Raleigh is an excellent place to live, and I couldn't trade my time here for anything, unless of course that anything is including a high paying position in industry somewhere else, in which case I'll be seeing you Raleigh. Of course, I would be completely remiss if I didn't thank the Williams group (and a significant portion of Dabney) for partaking in the first ever occasional soccer match between the Castellano Group and the Williams group (AKA second place). It is tough to lose gracefully, and I think they do it better than anyone I've met in grad school… the losing part that is… the grace bit is still up for discussion. Truly though, jokes aside, the team of people that Felix N. Castellano (Phil) has assembled have really made this an effortless research environment and I can't thank him, my committee, and the team of researchers I have had the distinct pleasure of working with enough. You all have truly been tremendous. *Cue the Music*

TABLE OF CONTENTS

LIST OF TABLES

LIST OF FIGURES

Chapter 1: The Sun is Gone, But I Have a Light.

1.1: Relevant Background and Historical Anecdotes

1.1.1 Introduction to Photochemistry and Photophysics

Light and the subsequent reactions that occur through interaction with light have long been a subject of wonder and amazement. Ancient civilizations often would generate lore centered around their major source of light, the sun. These civilizations would regularly assign deities of enormous power to the association of the sun. In modern times, society has largely left behind belief of some mythical omniscient being controlling the power of the sun. Modern society instead focuses on bettering their understanding of the true fundamentals of light and its interactions. This is done via rigorous scientific efforts in physics, chemistry, and numerable other fields. These studies have provided a plethora of information that are now at the disposal of photochemists. This information includes the duality of light, the characteristic of light to act both as a wave and a particle, the speed of light, 3×10^8 m/s, and the phenomena of characteristic light absorption/emission. Using this information, researchers have made numerous advances in spectroscopic characterization and furthered the understanding of how our world operates at a fundamental level. A brief explanation of several of these characterization methods and applications of photophysical processes follows.

1.1.2 Ultraviolet-visible absorbance spectroscopy

Ultraviolet-visible absorbance spectroscopy or UV-vis absorption measurements are one of the most basic techniques available to a photochemist. Light, upon interaction with matter, will be absorbed at select wavelengths following the Bohr equation, Eq. 1.1, where $h\nu$ is the photon energy and E_f and E_i are the energies of the excited (Ψ_f) and ground (Ψ_i) state wavefunction respectively, and the rest of the light will scatter.

$$h\nu = E_f - E_i \qquad \text{Eq. 1.1}$$

This process of light absorption gives rise to the wonderous colors that make up our reality. The principles of absorption play an important role in several applications in the fields of renewable energy, remote detection, sensor technology, biological imaging, photocatalysis, energy scavenging, and aerospace technology. Scientists utilize the principles of absorbance spectroscopy to experimentally determine what wavelengths of light a compound absorbs. These experiments take a compound, illuminate it with light and then measure the light that is transmitted via a detector. By using Eq. 1.2 (Beer-Lambert law), the absorbance may be calculated.[1, 2]

$$A = log\left(\frac{I_0}{I}\right) \qquad \text{Eq. 1.2}$$

Here A is absorbance, I_0 is the initial intensity of light at the detector (reference light intensity), and I is the intensity of light after a sample is measured (sample light intensity). Absorbance is also known to be directly proportional to the concentration and the path length, as such, Beer-Lambert law may be rewritten as Eq. 1.3:

$$A = \varepsilon lc \qquad \text{Eq. 1.3}$$

Here, A is represented by ε, the extinction coefficient, l, the path length, and c, the concentration of the sample. For known substances, this is a particularly useful tool to determine the concentration of an analyte in solution or the extinction coefficient of an analyte of known concentration. In Addition, UV-vis absorbance spectroscopy provides valuable information about the electronic transitions that occur in a molecule and is used to help resolve complex photophysical mechanisms. This is the fundamental principle underlying absorbance. As a photon of specific wavelength is absorbed, that energy is transferred to an electron that is promoted to an

excited state. **Figure 1.1** contains a Jablonski diagram demonstrating absorption and other relevant photophysical processes.[3] Once a photon is absorbed, an electron hole pair, or an exciton is generated. Once formed, the electron hole pair will recombine, this may include several mechanisms including radiative decay processes, or the pair will split often leading to what is known as photolysis, radical generation or redox chemistry, these processes are discussed further in section 1.2.1. This electron hole recombination step is the corollary process to absorption.

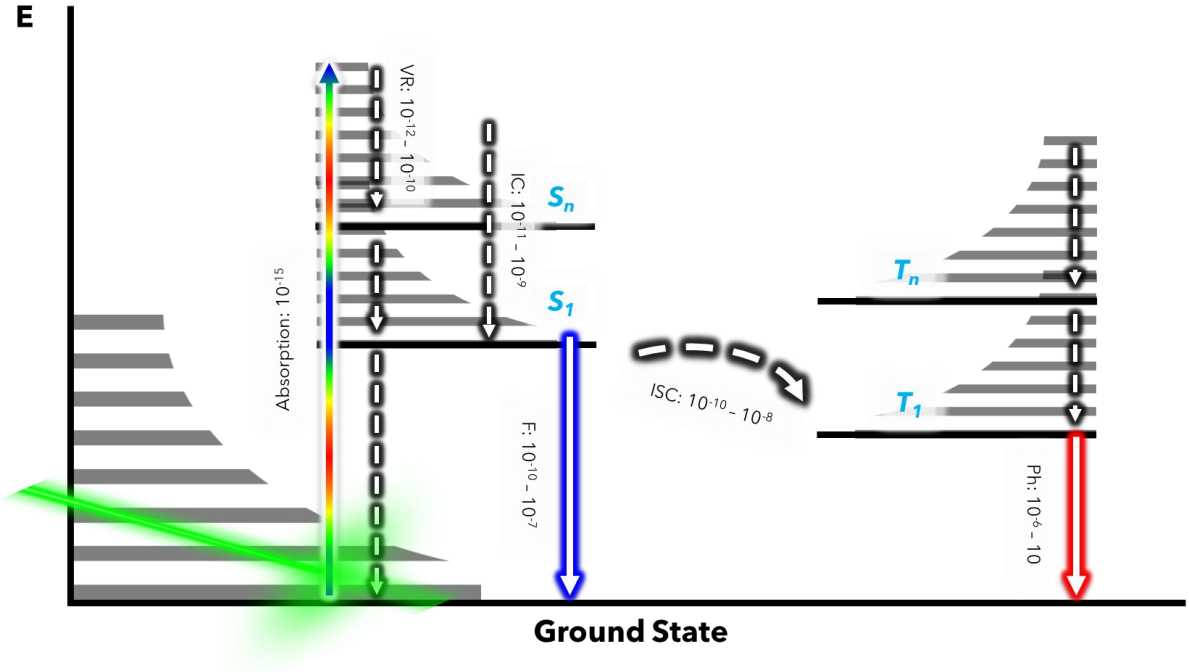

Figure 1.1. Jablonski diagram depicting available photophysical processes upon absorption.

1.1.3 Steady-state Photoluminescence Spectroscopy

Photoluminescence processes are the radiative processes that occur upon the recombination of an electron-hole pair. These processes are used in a variety of applications including display technology, lighting applications, bioimaging, sensor technology, photocatalysis and energy scavenging. The energy of the emitted photon will correspond to the energy gap between the electron and hole, **Figure 1.1**. Typical emission decay pathways include fluorescence and phosphorescence.

Fluorescence is the emission of a photon due to a spin allowed recombination of an exciton. As this process is allowed, fluorescent lifetimes are usually on the order of nanoseconds or less and usually have higher quantum yields than phosphorescent processes. Phosphorescent decays take place from a spin forbidden electron-hole recombination to the ground state. This decay, being spin forbidden, usually takes place over time periods on the order of μs – ms and typically result in lower PLQYs when compared to a fluorescent process. For both fluorescence and phosphorescence, the emission of photons may be monitored experimentally via a fluorimeter. The intensity, I_{PL}, of these processes follow Eq. 1.4.

$$I_{PL} = kI_0\Phi[1 - (10^{-\varepsilon lc})] \qquad \text{Eq. 1.4}$$

Here, k is a proportionality constant dependent on the instrument, Φ is the photoluminescence quantum yield, I_0 is the excitation intensity, ε is the extinction coefficient, l is the path length and c is the concentration of the sample. By using dilute samples to measure the PL (optical density (OD) < 0.1) Eq. 1.4 is simplified to Eq. 1.5 via a Taylor expansion approximation.

$$I_{PL} = kI_0\Phi\varepsilon lc \qquad \text{Eq. 1.5}$$

From these experiments, the photoluminescence quantum yield (PLQY), the full − width at half maximum (FWHM) and other important characteristics about the emitted photons may be extracted. When this technique is coupled with UV-vis absorbance spectroscopy, the energy gap between the ground state and the emitting state is capable of being teased out. In both absorption and photoluminescence under steady state conditions, the average processes that occur over time are being monitored. To gain a more complete understanding of the processes occurring in the excited state, time resolved experiments are necessary.

1.1.4 Transient Absorption Spectroscopy

Excited state dynamics often involve multiple steps that may be lost when monitoring steady state processes. El Sayed's rule, Energy Gap Law and Kasha's rule inherently express the complexities of the excited state dynamics that are difficult to identify from steady state measurements. Analysis with transient absorption spectroscopy provides a means to analyze the migration of excitons within the upper excited states by monitoring the change in absorbance as a function of time. To execute experiments of this type, pump-probe techniques become necessitated. Effectively, the initial spectrum is monitored following a pump beam pulse; then at a specified delay time, a probe beam monitors the change in the spectrum. These changes are tracked by changing the delay time between the pulses to give a difference spectrum following Eq. 1.6.

$$\Delta A = A_{ES} - A_{GS} \qquad \text{Eq. 1.6}$$

Here ΔA is the output signal generated in the TA spectrum, A_{ES} is the excited state absorbance and A_{GS} is the ground state absorbance. For suprananosecond time domains, time delays to monitor these processes are electronically controlled, for femtosecond time domains, it becomes necessary to use mechanical delays to control the output time delays. nsTA and fsTA methods are powerful tools to corroborate other analysis techniques and to distinguish excited state dynamics beyond the typical steady state techniques.

1.1.5 Time-Resolved Photoluminescence Spectroscopy

Resembling steady state methods, transient experiments monitoring absorption may be coupled to time-resolved photoluminescence measurements. A typical methodology to monitor photoluminescence decay over time is time gated emission (TGE). These experiments abide by the same rules as steady state photoluminescence, however, instead of scanning the

photoluminescence across a wavelength range, typically a camera is used to monitor the entire wavelength range all at once to give a snapshot of the PL at specific time delays. This is accomplished using a shutter before the detector to optically gate the PL signal. Alternatively, single wavelength time-resolved emission may be monitored with a PMT monitoring the output signal as it decays over time. Time-correlated single photon couniting (TCSPC) is another technique that is available. TCSPC uses statistical binning across time to place photons into a histogram. The population in each bin is representative of the decay intensity at each time point. These techniques provide information regarding the emitting state and may be coupled to TA data to distinguish observed states.

1.2: Triplet Energy Transfer Reactions:

1.2.1 Photophysical Processes

In addition to absorption and photoluminescence processes, other excited state dynamics exist that determine exciton decay. These are what are commonly referred to as the non-radiative processes in excited state dynamics' studies. Intersystem crossing (the process by which singlet states are converted to triplet states), internal conversion (the decay from upper excited states to lower excited states with the same spin), and vibrational relaxation (the decay from upper vibrational levels to lower vibrational levels within a manifold) are all examples of these types of processes in a molecule and are depicted in **Figure 1.1**.[3] Using the aforementioned techniques, excited state dynamics may be unveiled, researched and ultimately understood. It is by this understanding that new technology is developed by photochemists and photophysicists. Furthering our understanding has led scientists to exploit excited state dynamics in donor acceptor systems using triplet energy transfer reactions.[4-14]

1.2.2 Evolution and Utility

Triplet energy transfer reactions are a means to alter excited state dynamics for applications in exciton scavenging, sensitization reactions, photocatalysis and other excited state processes. Work on triplet energy transfer reactions around the turn of the millennia distinguished several properties that may be manipulated to alter energy transfer reactions such as energy gaps between interacting states, number of acceptor molecules used in the energy transfer reactions, the effects of spin orbit coupling (SOC), and other important characteristics that are well documented in many works from the turn of the millennia.[4, 6, 7, 13, 15-20] More recent works further manipulate the excited state dynamics through complex pairing of donor acceptor systems to yield a variety of end photophysical properties. These properties range from triplet−triplet annihilation for photochemical upconverision,[9, 11, 21-26] singlet fission,[27, 28] and thermally induced excited state equilibriums.[10, 29-31] The origin of many of these complex excited state dynamics are built upon early work by Parker and Hatchard, their discoveries of p–type and e–type delayed fluorescence, **Figure 1.2** provides a cartoon depiction of their seminal research discoveries.[32-34]

a.

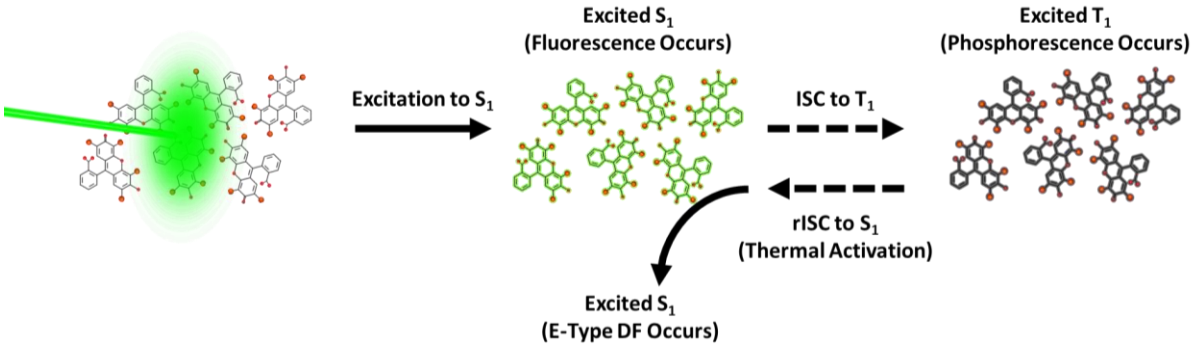

b.

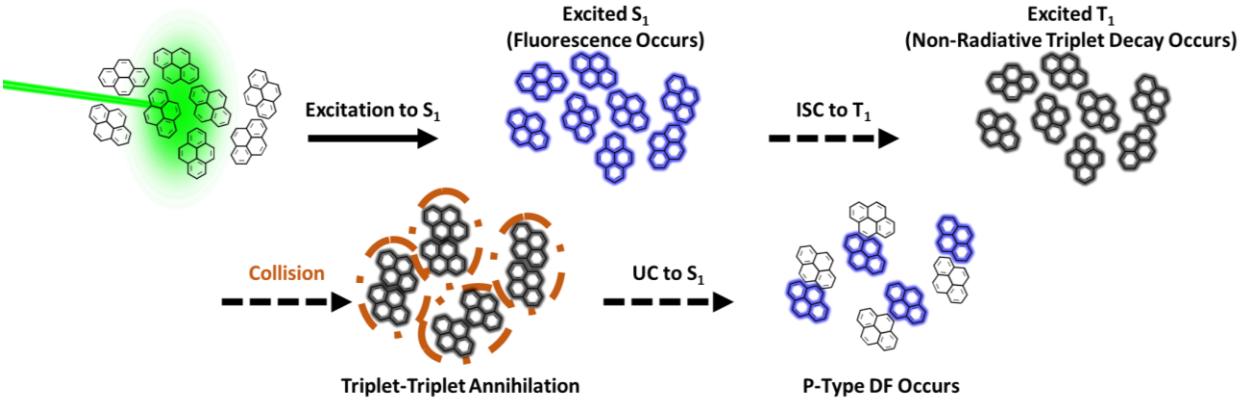

Figure 1.2. Cartoon depiction of available photophysical processes in a. eosin and b. pyrene, including complex processes such as TADF and P-Type DF, respectively.

1.2.3 Desired Characteristics for TADPL

Thermally activated delayed photoluminescence (TADPL) is a radiative energy transfer process that occurs from a thermally induced equilibrium. Typically speaking, the observed PL is generated from two interacting states, where the upper state acts as the radiative energy level that is thermally accessible and the lower state acts as an energy "reservoir."[10, 13, 31, 35-41] Often times this process is referred two as thermally activated delayed fluorescence (TADF) implying that the upper emitting state is singlet in character. This type of work has been popularized by the advent

of OLED technology and follows similar dynamics to the e-type process depicted in **Figure 1.2**.[30, 35, 39, 42-55] TADPL, however, allots for the inclusion of thermal equilibrium induced between two interacting triplet states. The underlying characteristics that control TADPL have undergone extensive study in attempts to identify the optimal TADPL complexes.[7, 8, 10, 12, 16, 18, 31, 41, 56-59] Work by Schmehl et. Al has identified a number of these processes and some of the information is pictorially encapsulated in **Figure 1.2**.[60] To summarize, the ideal case for TADPL systems is a highly tunable excited state design with a long lived lower lying triplet state. Systems with a strong equilibrium toward the low−lying triplet result in long lived TADPL character, and systems where the equilibrium is in favor of the nearly isoenergetic upper triplet result in rapid TADPL typically used in lighting applications. Chapter 2 provides a more in-depth review of TADPL and the components that dictate the end photophysical character.

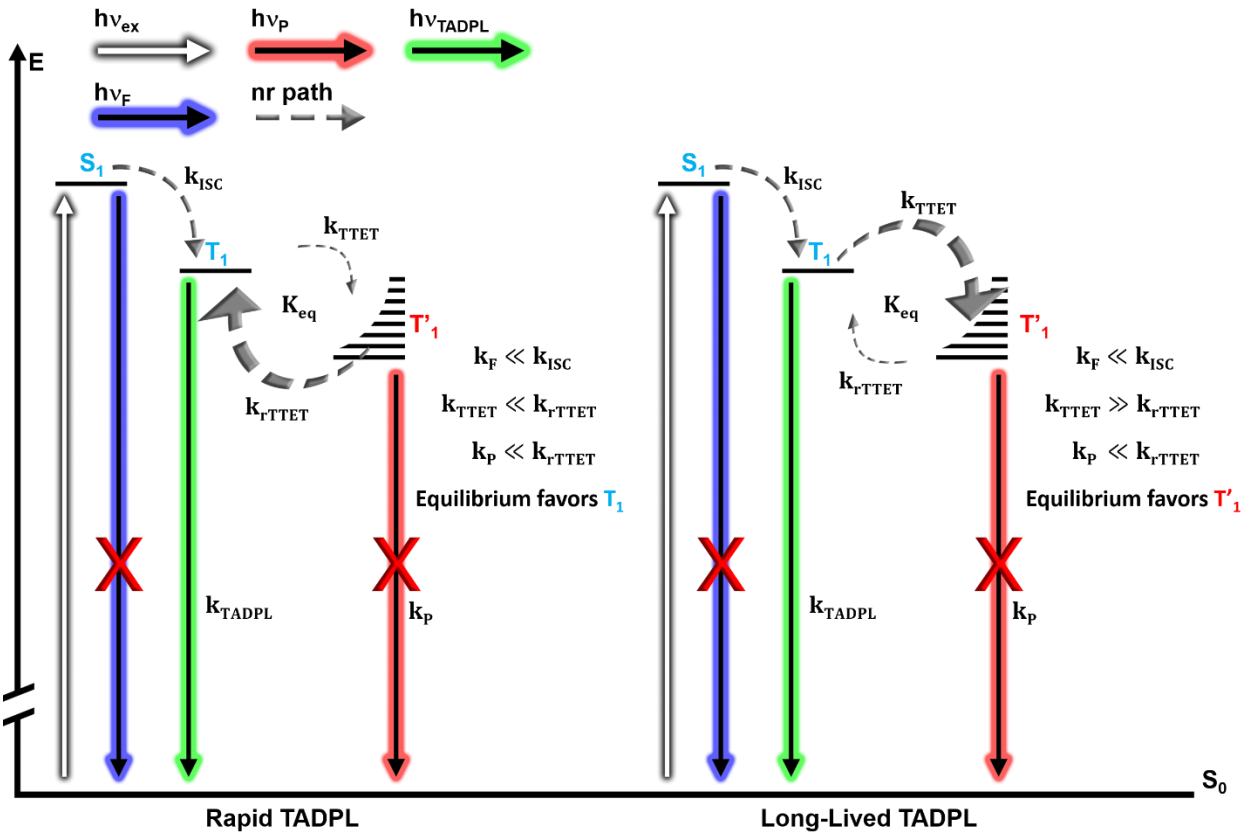

Figure 1.3. Depiction of rapid TADPL (left) and long-lived TADPL (right) between a donor (blue letters) and an appended acceptor triplet (red letters). Red Xs denote processes that are considered negligible relative to competing pathways.

1.3: Nanomaterials

1.3.1 Origin and Classes

Nanomaterial science has gained considerable interest in the last half century due interesting phenomena that occur at the nanoscale. However, the use of nanomaterials has been widespread for centuries. Early uses of nanomaterials admittedly were by accident in things such as stained-glass windows and as composites in Damascus steel.[61, 62] Modern uses are much more intentional and include several classes of nanomaterials. Small scale transistors have propelled the technology growth and have allotted for the continuation of Moore's law.[63] Many nanoscale

ceramics find use as filler materials to improve bulk material properties.[64, 65] Nanomaterials have also been implemented in responsive composites, conductive inks and other cutting-edge technology.[66, 67] Of particular interest to this research group and the photophysical research field are semiconductor nanocrystals or quantum dots (QDs). QDs enable the use of photophysical studies via quantum confinement, and are uniquely poised to enable a variety of next generation technologies.[52, 68-75]

1.3.2 Semiconductor Nanocrystals and Quantum Confinement

QDs are unique in that they exhibit size tunable photophysical properties coupled with large molar extinction coefficients and spin ambiguity. These properties coupled with their low cost and relative abundance position them as a potential photophysical holy grail.[76] These characteristics are driven by what is known as quantum confinement. Quantum confinement is the restriction of electron motion as a material's size approaches its Bohr exciton radius.[77-80] At this size regime, distinct energy transitions begin to appear in the QDs mimicking traditional molecular transitions. As a result, QDs have unique optical properties that separate them from bulk semiconductors and make them an interesting research topic.[76, 81-83]

1.3.3 Growing Pains of Nanomaterials

The past few decades have been marred by technological developments in nanomaterial technology, however the implementation has arguably outpaced its fundamental development.[84-86] This is a particularly important problem for mass production of nanotechnology. Several research thrusts focus on development of characterization tools, synthetic scale up and fundamental understanding of nanomaterials.[64, 87-89] As a result, nanomaterials are sometimes viewed as more art than science and understandably so. To remedy this designation, creative use of modern techniques needs to be coupled with advances in instrument technology to provide more

details about particle surface chemistries and generate consistent synthetic results. Many research labs have spent considerable effort in this area attempting to improve synthetic procedures in a variety of ways. Several rely on post processing of the materials to yield desired properties such as near unity photoluminescence quantum yields, minimal polydispersity, and other pertinent application-based characteristics. [87-96] Still, these procedures rely primarily on the use of tailored approaches and yield results that are often specific to the bespoke application space. Coupling these approaches with more systematic, scalable, and modular flow systems provide a means to yield procedures more cookbook in nature and standardize the synthetic pathways to obtain deterministic end materials that are both precise and accurate in their material properties. [97-105] A graphic representation of such a system is represented in **Figure 1.4**, demonstrating the potential of merging an in-house flow system with a commercial product to perform high throughput reaction condition screening which is easily modified to larger material production.

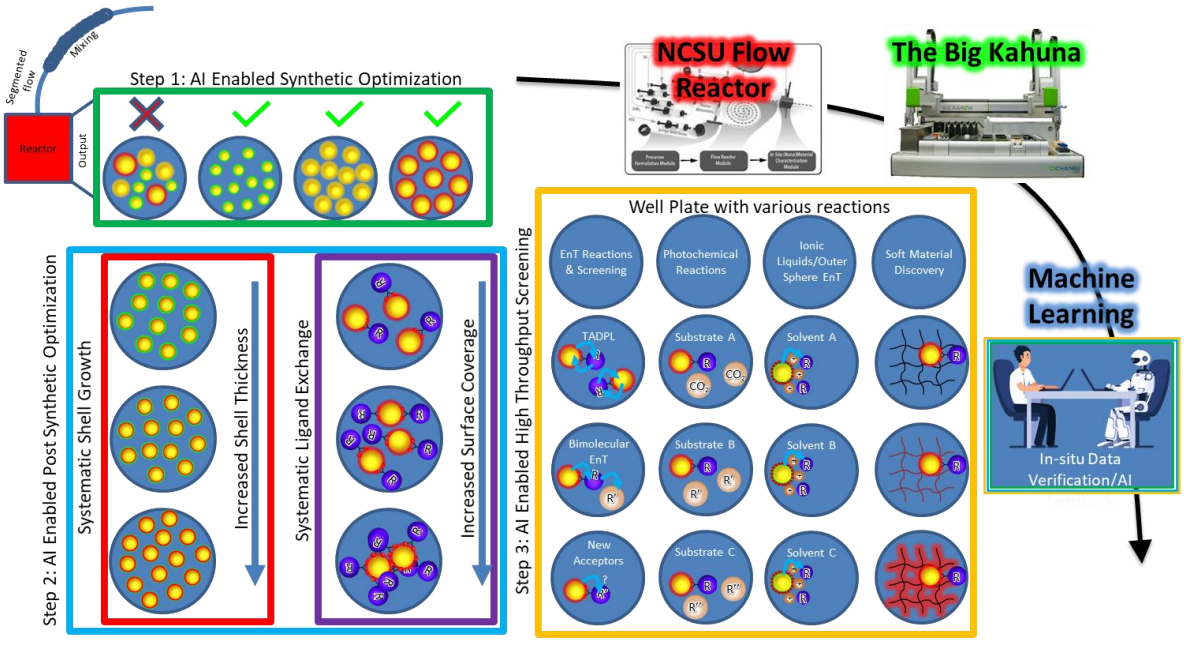

Figure 1.4. Graphical representation of a potential high throughput flow system enhanced with machine learning to develop reproducible and scalable reaction conditions.

Chapter 1 References:

1. Lakowicz, J. R., *Principles of Fluorescence Spectroscopy*. 3rd ed.; Springer, Boston, MA: 2006.

2. Balzani, V. C., Paola; Juris, Alberto, *Photochemistry and Photophysics Concepts, Research, Applications*. Wiley-VCH: Weinheim, Germany, 2014; p 472.

3. What is a Jablonski Diagram. https://www.edinst.com/blog/jablonski-diagram/.

4. Ford, W. E.; Rodgers, M. A. J., Reversible Triplet Triplet Energy-Transfer Within a Covalently Linked Bichromophoric Molecule. *J. Phys. Chem.* **1992,** *96*, 2917-2920.

5. Wilson, G. J.; Sasse, W. H. F.; Mau, A. W. H., Singlet and triplet energy transfer processes in ruthenium(II) bipyridine complexes containing covalently bound arenes. *Chem. Phys. Lett.* **1996,** *250*, 583-588.

6. Tyson, D. S.; Castellano, F. N., Intramolecular singlet and triplet energy transfer in a ruthenium(II) diimine complex containing multiple pyrenyl chromophores. *J. Phys. Chem. A* **1999,** *103*, 10955-10960.

7. Tyson, D. S.; Luman, C. R.; Zhou, X. L.; Castellano, F. N., New Ru(II) chromophores with extended excited-state lifetimes. *Inorg. Chem.* **2001,** *40*, 4063-4071.

8. McClenaghan, N. D.; Barigelletti, F.; Maubert, B.; Campagna, S., Towards ruthenium(II) polypyridine complexes with prolonged and predetermined excited state lifetimes. *Chem. Commun.* **2002**, 602-603.

9. Singh-Rachford, T. N.; Castellano, F. N., Photon upconversion based on sensitized triplet-triplet annihilation. *Coord. Chem. Rev.* **2010,** *254*, 2560-2573.

10. Yarnell, J. E.; Deaton, J. C.; McCusker, C. E.; Castellano, F. N., Bidirectional "Ping-Pong" Energy Transfer and 3000-Fold Lifetime Enhancement in a Re(I) Charge Transfer Complex. *Inorg. Chem.* **2011,** *50*, 7820-7830.

11. Zhao, J.; Wu, W.; Sun, J.; Guo, S., Triplet photosensitizers: from molecular design to applications. *Chem. Soc. Rev.* **2013,** *42*, 5323-5351.

12. Denisov, S. A.; Cudré, Y.; Verwilst, P.; Jonusauskas, G.; Marín-Suárez, M.; Fernández-Sánchez, J. F.; Baranoff, E.; McClenaghan, N. D., Direct Observation of Reversible Electronic Energy Transfer Involving an Iridium Center. *Inorg. Chem.* **2014,** *53*, 2677-2682.

13. Castellano, F. N., Altering Molecular Photophysics by Merging Organic and Inorganic Chromophores. *Acc. Chem. Res.* **2015,** *48*, 828-839.

14. Kholmicheva, N.; Moroz, P.; Eckard, H.; Jensen, G.; Zamkov, M., Energy Transfer in Quantum Dot Solids. *ACS Energy Lett.* **2017,** *2*, 154-160.

15. Tyson, D. S.; Bialecki, J.; Castellano, F. N., Ruthenium(II) complex with a notably long excited state lifetime. *Chem. Commun.* **2000**, 2355-2356.

16. Tyson, D. S.; Henbest, K. B.; Bialecki, J.; Castellano, F. N., Excited state processes in ruthenium(II)/pyrenyl complexes displaying extended lifetimes. *J. Phys. Chem. A* **2001,** *105*, 8154-8161.

17. Goze, C.; Kozlov, D. V.; Castellano, F. N.; Suffert, J.; Ziessel, R., Synthesis of bipyridine and terpyridine based ruthenium metallosynthons for grafting of multiple pyrene auxiliaries. *Tetrahedron Lett.* **2003,** *44*, 8713-8716.

18. Goze, C.; Kozlov, D. V.; Tyson, D. S.; Ziessel, R.; Castellano, F. N., Synthesis and photophysics of ruthenium(II) complexes with multiple pyrenylethynylene subunits. *New J. Chem.* **2003,** *27*, 1679-1683.

19. Kozlov, D. V.; Tyson, D. S.; Goze, C.; Ziessel, R.; Castellano, F. N., Room temperature phosphorescence from ruthenium(II) complexes bearing conjugated pyrenylethynylene subunits. *Inorg. Chem.* **2004,** *43*, 6083-6092.

20. Polyansky, D. E.; Danilov, E. O.; Castellano, F. N., Observation of triplet intraligand excited states through nanosecond step-scan Fourier transform infrared spectroscopy. *Inorg. Chem.* **2006,** *45*, 2370-2372.

21. Singh-Rachford, T. N.; Haefele, A.; Ziessel, R.; Castellano, F. N., Boron Dipyrromethene Chromophores: Next Generation Triplet Acceptors/Annihilators for Low Power Upconversion Schemes. *J. Am. Chem. Soc.* **2008,** *130*, 16164-16165.

22. Singh-Rachford, T. N.; Nayak, A.; Muro-Small, M. L.; Goeb, S.; Therien, M. J.; Castellano, F. N., Supermolecular-Chromophore-Sensitized Near-Infrared-to-Visible Photon Upconversion. *J. Am. Chem. Soc.* **2010,** *132*, 14203-14211.

23. Singh-Rachford, T. N.; Castellano, F. N., Triplet Sensitized Red-to-Blue Photon Upconversion. *J. Phys. Chem. Lett.* **2010,** *1*, 195-200.

24. Schulze, T. F.; Schmidt, T. W., Photochemical upconversion: present status and prospects for its application to solar energy conversion. *Energy Environ. Sci.* **2015,** *8*, 103-125.

25. Yanai, N.; Kimizuka, N., New Triplet Sensitization Routes for Photon Upconversion: Thermally Activated Delayed Fluorescence Molecules, Inorganic Nanocrystals, and Singlet-to-Triplet Absorption. *Acc. Chem. Res.* **2017,** *50*, 2487-2495.

26. El Roz, K. A.; Castellano, F. N., Photochemical upconversion in water. *Chem. Commun.* **2017,** *53*, 11705-11708.

27. Tritsch, J. R.; Chan, W.-L.; Wu, X.; Monahan, N. R.; Zhu, X. Y., Harvesting singlet fission for solar energy conversion via triplet energy transfer. *Nat. Commun.* **2013,** *4*, 2679.

28. Korovina, N. V.; Joy, J.; Feng, X.; Feltenberger, C.; Krylov, A. I.; Bradforth, S. E.; Thompson, M. E., Linker-Dependent Singlet Fission in Tetracene Dimers. *J. Am. Chem. Soc.* **2018,** *140*, 10179-10190.

29. McCusker, C. E.; Chakraborty, A.; Castellano, F. N., Excited State Equilibrium Induced Lifetime Extension in a Dinuclear Platinum(II) Complex. *J. Phys. Chem. A* **2014,** *118*, 10391-10399.

30. Gibson, J.; Monkman, A. P.; Penfold, T. J., The Importance of Vibronic Coupling for Efficient Reverse Intersystem Crossing in Thermally Activated Delayed Fluorescence Molecules. *Chemphyschem* **2016,** *17*, 2956-2961.

31. Yarnell, J. E.; McCusker, C. E.; Leeds, A. J.; Breaux, J. M.; Castellano, F. N., Exposing the Excited-State Equilibrium in an IrIII Bichromophore: A Combined Time Resolved Spectroscopy and Computational Study. *Eur. J. Inorg. Chem.* **2016,** *2016*, 1808-1818.

32. Parker, C. A.; Hatchard, C. G., Triplet-Singlet Emission in Fluid Solutions - Phosphorescence of Eosin. *Trans. Faraday Soc.* **1961,** *57*, 1894-&.

33. Parker, C. A., *Advances in Photochemistry*. Interscience Publishers: New York, New York, 1964.

34. Parker, C. A., *Photoluminescence of Solutions*. Elsevier Publishing Company: Amsterdam, New York, 1968; p 544.

35. Leitl, M. J.; Krylova, V. A.; Djurovich, P. I.; Thompson, M. E.; Yersin, H., Phosphorescence versus Thermally Activated Delayed Fluorescence. Controlling Singlet-Triplet Splitting in Brightly Emitting and Sublimable Cu(I) Compounds. *J. Am. Chem. Soc.* **2014,** *136*, 16032-16038.

36. Palmeira, T.; Berberan-Santos, M. N., Kinetic Criteria for Optimal Thermally Activated Delayed Fluorescence in Photoluminescence and in Electroluminescence. *J. Phys. Chem. C* **2017,** *121*, 701-708.

37. Zhang, Y.-N.; Liu, Y.-S.; Yan, M.-M.; Wei, Y.; Zhang, Q.-L.; Zhang, Y., Efficient Quantum-Dot Light-Emitting Diodes Employing Thermally Activated Delayed Fluorescence Emitters as Exciton Harvesters. *ACS Appl. Mater. Interfaces* **2018,** *10*, 7435-7441.

38. Shafikov, M. Z.; Suleymanova, A. F.; Schinabeck, A.; Yersin, H., Dinuclear Ag(I) Complex Designed for Highly Efficient Thermally Activated Delayed Fluorescence. *J. Phys. Chem. Lett.* **2018,** *9*, 702-709.

39. Penfold, T. J.; Dias, F. B.; Monkman, A. P., The theory of thermally activated delayed fluorescence for organic light emitting diodes. *Chem. Commun.* **2018,** *54*, 3926-3935.

40. Mongin, C.; Moroz, P.; Zamkov, M.; Castellano, F. N., Thermally activated delayed photoluminescence from pyrenyl-functionalized CdSe quantum dots. *Nat. Chem.* **2018,** *10*, 225.

41. Yarnell, J. E.; Wells, K. A.; Palmer, J. R.; Breaux, J. M.; Castellano, F. N., Excited-State Triplet Equilibria in a Series of Re(I)-Naphthalimide Bichromophores. *J. Phys. Chem. B* **2019,** *123*, 7611-7627.

42. Endo, A.; Ogasawara, M.; Takahashi, A.; Yokoyama, D.; Kato, Y.; Adachi, C., Thermally Activated Delayed Fluorescence from Sn4+-Porphyrin Complexes and Their Application to Organic Light-Emitting Diodes - A Novel Mechanism for Electroluminescence. *Adv. Mater.* **2009,** *21*, 4802-+.

43. Czerwieniec, R.; Yu, J. B.; Yersin, H., Blue-Light Emission of Cu(I) Complexes and Singlet Harvesting. *Inorg. Chem.* **2011,** *50*, 8293-8301.

44. Dias, F. B.; Bourdakos, K. N.; Jankus, V.; Moss, K. C.; Kamtekar, K. T.; Bhalla, V.; Santos, J.; Bryce, M. R.; Monkman, A. P., Triplet Harvesting with 100% Efficiency by Way of Thermally Activated Delayed Fluorescence in Charge Transfer OLED Emitters. *Adv. Mater.* **2013,** *25*, 3707-3714.

45. Chen, X. L.; Yu, R. M.; Zhang, Q. K.; Zhou, L. J.; Wu, C. Y.; Zhang, Q.; Lu, C. Z., Rational Design of Strongly Blue-Emitting Cuprous Complexes with Thermally Activated Delayed Fluorescence and Application in Solution-Processed OLEDs. *Chem. Mater.* **2013,** *25*, 3910-3920.

46. Zhang, Q. S.; Li, B.; Huang, S. P.; Nomura, H.; Tanaka, H.; Adachi, C., Efficient blue organic light-emitting diodes employing thermally activated delayed fluorescence. *Nat. Photonics* **2014,** *8*, 326-332.

47. Hofbeck, T.; Monkowius, U.; Yersin, H., Highly Efficient Luminescence of Cu(I) Compounds: Thermally Activated Delayed Fluorescence Combined with Short-Lived Phosphorescence. *J. Am. Chem. Soc.* **2015,** *137*, 399-404.

48. Bergmann, L.; Hedley, G. J.; Baumann, T.; Bräse, S.; Samuel, I. D. W., Direct observation of intersystem crossing in a thermally activated delayed fluorescence copper complex in the solid state. *Sci. Adv.* **2016,** *2*.

49. Fernando, B. D.; Thomas, J. P.; Andrew, P. M., Photophysics of thermally activated delayed fluorescence molecules. *Methods Appl. Fluoresc.* **2017,** *5*, 012001.

50. Steinegger, A.; Klimant, I.; Borisov, S. M., Purely Organic Dyes with Thermally Activated Delayed FluorescenceA Versatile Class of Indicators for Optical Temperature Sensing. *Adv. Opt. Mater.* **2017,** *5*, 13.

51. Yersin, H.; Czerwieniec, R.; Shafikov, M. Z.; Suleymanova, A. F., TADF Material Design: Photophysical Background and Case Studies Focusing on Cu-I and Ag-I Complexes. *Chemphyschem* **2017,** *18*, 3508-3535.

52. Li, T.; Yang, D.; Zhai, L.; Wang, S.; Zhao, B.; Fu, N.; Wang, L.; Tao, Y.; Huang, W., Thermally Activated Delayed Fluorescence Organic Dots (TADF Odots) for Time-Resolved and Confocal Fluorescence Imaging in Living Cells and In Vivo. *Adv. Sci. Weinh. Baden-Wurtt. Ger.* **2017,** *4*, 1600166-1600166.

53. Li, G. F.; Nobuyasu, R. S.; Zhang, B. H.; Geng, Y.; Yao, B.; Xie, Z. Y.; Zhu, D. X.; Shan, G. G.; Che, W. L.; Yan, L. K.; Su, Z. M.; Dias, F. B.; Bryce, M. R., Thermally Activated Delayed Fluorescence in Cu-I Complexes Originating from Restricted Molecular Vibrations. *Chem.-Eur. J.* **2017,** *23*, 11761-11766.

54. Wong, M. Y.; Zysman-Colman, E., Purely Organic Thermally Activated Delayed Fluorescence Materials for Organic Light-Emitting Diodes. *Adv. Mater.* **2017,** *29*.

55. Mieno, H.; Kabe, R.; Allendorf, M. D.; Adachi, C., Thermally activated delayed fluorescence of a Zr-based metal–organic framework. *Chem. Commun.* **2018,** *54*, 631-634.

56. Chakraborty, A.; Yarnell, J. E.; Sommer, R. D.; Roy, S.; Castellano, F. N., Excited-State Processes of Cyclometalated Platinum(II) Charge-Transfer Dimers Bridged by Hydroxypyridines. *Inorg. Chem.* **2018,** *57*, 1298-1310.

57. Yarnell, J. E.; Chakraborty, A.; Myahkostupov, M.; Wright, K. M.; Castellano, F. N., Long-Lived Triplet Excited State in a Platinum(II) Perylene Monoimide Complex. *Dalton Trans.* **2018,** *47*, 15071-15081.

58. McCusker, C. E.; Chakraborty, A.; Castellano, F. N., Excited State Equilibrium Induced Lifetime Extension in a Dinuclear Platinum(II) Complex. *J. Phys. Chem. A.* **2014,** *118*, 10391-10399.

59. McClenaghan, N. D.; Leydet, Y.; Maubert, B.; Indelli, M. T.; Campagna, S., Excited-state equilibration: a process leading to long-lived metal-to-ligand charge transfer luminescence in supramolecular systems. *Coord. Chem. Rev.* **2005,** *249*, 1336-1350.

60. Schmehl, R., Something New in Transition Metal Complex Sensitizers: Bringing Metal Diimine Complexes and Aromatic Hydrocarbons Together. *The Spectrum* **2000,** *13*.

61. Thompson, D., Michael Faraday's recognition of ruby gold: the birth of modern nanotechnology. *Gold Bull.* **2007,** *40*, 267-269.

62. Reibold, M.; Paufler, P.; Levin, A. A.; Kochmann, W.; Pätzke, N.; Meyer, D. C., Carbon nanotubes in an ancient Damascus sabre. *Nature* **2006,** *444*, 286-286.

63. Wu, J.; Shen, Y.-L.; Reinhardt, K.; Szu, H., *A NANO enhancement to Moore's law*. SPIE: 2012; Vol. 8401.

64. Gerung, H.; Boyle, T. J.; Tribby, L. J.; Bunge, S. D.; Brinker, C. J.; Han, S. M., Solution Synthesis of Germanium Nanowires Using a Ge2+ Alkoxide Precursor. *J. Am. Chem. Soc.* **2006,** *128*, 5244-5250.

65. Boyle, T. J.; Yonemoto, D. T.; Doan, T. Q.; Alam, T. M., Synthesis and Structural Characterization of Group 4 Metal Carboxylates for Nanowire Production. *Inorg. Chem.* **2014,** *53*, 12449-12458.

66. Treadwell, L. J.; Boyle, T. J.; Phelan, W. A.; Parkes, M. V.; Young, D. P., Synthesis and characterization of a series of nickel(ii) alkoxide precursors and their utility for Ni(0) nanoparticle production. *Dalton Trans.* **2017,** *46*, 5806-5815.

67. Boyle, T. J.; Yonemoto, D. T.; Sears, J. M.; Treadwell, L. J.; Bell, N. S.; Cramer, R. E.; Neville, M. L.; Stillman, G. A. K.; Bingham, S. P., Synthesis, characterization, and utility of trifluoroacetic acid lanthanide precursors for production of varied phase fluorinated lanthanide nanomaterials. *Polyhedron* **2017,** *131*, 59-73.

68. Lin, S.; Xie, X.; Patel, M. R.; Yang, Y.-H.; Li, Z.; Cao, F.; Gheysens, O.; Zhang, Y.; Gambhir, S. S.; Rao, J. H.; Wu, J. C., Quantum Dot Imaging for Embryonic Stem Cells. *BMC Biotechnol.* **2007,** *7*, 67.

69. Bao, Y.; Li, J.; Wang, Y.; Yu, L.; Wang, J.; Du, W.; Lou, L.; Zhu, Z.; Peng, H.; Zhu, J., Preparation Of Water Soluble Cdse and Cdse/Cds Quantum Dots and Their Uses in Imaging of Cell and Blood Capillary. *Opt. Mater.* **2012,** *34*, 1588-1592.

70. Stein, J. L.; Mader, E. A.; Cossairt, B. M., Luminescent InP Quantum Dots with Tunable Emission by Post-Synthetic Modification with Lewis Acids. *J. Phys. Chem. Lett.* **2016,** *7*, 1315-1320.

71. Garakyaraghi, S.; Mongin, C.; Granger, D. B.; Anthony, J. E.; Castellano, F. N., Delayed Molecular Triplet Generation from Energized Lead Sulfide Quantum Dots. *J. Phys. Chem. Lett.* **2017,** *8*, 1458-1463.

72. Caputo, J. A.; Frenette, L. C.; Zhao, N.; Sowers, K. L.; Krauss, T. D.; Weix, D. J., General and Efficient C–C Bond Forming Photoredox Catalysis with Semiconductor Quantum Dots. *J. Am. Chem. Soc.* **2017,** *139*, 4250-4253.

73. Ramalingam, G.; Saravanan, K. V.; Vizhi, T. K.; Rajkumar, M.; Baskar, K., Synthesis of Water-Soluble and Bio-Taggable Cdse@Zns Quantum Dots. *RSC Adv.* **2018,** *8*, 8516-8527.

74. Jiang, Y.; Wang, C.; Rogers, C. R.; Kodaimati, M. S.; Weiss, E. A., Regio- and Diastereoselective Intermolecular [2+2] Cycloadditions Photocatalysed by Quantum Dots. *Nature Chem.* **2019,** *11*, 1034-1040.

75. Xu, Z.; Jin, T.; Huang, Y.; Mulla, K.; Evangelista, F. A.; Egap, E.; Lian, T., Direct Triplet Sensitization of Oligothiophene by Quantum Dots. *Chem. Sci.* **2019,** *10*, 6120-6124.

76. Garakyaraghi, S.; Castellano, F. N., Nanocrystals for Triplet Sensitization: Molecular Behavior from Quantum-Confined Materials. *Inorg. Chem.* **2018,** *57*, 2351-2359.

77. Brus, L., Electronic Wave Functions in Semiconductor Clusters: Experiment and Theory. *J. Phys. Chem.* **1986,** *90*, 2555-2560.

78. Bohr, N., I. On the Constitution of Atoms and Molecules. *Lond. Edinb. Dublin Philos. Mag. J. Sci.* **1913,** *26*, 1-25.

79. Weller, H., Colloidal Semiconductor Q-Particles: Chemistry in the Transition Region Between Solid State and Molecules. *Angew. Chem. Int. Ed. Engl.* **1993,** *32*, 41-53.

80. Ekimov, A. I.; Hache, F.; Schanne-Klein, M. C.; Ricard, D.; Flytzanis, C.; Kudryavtsev, I. A.; Yazeva, T. V.; Rodina, A. V.; Efros, A. L., Absorption and Intensity-Dependent Photoluminescence Measurements on Cdse Quantum Dots: Assignment of the First Electronic Transitions. *J. Opt. Soc. Am. B* **1993,** *10* (1), 100-107.

81. Wang, C.; Dong, H.; Jiang, L.; Hu, W., Organic Semiconductor Crystals. *Chem. Soc. Rev.* **2018,** *47*, 422-500.

82. Moroz, P.; Royo Romero, L.; Zamkov, M., Colloidal Semiconductor Nanocrystals in Energy Transfer Reactions. *Chem. Commun.* **2019,** *55*, 3033-3048.

83. Luo, X.; Han, Y.; Chen, Z.; Li, Y.; Liang, G.; Liu, X.; Ding, T.; Nie, C.; Wang, M.; Castellano, F. N.; Wu, K., Mechanisms of Triplet Energy Transfer Across the Inorganic Nanocrystal/Organic Molecule Interface. *Nature Comm.* **2020,** *11*, 28.

84. Grassian, V. H.; Haes, A. J.; Mudunkotuwa, I. A.; Demokritou, P.; Kane, A. B.; Murphy, C. J.; Hutchison, J. E.; Isaacs, J. A.; Jun, Y.-S.; Karn, B.; Khondaker, S. I.; Larsen, S. C.; Lau, B. L. T.; Pettibone, J. M.; Sadik, O. A.; Saleh, N. B.; Teague, C., NanoEHS –

Defining Fundamental Science Needs: No Easy Feat When the Simple Itself is Complex. *Environ. Sci. Nano* **2016,** *3*, 15-27.

85. Baer, D. R.; Amonette, J. E.; Engelhard, M. H.; Gaspar, D. J.; Karakoti, A. S.; Kuchibhatla, S.; Nachimuthu, P.; Nurmi, J. T.; Qiang, Y.; Sarathy, V.; Seal, S.; Sharma, A.; Tratnyek, P. G.; Wang, C.-M., Characterization challenges for nanomaterials. *Surf. Interface Anal.* **2008,** *40*, 529-537.

86. Richman, E. K.; Hutchison, J. E., The Nanomaterial Characterization Bottleneck. *ACS Nano* **2009,** *3*, 2441-2446.

87. Jeevanandam, J.; Barhoum, A.; Chan, Y. S.; Dufresne, A.; Danquah, M. K., Review On Nanoparticles and Nanostructured Materials: History, Sources, Toxicity and Regulations. *Beilstein J. Nanotechnol.* **2018,** *9*, 1050-1074.

88. Kolahalam, L. A.; Kasi Viswanath, I. V.; Diwakar, B. S.; Govindh, B.; Reddy, V.; Murthy, Y. L. N., Review on nanomaterials: Synthesis and applications. *Mater. Today: Proc.* **2019,** *18*, 2182-2190.

89. van der Heijden, A. E. D. M., Developments and Challenges in the Manufacturing, Characterization and Scale-Up of Energetic Nanomaterials – A Review. *Chem. Eng. J.* **2018,** *350*, 939-948.

90. Zhou, J.; Zhu, M.; Meng, R.; Qin, H.; Peng, X. Ideal CdSe/CdS Core/Shell Nanocrystals Enabled by Entropic Ligands and Their Core Size-, Shell Thickness-, and Ligand-Dependent Photoluminescence Properties. *J. Am. Chem. Soc.* **2017**, *139* (46), 16556–16567.

91. Houtepen, A. J.; Hens, Z.; Owen, J. S.; Infante, I. On the Origin of Surface Traps in Colloidal II–VI Semiconductor Nanocrystals. *Chem. Mater.* **2017**, *29* (2), 752–761.

92. Kirkwood, N.; Monchen, J. O. V.; Crisp, R. W.; Grimaldi, G.; Bergstein, H. A. C.; du Fossé, I.; van der Stam, W.; Infante, I.; Houtepen, A. J. Finding and Fixing Traps in II–VI and III–V Colloidal Quantum Dots: The Importance of Z-Type Ligand Passivation. *J. Am. Chem. Soc.* **2018**, *140* (46), 15712–15723.

93. Hughes, K. E.; Stein, J. L.; Friedfeld, M. R.; Cossairt, B. M.; Gamelin, D. R. Effects of Surface Chemistry on the Photophysics of Colloidal InP Nanocrystals. *ACS Nano* **2019**, *13*, 14198–14207.

94. Hartley, C. L.; Kessler, M. L.; Dempsey, J. L. Molecular-Level Insight into Semiconductor Nanocrystal Surfaces. *J. Am. Chem. Soc.* **2021**, *143*, 1251–1266.

95. Kim, T.-G.; Zherebetskyy, D.; Bekenstein, Y.; Oh, M. H.; Wang, L.-W.; Jang, E.; Alivisatos, A. P. Trap Passivation in Indium-Based Quantum Dots through Surface Fluorination: Mechanism and Applications. *ACS Nano* **2018**, *12*, 11529–11540.

96. Zhang, X.; Hudson, M. H.; Castellano, F. N. Passivation of Electron Trap States in InP Quantum Dots with Benzoic Acid Ligands. *J. Phys. Chem. C* **2021**.

97. Abdel-Latif, K.; Bateni, F.; Crouse, S.; Abolhasani, M. Flow Synthesis of Metal Halide Perovskite Quantum Dots: From Rapid Parameter Space Mapping to AI-Guided Modular Manufacturing. *Matter* **2020**, *3*, 1053–1086.

98. Abdel-Latif, K.; Epps, R. W.; Kerr, C. B.; Papa, C. M.; Castellano, F. N.; Abolhasani, M. Facile Room-Temperature Anion Exchange Reactions of Inorganic Perovskite Quantum Dots Enabled by a Modular Microfluidic Platform. *Adv. Funct. Mater.* **2019**, *29*,

99. Abolhasani, M.; C. Bruno, N.; F. Jensen, K. Oscillatory Three-Phase Flow Reactor for Studies of Bi-Phasic Catalytic Reactions. *Chem. Commun.* **2015**, *51*, 8916–8919.

100. Abolhasani, M.; Coley, C. W.; Xie, L.; Chen, O.; Bawendi, M. G.; Jensen, K. F. Oscillatory Microprocessor for Growth and in Situ Characterization of Semiconductor Nanocrystals. *Chem. Mater.* **2015**, *27*, 6131–6138.

101. Epps, R. W.; Bowen, M. S.; Volk, A. A.; Abdel-Latif, K.; Han, S.; Reyes, K. G.; Amassian, A.; Abolhasani, M. Artificial Chemist: An Autonomous Quantum Dot Synthesis Bot. *Adv. Mater.* 2001626.

102. Kirmani, A. R.; Luther, J. M.; Abolhasani, M.; Amassian, A. Colloidal Quantum Dot Photovoltaics: Current Progress and Path to Gigawatt Scale Enabled by Smart Manufacturing. *ACS Energy Lett.* **2020**, *5*, 3069–3100.

103. Shen, Y.; Abolhasani, M.; Chen, Y.; Xie, L.; Yang, L.; Coley, C. W.; Bawendi, M. G.; Jensen, K. F. In-Situ Microfluidic Study of Biphasic Nanocrystal Ligand-Exchange Reactions Using an Oscillatory Flow Reactor. *Angew. Chem. Int. Ed.* **2017**, *56*, 16333–16337.

104. W. Epps, R.; A. Volk, A.; Abdel-Latif, K.; Abolhasani, M. An Automated Flow Chemistry Platform to Decouple Mixing and Reaction Times. *React. Chem. Eng.* **2020**, *5*, 1212–1217.

105. Volk, A. A.; Epps, R. W.; Yonemoto, D.; Castellano, F. N.; Abolhasani, M. Continuous Biphasic Chemical Processes in a Four-Phase Segmented Flow Reactor. *React. Chem. Eng.* **2021**, *6*, 1367–1375.

Chapter 2: Thermally Activated Delayed Photoluminescence: Deterministic Control of Excited State Decay

This chapter has been previously published: *J. Am. Chem. Soc.* **2020**, *142*, 10883–10893. DOI: 10.1021/jacs.0c03331

Abstract: Thermally activated photophysical processes are ubiquitous in numerous organic and metal-organic molecules, leading to chromophores with excited state properties that can be considered an equilibrium mixture of the available low-lying states. Relative populations of the equilibrated states are governed by temperature. Such molecules have been devised as high quantum yield emitters in modern organic light-emitting diode technology and for deterministic excited state lifetime control to enhance chemical reactivity in solar energy conversion and photocatalytic schemes. The recent discovery of thermally activated photophysics at CdSe nanocrystal-molecule interfaces enables a new paradigm wherein molecule-quantum dot constructs are used to systematically generate material with predetermined photophysical response and excited state properties. Semiconductor nanomaterials feature size-tunable energy level engineering, which considerably expands the purview of thermally activated photophysics beyond what is possible using only molecules. This Perspective is intended to provide a non-exhaustive overview of the advances that led to the integration of semiconductor quantum dots in thermally activated delayed photoluminescence (TADPL) schemes and to identify important challenges moving into the future. The initial establishment of excited state lifetime extension utilizing triplet-triplet excited-state equilibria is detailed. Next, advances involving the rational design of molecules composed of both metal-containing and organic-based chromophores that produce the desired TADPL are described. Finally, the recent introduction of semiconductor nanomaterials into hybrid TADPL constructs is discussed, paving the way towards the realization of fine-tuned

deterministic control of excited state decay. It is envisioned that libraries of synthetically facile composites will be broadly deployed as photosensitizers and light emitters for numerous synthetic and optoelectronic applications in the near future.

2.1 Introduction

At its very core, luminescence has been a research topic of extensive scientific interest for centuries. As noted in Cecil Parker's book, *Photoluminescence of Solutions*, topics of light emission phenomena encompass electroluminescence, radioluminescence, chemiluminescence, bioluminescence, triboluminescence, sonoluminescence, and photoluminescence (PL).[1] In each instance, light is emitted from excited states generated by a variety of excitation stimuli. As most organic molecules possess closed-shell (singlet) ground states, the study of molecular light emission pathways primarily focuses on the relative populations of the lowest energy singlet and triplet excited states.[2] In organic molecular photochemistry, triplet excited states are typically accessed by initial spin-allowed population of a singlet excited state, followed by intersystem crossing (ISC) to a lower energy triplet excited state. As one would expect from Hund's rules, this triplet excited state is generally lower in energy with respect to the initially populated singlet excited state due to the exchange interaction. Exchange is a quantum-mechanical phenomenon, with no classical analogue, that arises as a consequence of electron indistinguishability and the Pauli exclusion principle. The aligned electron spins of the triplet state provide an energetic stabilization relative to the opposite spins of the singlet state. Spin-allowed photon emission is typically referred to as fluorescence, whereas formally spin-forbidden light emission processes are termed phosphorescence.

The dominant process of ISC in molecular photophysics occurs through spin-orbit coupling (SOC). The ISC transition can occur by direct SOC of the lowest singlet to higher vibrational

levels of the lowest triplet, or by SOC to an upper triplet excited state, followed by rapid internal conversion to the lowest triplet. Spin-orbit coupling is induced in part by conservation of the total angular momentum of the electrons in the molecule. The two most common manifestations of SOC in molecular photophysics are perturbation by a magnetic field, as seen in the heavy atom effect[3] or the presence of paramagnetic molecules, and El-Sayed's rules.[4] From a molecular design perspective, proximal effects are eschewed in favor of direct integration of functionalities that can directly induce SOC. For El-Sayed considerations, this requires molecules with energetically proximate (n,π*) and (π,π*) excited states. The heavy atom effect entails including atoms of high atomic number (Z), including halogens such as iodine or 2nd and 3rd row transition metals.

Increasing SOC can increase the rates of ISC into spin-forbidden triplet states. By the same token, increased proclivity toward ISC will also enhance the phosphorescence efficiency by increasing the "allowed-ness" of radiative relaxation to the ground state. Combining discrete molecular subunits with vastly dissimilar rates of ISC can fuse these disparate excited state behaviors into new functionalities. Research along this seam of innovation has progressed steadily over the past two decades.[5] Equilibria between excited states can be established by meeting certain energetic and electronic coupling requirements, which will be detailed below. These equilibrated photo-processes offer a route to systematic control of excited state properties, particularly lifetime tuning, that are not accessible by simply adjusting non-radiative decay rates using established structure-property relationships. With the continued development of this technology, it should be possible to optimize combined constructs with applications in sensing,[6-15] photoredox catalysis,[16-18] and photochemical upconversion.[19] In any case, investigation of these photophysical phenomena has already yielded fundamental insights, and further knowledge gains can be expected to increase the parameter space for specific applications.

Exerting control over the excited state energetics, lifetime, and spin characteristics in molecules is essential for guiding light emission processes and exploiting chemical reactivity following light activation. Work dating back to the origins of quantum mechanics has led to comprehensive understanding of molecular excited states and the factors influencing their decay kinetics. However, it was not until the 1990's when researchers realized that combinations of two different chromophores, covalently linked together, gave rise to "cooperative" behavior wherein each entity imparted new photophysical properties to the other. This ultimately led to the design of numerous molecules featuring thermally equilibrated excited states, which were later harnessed for efficient triplet sensitization of both electron and energy transfer reactions, including photoredox catalysis.[16] More recently, this concept has been expanded to include delayed PL from semiconductor nanocrystal-molecule constructs, thermally activated in nature, whose space for research exploration appears limitless. Interested in capturing all possible electrically-generated spin states, modern organic light emitting diode (OLED) technology has turned to classic thermally activated delayed fluorescence (TADF) processes to generate light in these devices with promising results.[20-21] Given the continuously expanding scope of TADF, lifetime engineering, and related processes, a detailed appreciation of these topics is deemed timely and appropriate. It is the purpose of this Perspective to recognize numerous important contributions focused on thermally activated excited state processes while providing insight into the design criteria utilized and their intended (and sometimes unintentional) photophysical consequences.

2.2 Excited-State Equilibria

When multiple excited states of interest are not completely isoenergetic with each other, the repopulation of the higher-energy state is referred to as thermal activation. The best known of the thermally activated excited state processes is TADF. The first quantitative experimental

characterization of TADF dates back to 1941, when G.N. Lewis (of the eponymous dot structures) and coworkers reported long-lifetime and temperature dependent fluorescence and phosphorescence emanating from fluorescein molecules encapsulated in boric acid glasses.[22] It was not until 20 years later when Parker and Hatchard successfully measured the delayed emission properties of eosin in solution, termed E-type delayed fluorescence.[1, 5, 23-27] In classic work by Parker and Hatchard,[25] the E-type process consists of excitation to S_1 followed by ISC to T_1 and reverse intersystem crossing (rISC) back to S_1. With rISC dependent on drawing energy from a thermal bath, more delayed emission events are observed from S_1 at higher temperatures. This is displayed schematically in Figure 2.1. As long as the two states are nearly isoenergetic, (typically ΔE < 0.15 eV), the equilibrium between the two states should be thermally accessible at non-cryogenic temperatures. Following the demonstration of their utility in organic light emitting diodes near the beginning of the decade, research on TADF molecules has exploded over the past 8 years.[20, 28-30] The temperature dependence of repopulation to the S_1 state is modeled well using an Arrhenius expression of the form in Eq. 2.1,[31] where ΔE represents the energy gap between the S_1 and T_1 states.

$$k_{rISC} = Ae^{-\Delta E/k_B T} \qquad (2.1)$$

In this treatment, k_{rISC} is the rate of rISC, k_B is Boltzmann's constant, T is temperature and A is a pre-exponential factor. In a process analogous to TADF, excited-state equilibrium can also be established between two nearly isoenergetic electronic states, now featuring identical spin multiplicity, and the higher energy state will produce delayed emission at elevated temperatures. With the PL no longer necessarily being spin allowed, we will refer to it as thermally activated delayed photoluminescence (TADPL). Unlike TADF, TADPL expands the scope of chromophores beyond singlet emitters to include triplet emitters that require donor and acceptor triplet states,

displayed schematically in Figure 2.1. In specific contexts, which will be expanded below, these donor-acceptor pairs undergo Dexter triplet energy transfer (TTET) in the forward and reverse direction to establish an excited-state equilibrium. The behavior of these constructs is still modeled by an Arrhenius expression, but the two interacting excited states are triplet in nature and k_{rTTET} becomes the rate constant for reverse triplet-triplet energy transfer (rTTET) in Eq. 2.1.[31] The conceptual framework for TADPL is subtly different from that for TADF due to the matched or mismatched spin multiplicities at play. In TADF, the S_1 state is likely to have a significantly larger radiative rate constant than the T_1 state due to the spin-allowed nature of the transition. Combined with the exchange interaction that stabilizes the lowest triplet with respect to the singlet leads to a situation where the lower state is necessarily triplet and therefore longer lived. In TADPL, these conditions still need to be operative. First, the radiative rate constant for the upper state needs to be competitive with the rate constant for forward TTET to the lower state. If TTET outcompetes light emission from the upper state, populating that state will mostly lead to nonradiative TTET. Second, the rate constant for rTTET to the upper state needs to be competitive with the overall rate constant for relaxation of the lower excited state. If rTTET becomes noncompetitive with relaxation from the lower state, it will simply relax before it has a chance to repopulate the upper state. Considering that this process leverages the photophysical properties of two partner chromophores, any apparent increases in lifetime of the shorter-lived species (upper lying state) does not increase the PL quantum yield. Rather, the quantum yield will echo that inherent of the shorter-lived species as long as no additional deactivation processes are accessed. Moreover, the "extended" lifetime achieved in TADPL will always fall between those independently exhibited by the two partner chromophores and is determined by the energy gap and the rates of both TTET and rTTET, akin to TADF.

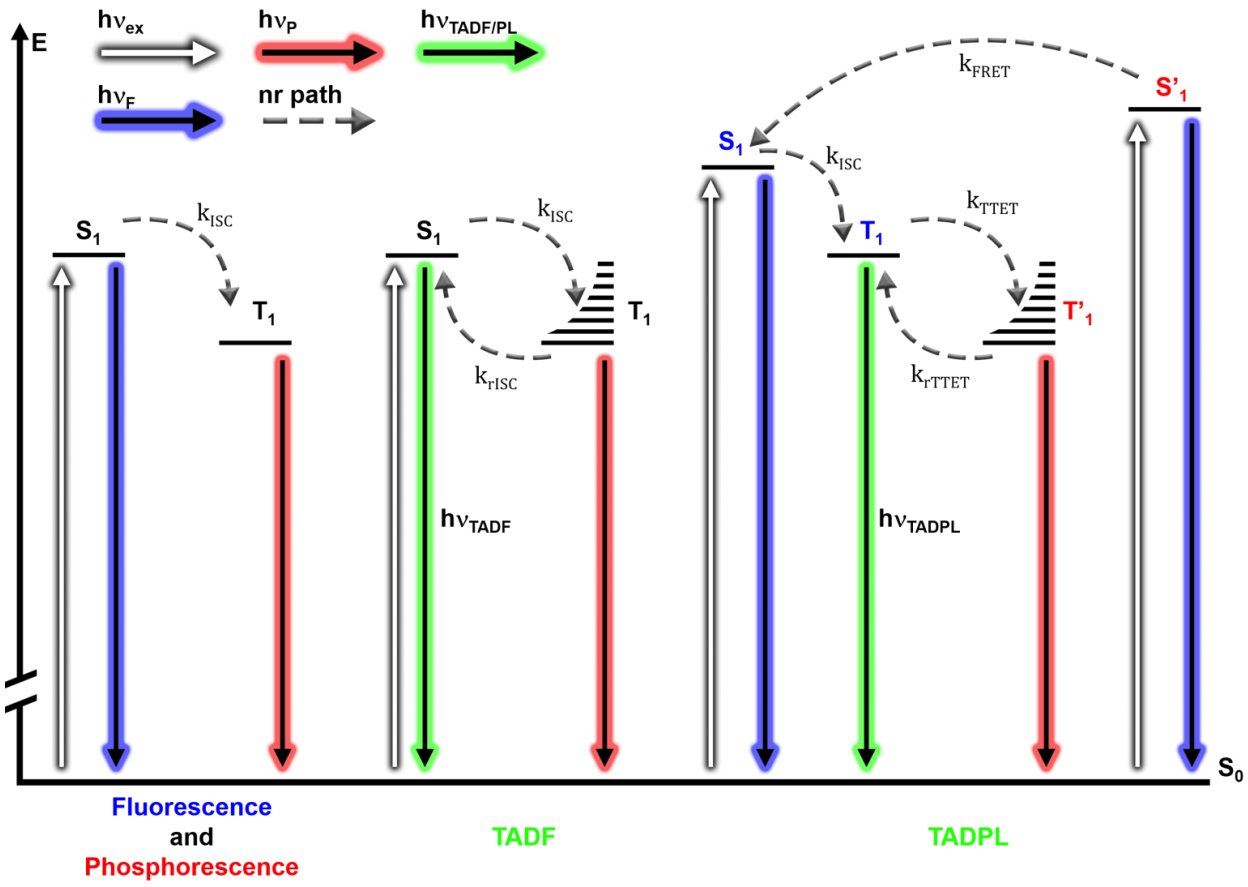

Figure 2.1. Qualitative energy level diagrams of fluorescence and phosphorescence (left), TADF (center), and triplet mediated TADPL (right).

2.3 Excited-State Lifetime Extension

Several publications in the 1990s and early 2000s demonstrated the effects of TADPL by using metal-organic Ru(II) metal-to-ligand charge transfer (MLCT) derivatives decorated with pyrene moities.[32-38] In these works, PL lifetimes of the compounds were greatly enhanced, in some cases by over 100-fold with respect to the "naked" MLCT chromophore.[33] This research, most notably by Tyson,[34-35, 39-40] Simon,[37] Guerzo,[38] Goze,[36, 41] McClenaghan[42] and their respective coworkers, was inspired by the original findings of Ford and Rodgers.[32] Manipulating the photophysical characteristics through alteration of the appended acceptor ligand, lifetimes were

extended through triplet-triplet equilibrium established between the triplet charge transfer state, ^{3}MLCT*, and the triplet excited state of the acceptor, ^{3}A*. The organic acceptor triplet excited states function as lower energy, longer-lived triplet reservoirs that thermally repopulates the emitting ^{3}MLCT* state with lifetimes extended relative to the bare MLCT chromophore. These early works established that the triplet-triplet equilibrium obeys Eq. 2.2, where k_{TTET} is the forward TTET rate constant and k_{rTTET} is the reverse TTET rate constant occurring between the two states.[32, 34-35, 42]

$$K_{eq} = \frac{k_{TTET}}{k_{rTTET}} \qquad (2.2)$$

Tyson's work was the first to suggest a linear lifetime dependence based on the number of pyrenyl groups appended to the Ru(II) core which was later confirmed by McClenaghan and colleagues.[34-35, 42] The combined results provided a foundation for manipulating the TADPL process to yield desired photophysical characteristics. This demonstrated that modification of energy transfer rates,[34-35, 42] spatial separation of localized states,[32] energetic matching of excited states ($\Delta E \lesssim 0.15$ eV),[32] changing temperature,[22, 25] and manipulation of K_{eq} in Eq. 2[34-35, 42] all conspire to control the TADPL dynamics. With careful design of the appended chromophores, researchers can theoretically engineer excited states to match desired applications in a deterministic manner.[5, 19, 43-44]

Recently, excited state engineering of this type has been documented using several different metal complexes as the fast ISC, higher energy triplet.[44-49] In 2011, utilizing a naphthalimide-bearing phenanthroline derivative called PNI-phen, Yarnell *et al.* were able to develop a three-order-of-magnitude lifetime enhancement in a Re(I) carbonyl complex outfitted with this particular ligand.[46] To see an illustrated example of PNI-phen, please refer to the moiety highlighted in blue in Figure 2.2. In that study, the TADPL process ensues subsequent to an initial

Förster resonance energy transfer from the PNI moiety to the Re(I) complex. A representative energy level diagram is shown in the TADPL section of Figure 2.1, where the red S_1' and T_1' represent the PNI ligand centered (LC) states and the blue S_1 and T_1 represent the MLCT states. This is also schematically analogous to the process illustrated in Figure 2.2 for a structurally related molecule. The closely matched triplet state energies generate a thermal equilibrium between the emissive $^3MLCT^*$ and the long-lived $^3LC^*$ states, resulting in an observed lifetime of 651 μs at room temperature. This is the longest reported lifetime from a Re(I) MLCT luminophore measured at room temperature.[46] Using the same PNI-phen derivative, McCusker *et. al.* developed a dinuclear Pt complex with a lifetime of 65 μs.[45] Here, the authors employed dz^2 overlap of the two Pt(II) metal centers to generate a triplet metal-metal-to-ligand charge transfer ($^3MMLCT^*$) state in close energetic proximity to the $^3LC^*$ state resident on the PNI moiety. It is from this $^3MMLCT^*$ state that TADPL was observed.

Ir(III) complexes have also been shown to exhibit TADPL via triplet-triplet equilibrated excited states. In 2014, Denisov *et al.* reported that separating the Ir(III) MLCT core from the appended organic chromophore by using aliphatic groups induced a *ca*. 30 fold excited state lifetime extension without lessening the PL quantum yield.[49] This separation effectively prevents quenching of the MLCT chromophore. Two years later, Yarnell *et al*. published an Ir(III) bichromophore, again using PNI-phen, with an excited state lifetime of 8.8 ms, a four-order-of-magnitude increase with respect to the model chromophore.[50] The TADPL process in this record-setting bichromophore follows the excited state dynamics observed in Figure 2.1. To aid in the visualization of this process, the dynamics are represented schematically by the illustration in Figure 2.2. Undoubtedly, each of these individual studies produced substantial lifetime improvements by utilizing TADPL, thereby expanding the library of molecules poised for

integration in the development of new photonic applications. However, increased consumer-driven demand in light-emitting technologies, such as is used in displays, continues to motivate the search for alternative chromophores for integration in these applications. Concurrently, it may be feasible to develop a more cost-effective approach to achieve these desirable photophysical properties than is possible with coordination compounds composed from rare and expensive metals.

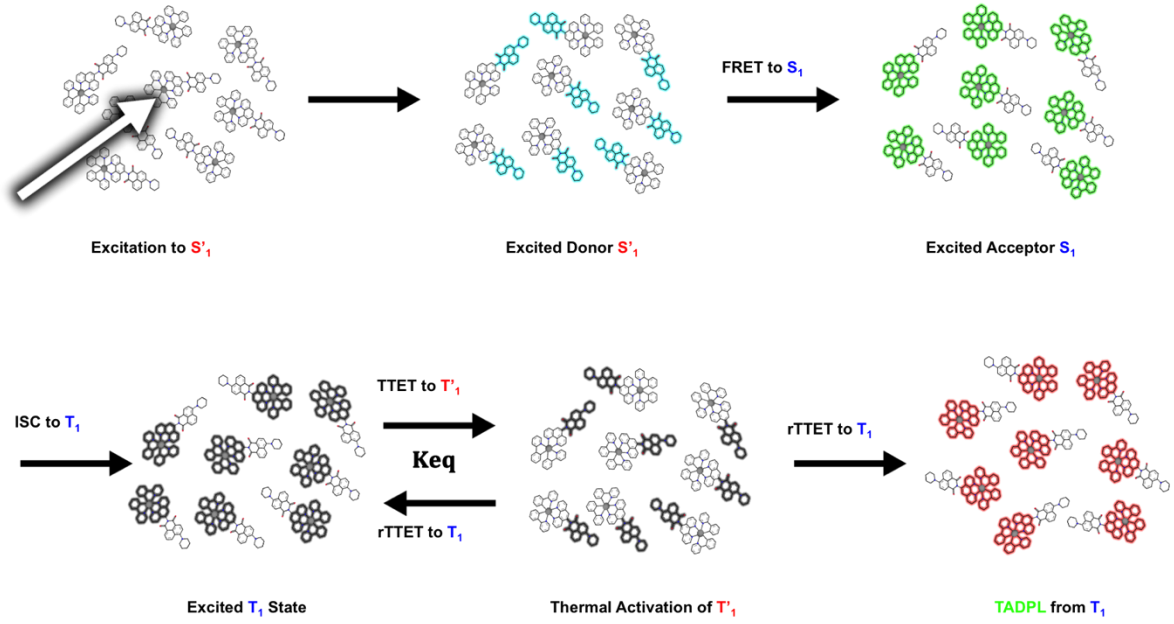

Figure 2.2. Schematic illustration of TADPL process observed in $[Ir(ppy)_2(PNI\text{-}phen)]^+$ as reported by Yarnell *et al.* (ref. 50).

2.4 Controlling TADPL

As noted previously, the major parameters that control TADPL are ΔE between the relevant excited states, k_{TTET} and k_{rTTET}, temperature, molecular geometry, and K_{eq}, some of which cannot be fully deconvoluted from one another. While all these parameters are necessary to observe TADPL, the manipulation of K_{eq} plays a significant role in determining the resultant TADPL characteristics. By shifting the equilibrium concentrations of the two excited states, the PL lifetime can be dramatically altered. In Schmehl's contribution in *The Spectrum*, a former publication of

the Center for Photochemical Sciences at Bowling Green State University, he discusses these details in depth.[51] Briefly, the relevant states in equilibrium must have rate constants significantly larger than the requisite radiative rate constants in order to establish the equilibrium in the first place. For this to occur, the k_{TTET} and k_{rTTET} values must be large relative to the radiative rate of the lower energy chromophore, which is denoted as k_P in Figure 2.3. With an equilibrium established, the relative concentrations of the two excited states can then be shifted toward either state to control the overall excited state lifetime. Under the assumptions outlined in Figure 2.3, when k_{TTET} is significantly greater than k_{rTTET}, long TADPL lifetimes are observed. As k_{rTTET} approaches k_{TTET} in magnitude, progressively shorter TADPL lifetimes will be observed. It is necessary that the equilibrated states be closely matched for TADPL to be detectable near room temperature. However, it becomes evident that, once within a suitable energetic regime, the efficiency of the TADPL is determined by the relative rate constants k_{TTET} and k_{rTTET}, while the observed lifetime is largely dominated by the inherent lifetime of the lower state.

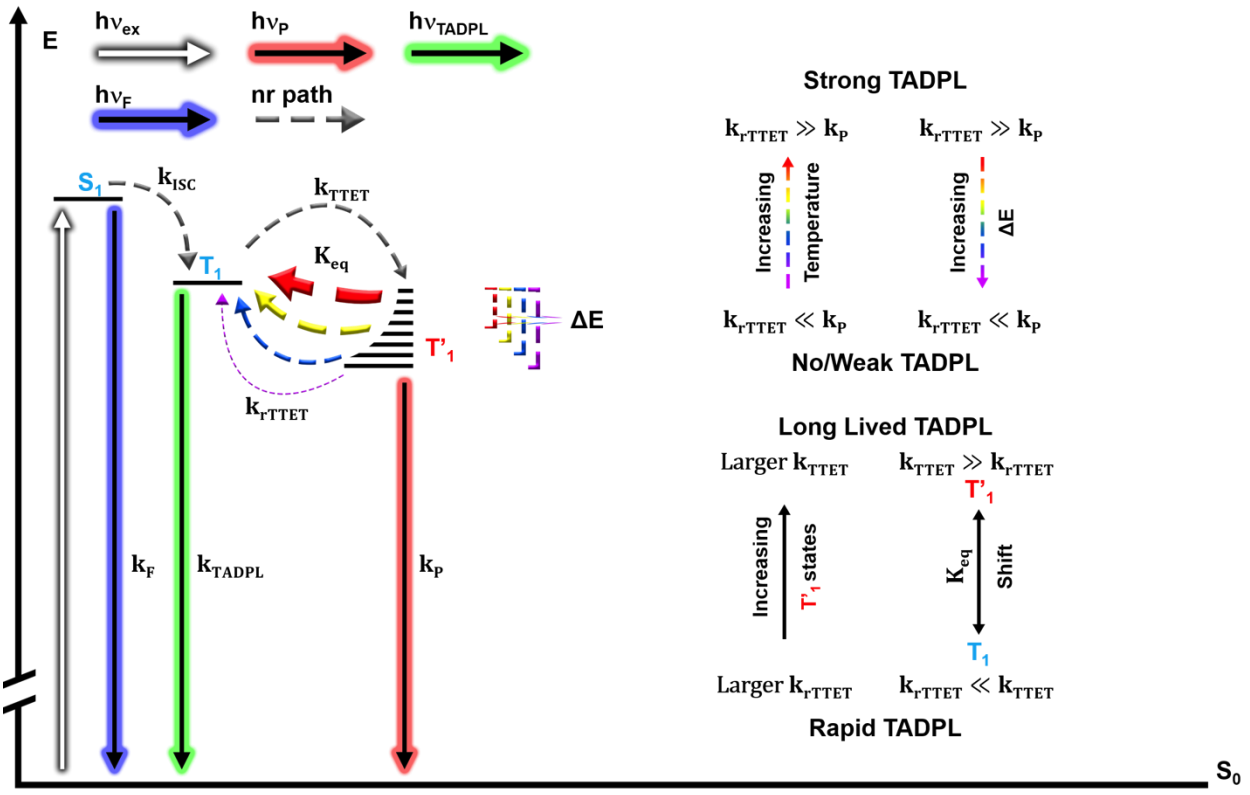

Figure 2.3. Qualitative energy level diagram depicting the effects of altering specific excited-state parameters and their influence on the decay characteristics of TADPL.

2.5 TADPL From Nanomaterials

Semiconductor nanocrystals (NCs) or quantum dots (QDs) can serve as the emissive higher energy excited state in concert with organic triplets because of their strong band-edge spin orbit coupling and excited state spin ambiguity.[52-53] NCs have been extensively studied due to their unique size-dependent, quantum confined optical properties.[54-58] Within the specific context of photochemistry, QDs have been regarded as having outstanding potential.[59] In fact, many recent studies have demonstrated the benefit of these nanomaterials being paired with traditional organic chromophores to achieve exceptional triplet-triplet energy transfer efficiencies; however their utility as TADPL materials was still undiscovered. Tabachnyk *et al.* and Thompson *et al.* independently demonstrated TTET from organic molecules (as thin films) to PbS and PbSe QDs

in 2014.[60-61] These reports were followed in 2016 by the first direct observation of the reverse process, TTET from selectively excited CdSe NCs to surface-appended molecules.[62] In addition to observing TTET from CdSe to various organic molecules,[63-64] the types of QDs that have successfully served as energized donors in TTET to surface anchored chromophores has recently expanded to include PbS,[65-69] $CsPbBr_3$,[70-73] Si,[74] and $CuInS_2$.[75]

In 2018, for the first time, rTTET from appended molecules to CdSe NCs of variable size was demonstrated by Mongin *et al*.,[52] yielding photon emission characteristic of the QDs, thereby mimicking the molecular systems described earlier. It was the first instance of rTTET because in this report, hybrids of CdSe QDs and 1-pyrenecarboxylic acid (PCA) were shown to initially undergo TTET from the NC to the surface anchored molecule as previously demonstrated.[62] This suggested the broad applicability of NCs in TADPL constructs. As the decay kinetics in these and related nanomaterials generally follow complex rate distribution models,[76-78] using a singular "lifetime" characteristic of molecular species is not readily applicable so average lifetime or average time constant are used. As a result, these materials demonstrated PL average lifetimes ranging from microseconds to tens of milliseconds through simple size-dependent tuning of the CdSe NC band gap energy. The QD with the energy nearest to the PCA triplet exhibited the most rapidly decaying TADPL while the larger energy gaps between the NC exciton and the molecular triplet bore longer-lived species. The full suite of differently sized NCs spanned to both extremes of the possible TADPL regime. Figure 2.4 provides an illustration of the effect of NC size on the resultant TADPL. Nearly concurrently, McClenaghan *et al.* reported analogous results using similarly PCA-functionalized CdSe NCs suspended in hexanes.[53] These two studies paved the way for designer nanomaterials with systematically varied excited state average lifetimes, tunable through both particle size and temperature. In both reports, the tunable nature of the NC first

exciton band (E_g) was crucial to control the repopulation of the NC bright state through rTTET. This tunability of the rTTET allows for the design of materials with different TADPL characteristics tailored to targeted functionalities.

It should be noted that the surface environment of semiconductor nanomaterials inherently changes with NC size, and that could affect the observable photophysical characteristics through concentration dependent effects on K_{eq}. The surface environment can also significantly impact the PL efficiency of these materials through the presence or absence of surface passivation.[79-82] The need for increased control over the surface concentration and reactivity of these materials is emerging as a nontrivial piece of this research puzzle. Additionally, systematic control and refined experimental design become necessary elements when dealing with QD-molecule systems because of the subtle complexities they can exhibit. Discussion of pump fluence, material synthetic reproducibility, surface quality control, thermodynamic constraints, molecule-nanocrystal interfacial binding, and methodologies to standardize all of these characteristics, would greatly enhance the impact of research in this field.[83] Technological advances for executing facile and systematic variable temperature transient absorption measurements would be particularly useful to distinguish thermally activated dynamics and other excited state processes.

While the mechanism responsible for TTET from QDs to molecules can vary, numerous studies have identified signals indicative of a direct TTET mechanism.[62-64, 66-67, 70-71, 74-75] By the principle of microscopic reversibility, one can expect direct TTET to allow for direct rTTET. Any QD-molecule system that satisfies the twin requirements of a direct TTET mechanism and a sufficiently small energy gap ($\Delta E \lesssim 0.15$ eV) should display thermally activated photophysics. Following similar logic, complete absence of thermal activation, regardless of energy gap, may be considered characteristic of an indirect triplet sensitization mechanism being operative. It is

incumbent upon the field to recognize the potential for this phenomenon and to carefully evaluate for it when interrogating new synthetic constructs.

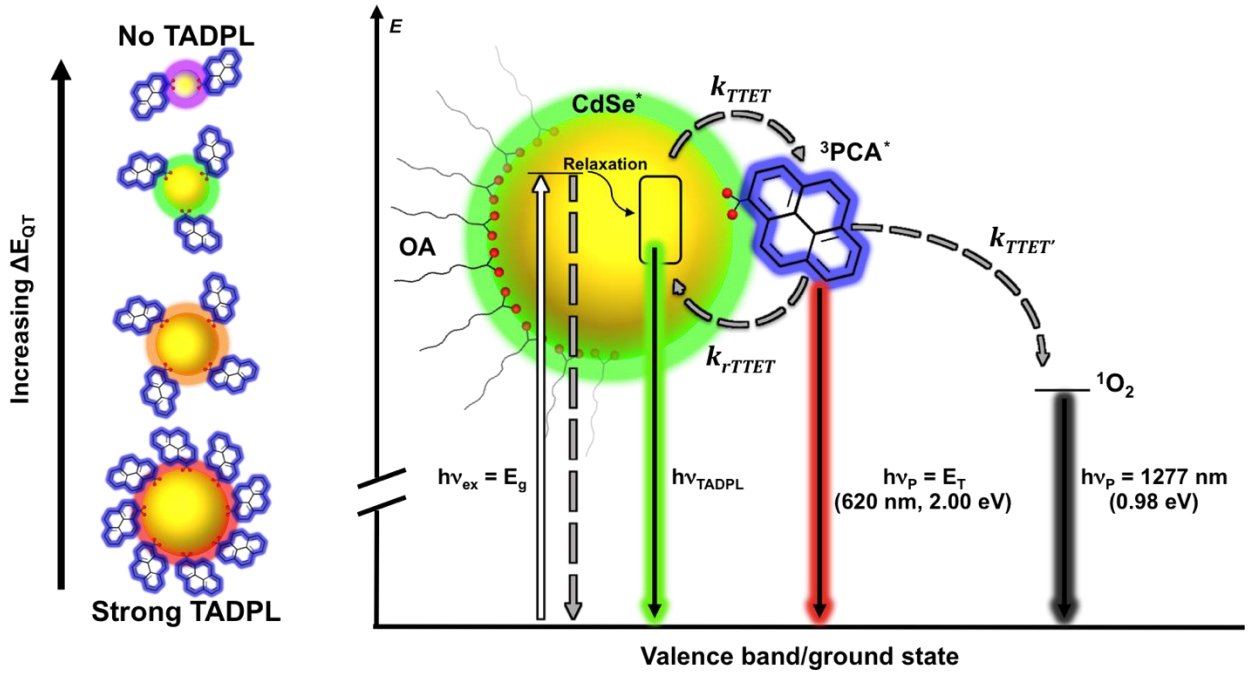

Figure 2.4. Illustration (left) of the effects on TADPL of ΔE between the nanocrystal band edge exciton and the molecular triplet exciton. Energy level diagram (right) illustrating the observed TADPL processes in CdSe/PCA hybrid constructs as reported by Mongin *et al.* (ref. 52).

2.6 Modeling TADPL Decay Kinetics

A pragmatic equation for modeling TADF lifetimes was first derived by McMillin and coworkers to describe the TADF behavior in Cu(I) MLCT excited states.[84] That equation is presented here as Eq. 2.3,[23, 84] where k_{obs} is the observed decay rate ($1/\tau_{obs}$) while k_S and k_T are the decay rates of the singlet and triplet states, respectively.

$$k_{obs} = \frac{3k_T + k_S \exp(-\Delta E/k_B T)}{3 + \exp(-\Delta E/k_B T)} \qquad (2.3)$$

The 3:1 ratio in the coefficients for k_T and k_S Acc. for the presence of three triplet sublevels (triply degenerate) compared to one singlet (singly degenerate) level. Eq. 2.3 is only valid at temperatures high enough that the zero-field splitting of the triplet sub-levels is negligible.[23]

Accounting for the different spin statistics when both states are triplets, the TADPL equivalent expression can be written as Eq. 2.4. Here, k_{UT} is the observed rate constant for the emissive upper triplet and k_{LT} is for the longer-lived lower triplet.

$$k_{obs} = \frac{k_{LT} + k_{UT}\exp(-\Delta E/k_B T)}{1 + \exp(-\Delta E/k_B T)} \qquad (2.4)$$

Applying this fitting procedure to the TADPL decay kinetics from Mongin et al.[52] yields the results summarized in Table 2.1. This fitting generates parameters that well model the experimentally determined values for ΔE[52] and τ_{CdSe}.[62] The k_{LT} value for PCA is held constant throughout fitting as a result of the k_{obs} value for the smallest ΔE constructs being positioned intermediately between k_{LT} and k_{UT}. At larger values of ΔE, k_{TTET} from CdSe to PCA starts to outcompete the prompt CdSe PL, and this can be seen in the increased value of k_{UT} for CdSe with PL at shorter wavelengths. To generate the data in Table 2.1, the k_{LT} values were fixed to 14.3 s^{-1}, the average value of k_{LT} for CdSe-488 below 273 K, when TADPL is assumed to be inoperative.[52] Likewise, the k_{UT} values for CdSe-520, CdSe-510, and CdSe-488 were fixed to 4.5×10^8 s^{-1}, the value reported for k_{TTET} from CdSe-505 to PCA.[62] There are still discrepancies in the fitting results for ΔE at experimental gaps greater than 0.25 eV. These could be due to the model failing to account for temperature-dependence of the nonradiative rates of decay,[23] a plausibly operative condition due to potential thermal activation of low-lying CdSe surface traps.[79, 85]

Table 2.1. Parameters Derived from Fitting TADPL Data in ref. 52 Using Eq. 2.4

	CdSe-600	CdSe-570	CdSe-553	CdSe-520	CdSe-510	CdSe-488
ΔE_{gap} (eV)[a]	0.069	0.177	0.244	0.387	0.433	0.543
ΔE_{fit} (eV)	0.072	0.186	0.248	0.330	0.348	0.463
k_{LT} (s^{-1})[b]	14.3	14.3	14.3	14.3	14.3	14.3
k_{UT} ($\times 10^7$ s^{-1})	1.16	3.05	3.94	45[c]	45[c]	45[c]

[a]Experimental values from ref. 52. [b]Parameter fixed to experimental value from ref. 52. [c]Parameter fixed to experimental value from ref. 62.

While matching the energy gaps and observed PL lifetimes is useful as an academic exercise, the fitting is also worthwhile because it demonstrates the broad applicability of TADPL principles. These principles illuminate the possibility of dialing in precise excited state average lifetimes by selecting from the panoply of highly tunable semiconductor nanomaterials and organic (and inorganic) molecular chromophores available to researchers. The semiconductor composition, nanomaterial size, and choice of surface-appended molecule(s) can be conceptualized as coarse-tuning knobs. One can imagine selecting a class of semiconductor capable of producing PL at a specific desired energy, which would also provide the lower limit of the excited state average decay rate as k_{UT}. Controlling the size of the nanometer-regime semiconductor material would further target the desired photon energy/desired wavelength. A molecular chromophore, which would also dictate the upper limit of the observed excited state average time constant, could then be selected on the basis of its T_1 level and ΔE considerations. It is important to note that temperature is clearly feasible as a final fine-tuning knob for precise lifetimes, but this is likely impractical. However, we foresee the ability to compensate by instead varying the concentration of the molecular chromophore bound on the nanomaterial surface. This

would function in an analogous sense to the impact of the precise number of appended $^{3}LC^{*}$-bearing moieties in equilibrium with the emissive triplet states observed in the molecular TADPL literature.

2.7 Outlook and Potential Research Directions

One goal in composing this Perspective was to challenge the field to correctly model chromophore surface coverage on specific QDs such as CdSe, resulting in predictable PL time constants as has been done with triplet equilibria in molecules.[34-35, 37-38, 42] With the correct framework in hand, it should be possible to model *a priori* the observed TADPL decay kinetics. As discussed above, this task comprises serious complexity featuring numerous considerations; this includes the nature of the QD and its size, the density of QD surface defects that may have been incorporated during functionalization, the nature of the molecular chromophore(s) used, and the surface linker used that can dramatically affect the electronic coupling, just to name a few.

This Perspective also calls to attention that newly conceived CdSe-based QD-molecular constructs will likely feature thermally activated processes and we encourage all researchers studying TTET across these interfaces to test for this phenomenon. Such observations of TADPL emanating from the QD itself immediately suggests Dexter-like TTET processes are indeed operative and ultrafast transient absorption spectroscopy will no longer be explicitly required for making this assignment. Rather, simple temperature-dependent static PL measurements accessible in most laboratories would enable the direct observation of the rTTET process, which in itself confirms the nature of forward TTET reaction (microscopic reversibility). As there has been growing evidence for "indirect" triplet sensitization mechanisms in select nanomaterials such as PbS,[65, 68-69] the lack of TADPL may confirm that the forward Dexter process is inoperative and other phenomena are likely responsible.[69, 72-73] While bimolecular TTET has been clearly

demonstrated from energized surface anchored molecular acceptors to freely diffusing molecules,[62, 64, 66, 74-75, 86-91] it remains unproven whether QDs can directly engage in collisional TTET. This would represent a significant advance as it would eliminate the need for complex and time-consuming post-synthetic modification of the QDs.

It should be noted that QDs can also sensitize phosphorescence emission from surface appended molecular chromophores.[52, 92] While this phenomenon appears to be general for aromatic hydrocarbons appended to QD surfaces, it remains largely unexplored for all other classes of tethered organic and inorganic molecules as well as whether TTET can be observed between different QDs themselves. Due to their large extinction coefficients, QDs can readily serve as light-harvesting species enabling low concentrations to be used in PL-based detection schemes. This was originally recognized in FRET-based experiments using QD donors and molecular fluorescent acceptors.[93-96] Interestingly, CdSe exhibits characteristics of being an exceptional singlet or triplet energy donor, depending upon the molecular species in which it is partnered. This is akin to metal-to-ligand charge transfer (MLCT) based photosensitizers such as $[Ru(bpy)_3]^{2+}$.[97-100] The admixture of singlet/triplet character enable observations of both efficient FRET and TTET from the MLCT excited state.[34-35, 39-41, 98, 101-105] This suggests that the photophysical processes occurring in QDs echo those in molecular based photosensitizers and they can be envisioned in the same manner. For example, it was recently shown that CdSe QDs were able to triplet sensitize [2+2] cycloaddition chemistry in a variety of surface-bound organic substrates.[106] This illustrates how QDs can be reimagined for applications in photochemistry by using their molecular-like photophysical properties to sensitize reactions, such as photoredox processes.[16-18, 107-109] Finally, the size-dependent absorption and PL properties inherent in QDs could be exploited for evaluating

the tenet of spin conservation (conservation of angular momentum) in dipolar (Förster) energy transfer reactions of QDs with molecular acceptors.[110]

2.8 Conclusions

Blending chromophores with vastly different excited state properties into a single molecule can yield equilibrium-controlled excited state processes that can be conceptualized as a superposition of their individual properties. Continued development of these multi-chromophores led to numerous molecular designs targeted at a suite of both fundamental and applied topical areas including light emission, photoredox catalysis, PL sensing, solar energy conversion, and excited state decay engineering. Building on these advances, the introduction of semiconductor QDs as a class of chromophores poised for integration into thermally activated excited state composites has opened a vast parameter space for future investigation. The dream of an expansive assembly of synthetically

Chapter 2 Acknowledgments

Many thanks are offered to Dr. Samuel G. Shepard at NC State University for insightful discussions on methods to mathematically model multiple excited states with intrinsic rate constants. This work was supported by the U.S. Department of Energy, Office of Science, Office of Basic Energy Sciences, under Award No. DE-SC0011979 and the Organic Materials Chemistry program in the Air Force Office of Scientific Research (FA9550-18-1-0331). I'd also like to thank Christopher M. Papa, Cedric Mongin and Felix N. Castellano for their co-authorship.

Chapter 2 References:

1. Parker, C. A., *Photoluminescence of Solutions*. Elsevier Publishing Company: Amsterdam, New York, 1968; p 544.
2. Turro, N. J., *Modern Molecular Photochemistry*. 1991.
3. IUPAC, Compendium of Chemical Terminology. In *the "Gold Book"* [Online] 2nd ed.; A. D. McNaught, A. W., Ed. Blackwell Scientific Publications: Oxford, 1997.
4. El-Sayed, M. A., Origin of the Phosphorescence Radiation in Aromatic Hydrocarbons. **1963,** *197* (4866), 481-482.
5. Castellano, F. N., Altering Molecular Photophysics by Merging Organic and Inorganic Chromophores. *Accounts Chem. Res.* **2015,** *48* (3), 828-839.
6. Lakowicz, J. R., Emerging Biomedical Applications of Time-Resolved Fluorescence Spectroscopy. In *Topics in Fluorescence Spectroscopy: Probe Design and Chemical Sensing*, Lakowicz, J. R., Ed. Springer US: Boston, MA, 1994; pp 1-19.
7. Szmacinski, H.; Lakowicz, J. R., Fluorescence lifetime-based sensing and imaging. *Sensors and Actuators B: Chemical* **1995,** *29* (1), 16-24.
8. de Silva, A. P.; Gunaratne, H. Q. N.; Gunnlaugsson, T.; Huxley, A. J. M.; McCoy, C. P.; Rademacher, J. T.; Rice, T. E., Signaling Recognition Events with Fluorescent Sensors and Switches. *Chemical Reviews* **1997,** *97* (5), 1515-1566.
9. Beer, P. D., Transition-Metal Receptor Systems for the Selective Recognition and Sensing of Anionic Guest Species. *Accounts Chem. Res.* **1998,** *31* (2), 71-80.
10. Castellano, F. N.; Lakowicz, J. R., A Water-Soluble Luminescence Oxygen Sensor. *Photochemistry and Photobiology* **1998,** *67* (2), 179-183.
11. Lakowicz, J. R.; Castellano, F. N.; Dattelbaum, J. D.; Tolosa, L.; Rao, G.; Gryczynski, I., Low-Frequency Modulation Sensors Using Nanosecond Fluorophores. *Analytical Chemistry* **1998,** *70* (24), 5115-5121.
12. Slone, R. V.; Benkstein, K. D.; Bélanger, S.; Hupp, J. T.; Guzei, I. A.; Rheingold, A. L., Luminescent transition-metal-containing cyclophanes ("molecular squares"): covalent self-assembly, host-guest studies and preliminary nanoporous materials applications. *Coordination Chemistry Reviews* **1998,** *171*, 221-243.
13. Lakowicz, J. R., *Principles of Fluorescence Spectroscopy*. 2 ed.; Springer US: New York, 1999.
14. Sun, S.-S.; Lees, A. J., Anion recognition through hydrogen bonding: a simple, yet highly sensitive, luminescent metal-complex receptor. *Chemical Communications* **2000,** (17), 1687-1688.
15. Demas, J. N.; DeGraff, B. A., Applications of luminescent transition platinum group metal complexes to sensor technology and molecular probes. *Coordination Chemistry Reviews* **2001,** *211* (1), 317-351.

16. Pan, Q.; Freitag, L.; Kowacs, T.; Falgenhauer, J. C.; Korterik, J. P.; Schlettwein, D.; Browne, W. R.; Pryce, M. T.; Rau, S.; González, L.; Vos, J. G.; Huijser, A., Peripheral ligands as electron storage reservoirs and their role in enhancement of photocatalytic hydrogen generation. *Chemical Communications* **2016,** *52* (60), 9371-9374.

17. Arias-Rotondo, D. M.; McCusker, J. K., The photophysics of photoredox catalysis: a roadmap for catalyst design. *Chemical Society Reviews* **2016,** *45* (21), 5803-5820.

18. Prier, C. K.; Rankic, D. A.; MacMillan, D. W. C., Visible Light Photoredox Catalysis with Transition Metal Complexes: Applications in Organic Synthesis. *Chemical Reviews* **2013,** *113*, 5322-5363.

19. Singh-Rachford, T. N.; Castellano, F. N., Photon upconversion based on sensitized triplet-triplet annihilation. *Coordination Chemistry Reviews* **2010,** *254* (21-22), 2560-2573.

20. Uoyama, H.; Goushi, K.; Shizu, K.; Nomura, H.; Adachi, C., Highly efficient organic light-emitting diodes from delayed fluorescence. *Nature* **2012,** *492* (7428), 234-+.

21. Kabe, R.; Adachi, C., Organic long persistent luminescence. *Nature* **2017,** *550*, 384.

22. Lewis, G. N.; Lipkin, D.; Magel, T. T., Reversible photochemical processes in rigid media. A study of the phosphorescent state. *Journal of the American Chemical Society* **1941,** *63*, 3005-3018.

23. Deaton, J. C.; Switalski, S. C.; Kondakov, D. Y.; Young, R. H.; Pawlik, T. D.; Giesen, D. J.; Harkins, S. B.; Miller, A. J. M.; Mickenberg, S. F.; Peters, J. C., E-Type Delayed Fluorescence of a Phosphine-Supported Cu2(μ-NAr2)2 Diamond Core: Harvesting Singlet and Triplet Excitons in OLEDs. *Journal of the American Chemical Society* **2010,** *132* (27), 9499-9508.

24. Balzani, V. C., Paola; Juris, Alberto, *Photochemistry and Photophysics Concepts, Research, Applications*. Wiley-VCH: Weinheim, Germany, 2014; p 472.

25. Parker, C. A.; Hatchard, C. G., Triplet-Singlet Emission in Fluid Solutions - Phosphorescence of Eosin. *Transactions of the Faraday Society* **1961,** *57* (11), 1894-&.

26. Yersin, H.; Rausch, A. F.; Czerwieniec, R.; Hofbeck, T.; Fischer, T., The triplet state of organo-transition metal compounds. Triplet harvesting and singlet harvesting for efficient OLEDs. *Coordination Chemistry Reviews* **2011,** *255* (21-22), 2622-2652.

27. Parker, C. A., *Advances in Photochemistry*. Interscience Publishers: New York, New York, 1964.

28. Steinegger, A.; Klimant, I.; Borisov, S. M., Purely Organic Dyes with Thermally Activated Delayed FluorescenceA Versatile Class of Indicators for Optical Temperature Sensing. *Adv. Opt. Mater.* **2017,** *5* (18), 13.

29. Chen, H.-W.; Lee, J.-H.; Lin, B.-Y.; Chen, S.; Wu, S.-T., Liquid crystal display and organic light-emitting diode display: present status and future perspectives. *Light: Science &Amp; Applications* **2018,** *7*, 17168.

30. Fernando, B. D.; Thomas, J. P.; Andrew, P. M., Photophysics of thermally activated delayed fluorescence molecules. *Methods and Applications in Fluorescence* **2017,** *5* (1), 012001.

31. Baleizão, C.; Berberan-Santos, M. N., Thermally activated delayed fluorescence as a cycling process between excited singlet and triplet states: Application to the fullerenes. **2007,** *126* (20), 204510.

32. Ford, W. E.; Rodgers, M. A. J., Reversible Triplet Triplet Energy-Transfer Within a Covalently Linked Bichromophoric Molecule. *J. Phys. Chem.* **1992,** *96* (7), 2917-2920.

33. Harriman, A.; Hissler, M.; Khatyr, A.; Ziessel, R., A ruthenium(II) tris(2,2 '-bipyridine) derivative possessing a triplet lifetime of 42 mu s. *Chemical Communications* **1999,** (8), 735-736.

34. Tyson, D. S.; Castellano, F. N., Intramolecular singlet and triplet energy transfer in a ruthenium(II) diimine complex containing multiple pyrenyl chromophores. *J. Phys. Chem. A* **1999,** *103* (50), 10955-10960.

35. Tyson, D. S.; Henbest, K. B.; Bialecki, J.; Castellano, F. N., Excited state processes in ruthenium(II)/pyrenyl complexes displaying extended lifetimes. *J. Phys. Chem. A* **2001,** *105* (35), 8154-8161.

36. Goze, C.; Kozlov, D. V.; Castellano, F. N.; Suffert, J.; Ziessel, R., Synthesis of bipyridine and terpyridine based ruthenium metallosynthons for grafting of multiple pyrene auxiliaries. *Tetrahedron Letters* **2003,** *44* (48), 8713-8716.

37. Simon, J. A.; Curry, S. L.; Schmehl, R. H.; Schatz, T. R.; Piotrowiak, P.; Jin, X.; Thummel, R. P., Intramolecular Electronic Energy Transfer in Ruthenium(II) Diimine Donor/Pyrene Acceptor Complexes Linked by a Single C−C Bond. *Journal of the American Chemical Society* **1997,** *119* (45), 11012-11022.

38. Del, G.; Leroy, S.; Fages, F.; Schmehl, R. H., Photophysics of Re(I) and Ru(II) Diimine Complexes Covalently Linked to Pyrene: Contributions from Intra-Ligand Charge Transfer States. *Inorganic Chemistry* **2002,** *41* (2), 359-366.

39. Tyson, D. S.; Bialecki, J.; Castellano, F. N., Ruthenium(II) complex with a notably long excited state lifetime. *Chemical Communications* **2000,** (23), 2355-2356.

40. Tyson, D. S.; Luman, C. R.; Zhou, X. L.; Castellano, F. N., New Ru(II) chromophores with extended excited-state lifetimes. *Inorganic Chemistry* **2001,** *40* (16), 4063-4071.

41. Goze, C.; Kozlov, D. V.; Tyson, D. S.; Ziessel, R.; Castellano, F. N., Synthesis and photophysics of ruthenium(II) complexes with multiple pyrenylethynylene subunits. *New Journal of Chemistry* **2003,** *27* (12), 1679-1683.

42. McClenaghan, N. D.; Barigelletti, F.; Maubert, B.; Campagna, S., Towards ruthenium(II) polypyridine complexes with prolonged and predetermined excited state lifetimes. *Chemical Communications* **2002,** (6), 602-603.

43. McClenaghan, N. D.; Leydet, Y.; Maubert, B.; Indelli, M. T.; Campagna, S., Excited-state equilibration: a process leading to long-lived metal-to-ligand charge transfer luminescence

in supramolecular systems. *Coordination Chemistry Reviews* **2005,** *249* (13-14), 1336-1350.

44. Yersin, H.; Czerwieniec, R.; Shafikov, M. Z.; Suleymanova, A. F., TADF Material Design: Photophysical Background and Case Studies Focusing on Cu-I and Ag-I Complexes. *Chemphyschem* **2017,** *18* (24), 3508-3535.

45. McCusker, C. E.; Chakraborty, A.; Castellanet, F. N., Excited State Equilibrium Induced Lifetime Extension in a Dinuclear Platinum(II) Complex. *J. Phys. Chem. A* **2014,** *118* (45), 10391-10399.

46. Yarnell, J. E.; Deaton, J. C.; McCusker, C. E.; Castellano, F. N., Bidirectional "Ping-Pong" Energy Transfer and 3000-Fold Lifetime Enhancement in a Re(I) Charge Transfer Complex. *Inorganic Chemistry* **2011,** *50* (16), 7820-7830.

47. Shafikov, M. Z.; Suleymanova, A. F.; Schinabeck, A.; Yersin, H., Dinuclear Ag(I) Complex Designed for Highly Efficient Thermally Activated Delayed Fluorescence. *The Journal of Physical Chemistry Letters* **2018,** *9* (4), 702-709.

48. Hauke, C. E.; Oldacre, A. N.; Fulong, C. R. P.; Friedman, A. E.; Cook, T. R., Coordination-Driven Self-Assembly of Ruthenium Polypyridyl Nodes Resulting in Emergent Photophysical and Electrochemical Properties. *Inorganic Chemistry* **2018,** *57* (7), 3587-3595.

49. Denisov, S. A.; Cudré, Y.; Verwilst, P.; Jonusauskas, G.; Marín-Suárez, M.; Fernández-Sánchez, J. F.; Baranoff, E.; McClenaghan, N. D., Direct Observation of Reversible Electronic Energy Transfer Involving an Iridium Center. *Inorganic Chemistry* **2014,** *53* (5), 2677-2682.

50. Yarnell, J. E.; McCusker, C. E.; Leeds, A. J.; Breaux, J. M.; Castellano, F. N., Exposing the Excited-State Equilibrium in an IrIII Bichromophore: A Combined Time Resolved Spectroscopy and Computational Study. **2016**, 1808-1818.

51. Schmehl, R., Something New in Transition Metal Complex Sensitizers: Bringing Metal Diimine Complexes and Aromatic Hydrocarbons Together. *The Spectrum* **2000,** *13* (2).

52. Mongin, C.; Moroz, P.; Zamkov, M.; Castellano, F. N., Thermally activated delayed photoluminescence from pyrenyl-functionalized CdSe quantum dots. *Nature Chemistry* **2018,** *10* (2), 225-230.

53. La Rosa, M.; Denisov, S. A.; Jonusauskas, G.; McClenaghan, N. D.; Credi, A., Designed Long-Lived Emission from CdSe Quantum Dots through Reversible Electronic Energy Transfer with a Surface-Bound Chromophore. *Angewandte Chemie-International Edition* **2018,** *57* (12), 3104-3107.

54. Scholes, G. D., Controlling the Optical Properties of Inorganic Nanoparticles. **2008,** *18* (8), 1157-1172.

55. Smith, A. M.; Nie, S. M., Semiconductor Nanocrystals: Structure, Properties, and Band Gap Engineering. *Accounts Chem. Res.* **2010,** *43* (2), 190-200.

56. Jasieniak, J.; Smith, L.; van Embden, J.; Mulvaney, P.; Califano, M., Re-examination of the Size-Dependent Absorption Properties of CdSe Quantum Dots. *The Journal of Physical Chemistry C* **2009,** *113* (45), 19468-19474.

57. Yu, W. W.; Qu, L.; Guo, W.; Peng, X., Experimental Determination of the Extinction Coefficient of CdTe, CdSe, and CdS Nanocrystals. *Chemistry of Materials* **2003,** *15* (14), 2854-2860.

58. Wang, C.; Dong, H.; Jiang, L.; Hu, W., Organic semiconductor crystals. *Chemical Society Reviews* **2018,** *47* (2), 422-500.

59. Garakyaraghi, S.; Castellano, F. N., Nanocrystals for Triplet Sensitization: Molecular Behavior from Quantum-Confined Materials. *Inorganic Chemistry* **2018,** *57* (5), 2351-2359.

60. Tabachnyk, M.; Ehrler, B.; Gélinas, S.; Böhm, M. L.; Walker, B. J.; Musselman, K. P.; Greenham, N. C.; Friend, R. H.; Rao, A., Resonant energy transfer of triplet excitons from pentacene to PbSe nanocrystals. *Nature Materials* **2014,** *13*, 1033.

61. Thompson, N. J.; Wilson, M. W. B.; Congreve, D. N.; Brown, P. R.; Scherer, J. M.; Bischof, Thomas S.; Wu, M.; Geva, N.; Welborn, M.; Voorhis, T. V.; Bulović, V.; Bawendi, M. G.; Baldo, Marc A., Energy harvesting of non-emissive triplet excitons in tetracene by emissive PbS nanocrystals. *Nature Materials* **2014,** *13*, 1039.

62. Mongin, C.; Garakyaraghi, S.; Razgoniaeva, N.; Zamkov, M.; Castellano, F. N., Direct observation of triplet energy transfer from semiconductor nanocrystals. **2016,** *351* (6271), 369-372.

63. Xu, Z. H.; Jin, T.; Huang, Y. M.; Mulla, K.; Evangelista, F. A.; Egap, E.; Lian, T. Q., Direct triplet sensitization of oligothiophene by quantum dots. *Chem. Sci.* **2019,** *10* (24), 6120-6124.

64. De Roo, J.; Huang, Z.; Schuster, N. J.; Hamachi, L. S.; Congreve, D. N.; Xu, Z.; Xia, P.; Fishman, D. A.; Lian, T.; Owen, J. S.; Tang, M. L., Anthracene Diphosphate Ligands for CdSe Quantum Dots; Molecular Design for Efficient Upconversion. *Chemistry of Materials* **2020,** *32* (4), 1461-1466.

65. Garakyaraghi, S.; Mongin, C.; Granger, D. B.; Anthony, J. E.; Castellano, F. N., Delayed Molecular Triplet Generation from Energized Lead Sulfide Quantum Dots. *Journal of Physical Chemistry Letters* **2017,** *8* (7), 1458-1463.

66. Huang, Z.; Xu, Z.; Mahboub, M.; Li, X.; Taylor, J. W.; Harman, W. H.; Lian, T.; Tang, M. L., PbS/CdS Core–Shell Quantum Dots Suppress Charge Transfer and Enhance Triplet Transfer. *Angewandte Chemie International Edition* **2017,** *56* (52), 16583-16587.

67. Kroupa, D. M.; Arias, D. H.; Blackburn, J. L.; Carroll, G. M.; Granger, D. B.; Anthony, J. E.; Beard, M. C.; Johnson, J. C., Control of Energy Flow Dynamics between Tetracene Ligands and PbS Quantum Dots by Size Tuning and Ligand Coverage. *Nano Letters* **2018,** *18*, 865-873.

68. Bender, J. A.; Raulerson, E. K.; Li, X.; Goldzak, T.; Xia, P.; Van Voorhis, T.; Tang, M. L.; Roberts, S. T., Surface States Mediate Triplet Energy Transfer in Nanocrystal–Acene Composite Systems. *Journal of the American Chemical Society* **2018,** *140*, 7543-7553.

69. Papa, C. M.; Garakyaraghi, S.; Granger, D. B.; Anthony, J. E.; Castellano, F. N., TIPS-pentacene triplet exciton generation on PbS quantum dots results from indirect sensitization. *Chemical Science* **2020**.

70. Luo, X.; Lai, R. C.; Li, Y. L.; Han, Y. Y.; Liang, G. J.; Liu, X.; Ding, T.; Wang, J. H.; Wu, K. F., Triplet Energy Transfer from CsPbBr3 Nanocrystals Enabled by Quantum Confinement. *Journal of the American Chemical Society* **2019,** *141* (10), 4186-4190.

71. Han, Y. Y.; Luo, X.; Lai, R. C.; Li, Y. L.; Liang, G. J.; Wu, K. F., Visible-Light-Driven Sensitization of Naphthalene Triplets Using Quantum-Confined CsPbBr3 Nanocrystals. *Journal of Physical Chemistry Letters* **2019,** *10* (7), 1457-1463.

72. Luo, X.; Liang, G. J.; Wang, J. H.; Liu, X.; Wu, K. F., Picosecond multi-hole transfer and microsecond charge-separated states at the perovskite nanocrystal/tetracene interface. *Chemical Science* **2019,** *10* (8), 2459-2464.

73. Luo, X.; Han, Y.; Chen, Z.; Li, Y.; Liang, G.; Liu, X.; Ding, T.; Nie, C.; Wang, M.; Castellano, F. N.; Wu, K., Mechanisms of triplet energy transfer across the inorganic nanocrystal/organic molecule interface. *Nature Communications* **2020,** *11*, 28.

74. Xia, P.; Raulerson, E. K.; Coleman, D.; Gerke, C. S.; Mangolini, L.; Tang, M. L.; Roberts, S. T., Achieving spin-triplet exciton transfer between silicon and molecular acceptors for photon upconversion. *Nature Chemistry* **2020,** *12* (2), 137-144.

75. Han, Y.; He, S.; Luo, X.; Li, Y.; Chen, Z.; Kang, W.; Wang, X.; Wu, K., Triplet Sensitization by "Self-Trapped" Excitons of Nontoxic CuInS2 Nanocrystals for Efficient Photon Upconversion. *Journal of the American Chemical Society* **2019,** *141* (33), 13033-13037.

76. Soloviev, V. N.; Eichhöfer, A.; Fenske, D.; Banin, U., Size-Dependent Optical Spectroscopy of a Homologous Series of CdSe Cluster Molecules. *Journal of the American Chemical Society* **2001,** *123* (10), 2354-2364.

77. Jones, M.; Lo, S. S.; Scholes, G. D., Signatures of Exciton Dynamics and Carrier Trapping in the Time-Resolved Photoluminescence of Colloidal CdSe Nanocrystals. *The Journal of Physical Chemistry C* **2009,** *113* (43), 18632-18642.

78. Jones, M.; Scholes, G. D., On the use of time-resolved photoluminescence as a probe of nanocrystal photoexcitation dynamics. *Journal of Materials Chemistry* **2010,** *20* (18), 3533-3538.

79. Nirmal, M.; Norris, D. J.; Kuno, M.; Bawendi, M. G.; Efros, A. L.; Rosen, M., Observation of the "Dark Exciton" in CdSe Quantum Dots. *Physical Review Letters* **1995,** *75* (20), 3728-3731.

80. Morris-Cohen, A. J.; Donakowski, M. D.; Knowles, K. E.; Weiss, E. A., The Effect of a Common Purification Procedure on the Chemical Composition of the Surfaces of CdSe

Quantum Dots Synthesized with Trioctylphosphine Oxide. *The Journal of Physical Chemistry C* **2010,** *114* (2), 897-906.

81. Mooney, J.; Krause, M. M.; Saari, J. I.; Kambhampati, P., Challenge to the deep-trap model of the surface in semiconductor nanocrystals. *Physical Review B* **2013,** *87* (8), 081201.

82. Kambhampati, P., On the kinetics and thermodynamics of excitons at the surface of semiconductor nanocrystals: Are there surface excitons? *Chemical Physics* **2015,** *446*, 92-107.

83. Murphy, C. J.; Buriak, J. M., Best Practices for the Reporting of Colloidal Inorganic Nanomaterials. *Chemistry of Materials* **2015,** *27* (14), 4911-4913.

84. Kirchhoff, J. R.; Gamache, R. E.; Blaskie, M. W.; Delpaggio, A. A.; Lengel, R. K.; McMillin, D. R., Temperature-Dependence of Luminescence from Cu(NN)2+ Systems in Fluid Solution - Evidence for the Participation of 2 Excited-States. *Inorganic Chemistry* **1983,** *22*, 2380-2384.

85. Valerini, D.; Creti, A.; Lomascolo, M.; Manna, L.; Cingolani, R.; Anni, M., Temperature dependence of the photoluminescence properties of colloidal CdSe/ZnS core/shell quantum dots embedded in a polystyrene matrix. *Physical Review B* **2005,** *71* (23).

86. Huang, Z.; Li, X.; Mahboub, M.; Hanson, K. M.; Nichols, V. M.; Le, H.; Tang, M. L.; Bardeen, C. J., Hybrid Molecule-Nanocrystal Photon Upconversion Across the Visible and Near-Infrared. *Nano Letters* **2015,** *15* (8), 5552-5557.

87. Mahboub, M.; Huang, Z. Y.; Tang, M. L., Efficient Infrared-to-Visible Upconversion with Subsolar Irradiance. *Nano Letters* **2016,** *16* (11), 7169-7175.

88. Okumura, K.; Mase, K.; Yanai, N.; Kimizuka, N., Employing Core-Shell Quantum Dots as Triplet Sensitizers for Photon Upconversion. *Chemistry-a European Journal* **2016,** *22* (23), 7721-7726.

89. Mase, K.; Okumura, K.; Yanai, N.; Kimizuka, N., Triplet sensitization by perovskite nanocrystals for photon upconversion. *Chemical Communications* **2017,** *53* (59), 8261-8264.

90. He, S.; Luo, X.; Liu, X.; Li, Y.; Wu, K., Visible-to-Ultraviolet Upconversion Efficiency above 10% Sensitized by Quantum-Confined Perovskite Nanocrystals. *The Journal of Physical Chemistry Letters* **2019,** *10* (17), 5036-5040.

91. VanOrman, Z. A.; Bieber, A. S.; Wieghold, S.; Nienhaus, L., Green-to-Blue Triplet Fusion Upconversion Sensitized by Anisotropic CdSe Nanoplatelets. *Chemistry of Materials* **2020**.

92. Cossairt, B. M.; Juhas, P.; Billinge, S. J. L.; Owen, J. S., Tuning the Surface Structure and Optical Properties of CdSe Clusters Using Coordination Chemistry. *The Journal of Physical Chemistry Letters* **2011,** *2* (24), 3075-3080.

93. Kloepfer, J. A.; Cohen, N.; Nadeau, J. L., FRET between CdSe Quantum Dots in Lipid Vesicles and Water- and Lipid-soluble Dyes. *The Journal of Physical Chemistry B* **2004,** *108* (44), 17042-17049.

94. Clapp, A. R.; Medintz, I. L.; Mattoussi, H., Förster Resonance Energy Transfer Investigations Using Quantum-Dot Fluorophores. *ChemPhysChem* **2006,** *7* (1), 47-57.

95. Bae, S. H.; Yoo, S. I.; Bae, W. K.; Lee, S.; Lee, J.-K.; Sohn, B.-H., Single-Layered Films of Diblock Copolymer Micelles Containing Quantum Dots and Fluorescent Dyes and Their Fluorescence Resonance Energy Transfer. *Chemistry of Materials* **2008,** *20* (13), 4185-4187.

96. Shi, J.; Tian, F.; Lyu, J.; Yang, M., Nanoparticle based fluorescence resonance energy transfer (FRET) for biosensing applications. *Journal of Materials Chemistry B* **2015,** *3* (35), 6989-7005.

97. Navon, G.; Sutin, N., Mechanism of the quenching of the phosphorescence of tris(2,2'-bipyridine)ruthenium(II) by some cobalt(III) and ruthenium(III) complexes. *Inorganic Chemistry* **1974,** *13* (9), 2159-2164.

98. Kober, E. M.; Meyer, T. J., Concerning the absorption spectra of the ions M(bpy)32+ (M = Fe, Ru, Os; bpy = 2,2'-bipyridine). *Inorganic Chemistry* **1982,** *21* (11), 3967-3977.

99. Bhasikuttan, A. C.; Suzuki, M.; Nakashima, S.; Okada, T., Ultrafast Fluorescence Detection in Tris(2,2‘-bipyridine)ruthenium(II) Complex in Solution: Relaxation Dynamics Involving Higher Excited States. *Journal of the American Chemical Society* **2002,** *124* (28), 8398-8405.

100. Gawelda, W.; Johnson, M.; de Groot, F. M. F.; Abela, R.; Bressler, C.; Chergui, M., Electronic and Molecular Structure of Photoexcited [RuII(bpy)3]2+ Probed by Picosecond X-ray Absorption Spectroscopy. *Journal of the American Chemical Society* **2006,** *128* (15), 5001-5009.

101. Mandal, K.; Pearson, T. D. L.; Demas, J. N., Singlet energy transfer from the charge transfer excited state of tris (2,2′-bipyridine) ruthenium (II). *The Journal of Chemical Physics* **1980,** *73* (5), 2507-2509.

102. Mandal, K.; Demas, J. N., Surfactant-enhanced singlet energy transfer from the charge-transfer excited state of tris(2,2-bipyridine) ruthenium(II). *Chem. Phys. Lett.* **1981,** *84* (2), 410-414.

103. Luman, C. R.; Castellano, F. N., Lengthening of Fluorescence Lifetimes in Self-organized Metal–Organic Assemblies ¶. *Photochem. Photobiol.* **2003,** *77* (5), 510-514.

104. Wilson, G. J.; Launikonis, A.; Sasse, W. H. F.; Mau, A. W. H., Excited-State Processes in Ruthenium(II) Bipyridine Complexes Containing Covalently Bound Arenes. *The Journal of Physical Chemistry A* **1997,** *101* (27), 4860-4866.

105. Thompson, D. W.; Ito, A.; Meyer, T. J., [Ru(bpy)3]2+* and other remarkable metal-to-ligand charge transfer (MLCT) excited states. **2013,** *85* (7), 1257.

106. Jiang, Y.; Wang, C.; Rogers, C. R.; Kodaimati, M. S.; Weiss, E. A., Regio- and diastereoselective intermolecular [2+2] cycloadditions photocatalysed by quantum dots. **2019,** *11* (11), 1034-1040.

107. Caputo, J. A.; Frenette, L. C.; Zhao, N.; Sowers, K. L.; Krauss, T. D.; Weix, D. J., General and Efficient C–C Bond Forming Photoredox Catalysis with Semiconductor Quantum Dots. *Journal of the American Chemical Society* **2017,** *139*, 4250-4253.

108. Zhang, Z.; Edme, K.; Lian, S.; Weiss, E. A., Enhancing the Rate of Quantum-Dot-Photocatalyzed Carbon–Carbon Coupling by Tuning the Composition of the Dot's Ligand Shell. *J. Am. Chem. Soc.* **2017,** *139* (12), 4246-4249.

109. Zhu, X.; Lin, Y.; Sun, Y.; Beard, M. C.; Yan, Y., Lead-Halide Perovskites for Photocatalytic α-Alkylation of Aldehydes. *J. Am. Chem. Soc.* **2019,** *141* (2), 733-738.

110. Guo, D.; Knight, T. E.; McCusker, J. K., Angular Momentum Conservation in Dipolar Energy Transfer. *Science* **2011,** *334* (6063), 1684.

Chapter 3: Controlling Thermally Activated Delayed Photoluminescence in CdSe Quantum Dots through Triplet Acceptor Surface Coverage

This chapter has been previously published: *J. Phys. Chem. Lett.* **2021**, *12*, 3718–3723. DOI: 10.1021/acs.jpclett.1c00746

Abstract: Quantum−dot/molecule composites (QD/mol) have demonstrated useful photochemical properties for many photonic and optoelectronic applications, however, a comprehensive understanding of these materials remains elusive. This work introduces a series of cadmium(II) selenide/1-pyrenecarboxylic acid (CdSe/PCA) nanomaterials featuring bespoke PCA surface coverage on CdSe585 (coded by the peak of the first exciton absorption band) to glean insight into the QD/mol photophysical behavior. Tailoring the energy gap between the CdSe585 first exciton band (2.1 eV) and the lowest PCA triplet level (T_1 = 2.0 eV) to be nearly isoenergetic, strong thermally activated delayed photoluminescence (TADPL) is observed resulting from reverse triplet-triplet energy transfer. The resultant average decay time constant (τ_{obs}) of the photoluminescence emanating from CdSe585 is deterministically controlled with surface-bound PCA_n chromophores (n = average number of adsorbed PCA molecules) by shifting the triplet excited state equilibrium from the CdSe585 to the PCA molecular triplet reservoir as a function of n.

3.1 Introduction

The scientific community has invested considerable recent effort into the development of quantum dot-molecule composites (QD/mol) that leverage valuable properties engendered within each component.[1–14] These constructs merge highly tunable, strongly absorbing, and easy to synthesize semiconducting QDs with well-established molecular chromophores to exploit interfacial photo-induced energy transfer (EnT) reactions through the bespoke characteristics of both the molecule and the QD. Several examples of these molecularly modified nanomaterials have been reported for executing triplet sensitization chemistry, excited state lifetime extension, photochemical upconversion, as well as photocatalysis.[2–5,8,11,13–19] In each instance, the EnT reactions occurring between the QDs and appended molecules enable their photo-functionality. QD/mol cooperativity therefore represents a means to preparing highly modular photochemically-active systems poised to meet numerous application-specific demands.[20,21] Despite the potential utility of these materials, detailed understanding of their excited state reaction dynamics has remained somewhat elusive, particularly in comparison to their purely molecular counterparts.[2,13,18,19,22–40]

Among the remaining questions to QD/mol systems is the effect of molecular acceptor concentration/surface coverage on the resultant photophysical properties. Multiple studies have identified that the surface molecule concentration changes as a function of QD size, including those that have analyzed surface coverage in a more quantitative manner, however, the role of surface coverage remains incomplete.[3,4,6,8,11–14,17,41] In a recent Perspective, we postulated that *a priori* determination of excited state dynamics should be possible using a derived Boltzmann model for thermally activated delayed photoluminescence (TADPL)-active QD/mols.[42] To do so, however, requires precise control over the surface environment of the nanomaterials, which is

challenging to achieve in a reproducible manner. The present study specifically addresses this question regarding the influence of molecular acceptor surface concentration, revealing deterministic photophysical behavior akin to what has been observed in purely molecular-based triplet-triplet equilibria.

3.2 Identifying Effects of nPCA on CdSe

Previous reports have demonstrated that QD/mols using CdSe nanocrystals featuring triplet energy gaps smaller ~ < 0.4 eV display TADPL.[5,14] When the QD/mol triplet states become nearly isoenergetic, strong TADPL was observed, however, the lifetime extension becomes minimized as the thermal activation at RT readily accesses the upper (QD) triplet emitting state, efficiently quenching the lower molecular triplet.[5,14,42] In this contribution, we selected a single CdSe QD material having a bandgap energy centered at 585 nm (2.1 eV) in concert with surface-anchored 1-pyrenecarboxylic acid (PCA) having a triplet energy of 2.0 eV, yielding an energy gap of ~0.1 eV. By regulating the number of PCA molecules resident on the CdSe QD's surface, we expand upon previous work by providing a means to manipulate TADPL time constants in instances where reverse EnT becomes facile. Specifically, the average TADPL decay time constant (τ_{TADPL}) observed from the QD is predictably extended in CdSe585 by each additional bound PCA molecule (n) by ~160 ns until the process saturates when n = 27.

The CdSe585 QDs were synthesized using an adapted literature procedure and screened for selected photophysical properties as described in Experimental sections S3.1 – S3.3 of the Chapter 3 Supporting Information and **Figure S3.1**.[43] To illustrate the effects of PCA surface concentration on the QD/mol's photophysical properties, ligand exchange was undertaken with a systematic increase of chromophore loading on the QDs as described in Experimental section 4 of the Supporting Information. These materials are coded as CdSe585/PCA_n, where 585 represents

the first exciton band (E_g) in wavelength and n denotes the average number of surface anchored PCA molecules.

Comparison of the pristine as-synthesized CdSe585 to surface-exchanged CdSe585/PCA_n is an important step to ensure the ligand exchange has occurred and to verify that the QD/mol's material integrity has not been compromised. The toluene solution absorbance spectra of the various CdSe585/PCA_n materials indicate that the systematic increase of the PCA band at 341 nm, which is not observed in pristine CdSe585, coincides with PCA surface loading of CdSe585, **Figure 3.1a**. As additional chromophores are added to the surface, no spectral changes were noted in the QD first exciton band when compared to the pristine material. This suggests that the materials retain both their size and quantum confinement properties upon ligand exchange.[20,21] Representative TEM images (**Figures S3.2a and S3.2b**) show no change in the CdSe585 size or shape after ligand exchange, further corroborating the integrity of the CdSe585 is preserved after the ligand exchange chemistry. Representative FT-IR (ATR) spectra, **Figure S3.2c**, indicate the loss of native oleic carboxylates (OA) with the addition of PCA. Control studies using naphthoic acid (NCA) and 5-tetracene carboxylic acid (5TET) with CdSe585 were also performed, whose triplet energies are 2.5 and 1.3 eV, respectively. These surface anchored molecules energetically prohibit any TADPL processes from being observed and surface defects generated on CdSe585 through carboxylate ligand exchange may be directly monitored. Using NCA, no significant changes in the photophysical properties were observed in the final materials, **Figure S3.3a** and **Table S3.1**. In the case of 5TET, **Figure S3.3b**, quenching of the CdSe PL was observed as a function of increasing surface coverage but these materials did not display any TADPL behavior as the energy gap is simply too large (~0.8 eV) to enable any thermal activation at RT. No evidence of any red-shifted PL features emanating from the CdSe were observed in either series of samples

indicating there is no generation of trap states during the ligand exchange process. In addition, the PL band shape is retained for these materials suggesting the CdSe retains its surface stability and monodispersity. We therefore conclude that any surface defects generated through carboxylate ligand exchange are negligible and the intrinsic properties of CdSe remain largely unperturbed from this process, full details are available in Section 6 of the Supporting Information. These results collectively suggest the successful and non-destructive ligand exchange of CdSe585 producing the desired CdSe585/PCA_n materials.

Upon verification of successful ligand exchange chemistry, the absorption features attributed to CdSe585 and PCA leveraged the established extinction coefficients (ε) of their individual components as previously reported.[3,5,14] Subjecting the solution absorbance spectra for CdSe585/PCAn materials to the Beer-Lambert Law, $M_{PCA}/M_{CdSe} = (A_{PCA} \times \varepsilon_{PCA} \times l_{CdSe})/(A_{CdSe} \times \varepsilon_{CdSe} \times l_{PCA})$, yields the average number of PCA adsorbed per QD (n), ranging from 0 – 27 for CdSe585 in this inverstigation.[3,5,14] In quantifying the average number of appended PCA chromophores (n), it was found that n could be controlled through systematic variation of the initial PCA solution loading.

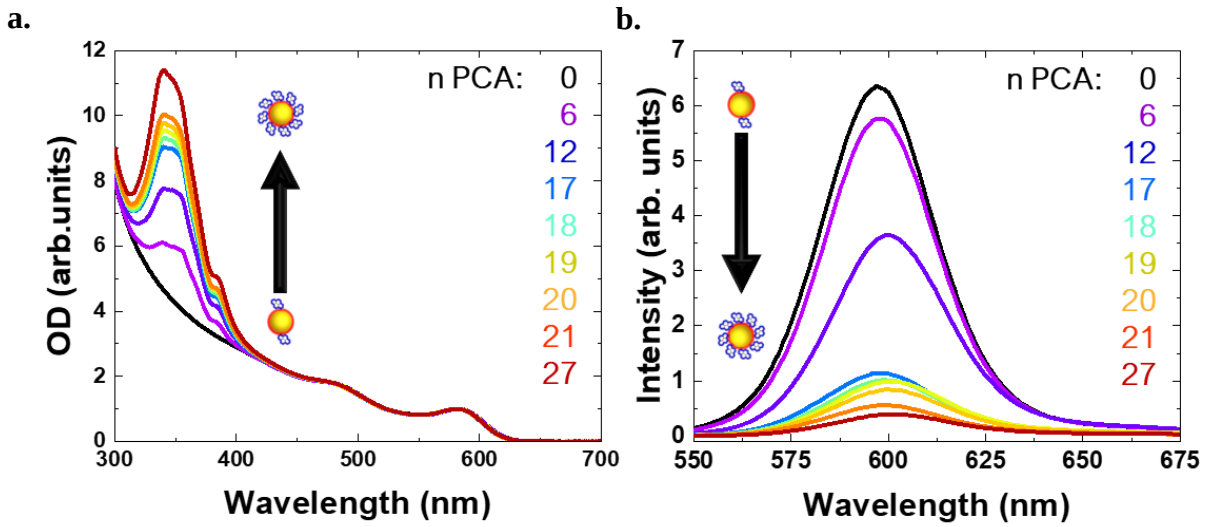

Figure 3.1. Solution UV-vis and photoluminescence spectra of CdSe585/PCA$_n$ composites measured in toluene. **(a)** normalized absorbance and **(b)** steady−state PL spectra measured with 475 nm excitation. Arrows indicate increasing n PCA units on the CdSe585 surface.

Previous studies of CdSe/PCA materials report substantial steady−state photoluminescence (PL) quenching with respect to the pristine CdSe PL signal resulting from efficient triplet-triplet energy transfer.[3,16] Here, quenching of the CdSe585 static PL signal was proportional to n PCA, **Figure 3.1b**, suggesting the rate of EnT indeed changes as a function of increasing n. Additionally, the PL intensity dependence on n also suggests the observed increase of PCA in the absorbance spectra remains correlated to the actual surface number density and not simply a result of freely diffusing PCA molecules in the bulk solution. Information regarding the role of n on CdSe585/PCA$_n$'s dynamics is necessary to establish a clear understanding of the photophysics in these materials. Therefore, more intricate time-resolved spectroscopic techniques were used to determine the underlying photophysics of the CdSe585/PCA$_n$ materials.

Supra-nanosecond time gated emission (TGE) experiments were performed to extract k_{obs} for the various CdSe585/PCA$_n$ materials. An equilibrium between CdSe585 and ^{3}PCA* states is expected as they are nearly isoenergetic. This equilibrium in effect results in PL lifetime extension in the CdSe PL by exploiting the long-lived ^{3}PCA* reservoir that can thermally

resupply the CdSe585 bright state resulting in TADPL.[5,14,27,36,39,40,44] To disentangle the prompt CdSe decay kinetics from the TADPL decay, these experiments were time-gated beyond the pristine CdSe585 native PL intensity decay, see Section 8 of the Supporting Information. As such, the observed average PL time constants gathered from TGE experiments represent solely the TADPL decay processes (τ_{TADPL}). By introducing additional PCA molecules to the surface of the CdSe585, the equilibrium between the two states is entropically shifted toward the long lived ^{3}PCA* resulting in systematic lifetime extension as a function of n, **Table 3.1,** and **Figure 3.2**.

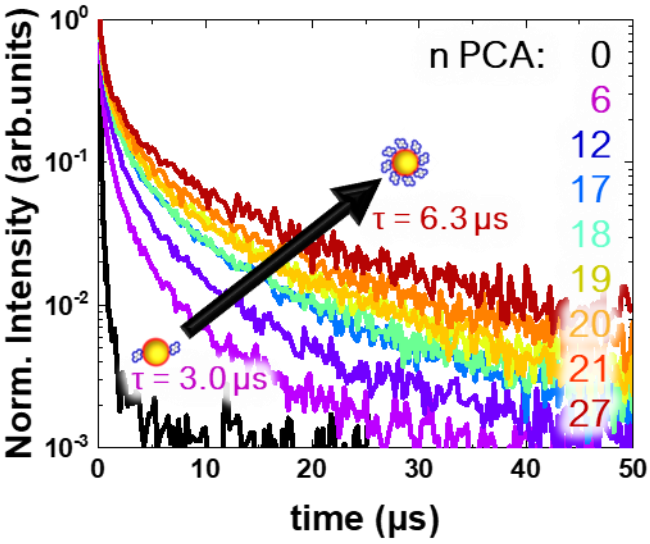

Figure 3.2. Normalized time-resolved PL intensity decay kinetic traces observed in the CdSe585/PCAn series measured in degassed toluene at 293 K following selective excitation (2 mJ, 5-7 ns FWHM) of CdSe at 475 nm. Representative lifetimes calculated using a stretch exponential fit, $I(t) = A \exp(-(t/\tau)^{\beta})$, full details available in Section 7 of the Supporting Information. The arrow indicates both an increase in n PCA units and the corresponding extension of excited state decay.

3.3 Developing a Deterministic Model

Previous reports have utilized a Boltzmann model to deconvolute the underlying contributions responsible for the observed lifetime extension in molecular TADPL systems.[42,45,46]

Using the same Boltzmann model, Eq. 3.1, the entropic change in driving force is determined to be ~1 meV/PCA, as presented in **Figure 3.3a**.

$$k_{obs} = \left[\frac{\left(k_{PCA} + k_{CdSe} \times \exp\left(\frac{-\Delta E}{k_B T} \right) \right)}{\left(1 + \exp\left(\frac{-\Delta E_{g585T}}{k_B T} \right) \right)} \right] \qquad (3.1)$$

In Eq. 3.1, k_{obs} is the observed average rate constant ($1/\langle \tau_{obs} \rangle$), k_{PCA} and k_{CdSe} represent the intrinsic rate constants of the unbound PCA and pristine CdSe585, respectively, and ΔE represents the effective energy gap between the CdSe585 bright state and ^{3}PCA* as a function of surface coverage. Fitting of this data indicates that the change in ΔE is directly proportional to n. This suggests the energy transfer reactions between the two triplet states is perturbed in a systematic fashion resulting in predictable changes in the equilibrium constant. As the triplet equilibrium is responsible for the changes in τ_{TADPL}, the systematic variation revealed in the Boltzmann model hints that a deterministic change related to the PCA surface coverage in these materials is operative.

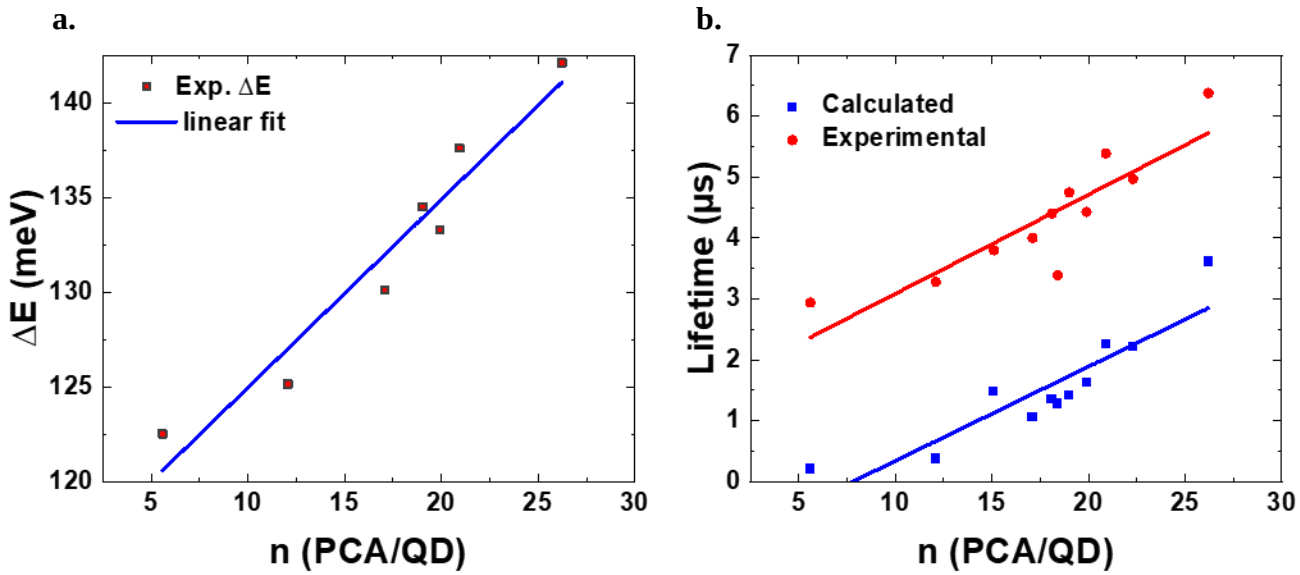

Figure 3.3. Graphical representation of Boltzmann models of **(a)** change in ΔE and **(b)** τ_{TADPL} as a function of n. Linear fitting is represented by solid lines denoting a 1 meV/PCA and ~160 ns/PCA increase in ΔE and τ_{TADPL}, respectively.

We further modeled the current triplet-triplet equilibrium in this system using a derived Boltzmann model, Eq. 3.2, adapted from the thermally activated delayed fluorescence (TADF) work by Ravinson et al.[47]

$$\tau_{TADPL} = \tau_{CdSe} \times K_{eq}^{-1} \qquad (3.2)$$

K_{eq}^{-1} in this equation represents k_{EnT}/k_{rEnT}, the ratio between the forward and reverse EnT reactions respectively, and τ_{CdSe}, the intrinsic lifetime of pristine CdSe585. For Eq. 3.2 to be acceptable, the assumptions $k_{CdSe} >> k_{PCA}$ and k_{rEnT}, $k_{EnT} >> k_{CdSe}$ must be met. Our experimental data combined with established literature values indicate the CdSe585/PCA_n materials are well within these boundary conditions.[5,14] K_{eq} was extracted from static PL measurements, utilizing the TADPL of CdSe585/PCAn with respect to the PL of pristine CdSe585; a full derivation of the K_{eq} calculation is available in Section 8 of the Supporting Information. Results from Eq. 3.2 are reported in **Table 3.1** and **Figure 3.3b**.

Table 3.1. CdSe585/PCA$_n$ tabulated values of n, K_{eq}, calculated lifetime, and experimental average lifetime.

n (PCA/CdSe585)	K_{eq}	Calc. τ_{TADPL} (s)	[a]Exp. $\langle\tau_{TADPL}\rangle$ (s)
0	-----	-----	[b]1.82×10^{-7}
6	0.88	2.08×10^{-7}	2.94×10^{-6}
12	0.49	3.77×10^{-7}	3.28×10^{-6}
17	0.17	1.05×10^{-6}	4.00×10^{-6}
18	0.14	1.28×10^{-6}	3.39×10^{-6}
19	0.13	1.41×10^{-6}	4.75×10^{-6}
20	0.11	1.62×10^{-6}	4.43×10^{-6}
21	0.08	2.26×10^{-6}	5.39×10^{-6}
27	0.05	3.61×10^{-6}	6.38×10^{-6}

[a]Experimental $\langle\tau\rangle$ derived using a stretch exponential fit, $I(t) = A \exp(-(t/\tau)^{\beta})$. [b]Pristine CdSe585 decay time constant derived from the same experiments

3.4 Results and Analysis

Under initial inspection, the calculated values appear to be offset from the experimental values. However, upon closer inspection, the change in lifetime per PCA unit represented by the slope of the calculated lifetime, $\langle m_{Calc}\rangle = 1.59 \pm 0.30 \times 10^{-7}$ s/PCA, and the slope of the experimental lifetime, $\langle m_{Exp}\rangle = 1.64 \pm 0.38 \times 10^{-7}$, are found to be within experimental error of one another, **Figure 3.3b**. The coalescence of these values suggests that the observed PL quenching and lifetime extension for TADPL active CdSe585/PCAn are directed by the triplet acceptor concentration in a similar fashion as observed in complementary TADPL active molecules.[48–50] Additionally, by measuring τ_{TADPL} directly from our TGE experiments, it is possible that our experimental data is artificially elongated as a result of a systematic error induced by the requisite gating of the early time PL signal. However, as this is a systematic error, the trends observed in the experimental data and the conclusions drawn by them remain valid. In this manner, PCA surface concentration is shown to regulate TADPL systematically in CdSe585, allowing for tailored photophysics in QD/mol constructs synonymous to molecular TADPL constructs. Furthermore, the combined results suggest simple static PL measurements may be used to

accurately predict the trend in TADPL lifetimes for QD/mols as a function of PCA units added, providing a means for deterministic design of TADPL active QD/mol composite materials.

3.5 Conclusions

This report illustrates that the photophysical properties of QD/mol composites can be deterministically controlled at RT by simply changing the number of appended triplet chromophore units when ΔE is small, similar to molecular systems that have been more widely studied.[39,48,49,51,52] The average τ_{TADPL} value varies linearly as a function of surface-anchored PCA molecules on CdSe585 and is shown to be reasonably modeled using Boltzmann approximations. Specifically, τ_{TADPL} is extended by ~160 ns per PCA molecule in CdSe585/PCA_n up to n = 27. While previous reports indicate the enthalpic driving force between the QD and triplet acceptor to be more substantial in altering the material's kinetics – changes in ΔE have been reported to alter lifetimes by orders of magnitude – the current results indicate that the QD/mol surface coverage cannot be ignored to achieve comprehensive photophysical design.[5,14] Bespoke QD/mol materials should consider the enthalpic thermodynamics of these systems as a method for coarse lifetime tuning whereas triplet acceptor surface coverage serves as a means for fine tuning the resultant decay kinetics. These combined effects are expected to be particularly important for non-0D morphologies, i.e. rods, wires, plates and wells wherein increased surface area may enable extensive chromophore adsorption to the nanomaterial surface. It should also be noted that surface acceptor coverage may dictate more substantial lifetime manipulation in cases where the thermodynamic landscape does not lend itself to activate strong rEnT i.e. TADPL materials with a larger ΔE may be more susceptible to entropic shifts in Keq due to weaker rEnT. Complete understanding of these effects ultimately contributes to more robust QD/mol designs poised to impact a variety of applications. Finally, this contribution illustrates that diverse photophysical

behavior is readily enabled using just one type of CdSe QD in concert with one molecular chromophore (PCA). Therefore, libraries of future QD/mol constructs are anticipated to provide enormous opportunities for controlling the output of photoluminescent materials.

Chapter 3 Acknowledgments

We thank Margaret H. Hudson and Tia S. Lee at NC State University for their fruitful discussions and suggestions. This work was supported by the Organic Materials Chemistry Program in the Air Force Office of Scientific Research (FA9550-18-1-0331). I'd also like to thank my coauthors Sara Sheykhi, Christopher M. Papa and Felix N. Castellano.

Chapter 3 References:

1. Moroz, P.; Romero, L. R.; Zamkov, M. Colloidal Semiconductor Nanocrystals in Energy Transfer Reactions. *Chem. Commun.* **2019**, *55* (21), 3033–3048.

2. Jiang, Y.; Wang, C.; Rogers, C. R.; Kodaimati, M. S.; Weiss, E. A. Regio- and Diastereoselective Intermolecular [2+2] Cycloadditions Photocatalysed by Quantum Dots. *Nat. Chem.* **2019**, *11* (11), 1034–1040.

3. Mongin, C.; Garakyaraghi, S.; Razgoniaeva, N.; Zamkov, M.; Castellano, F. N. Direct Observation of Triplet Energy Transfer from Semiconductor Nanocrystals. *Science* **2016**, *351* (6271), 369–372.

4. Garakyaraghi, S.; Mongin, C.; Granger, D. B.; Anthony, J. E.; Castellano, F. N. Delayed Molecular Triplet Generation from Energized Lead Sulfide Quantum Dots. *J. Phys. Chem. Lett.* **2017**, *8* (7), 1458–1463.

5. Mongin, C.; Moroz, P.; Zamkov, M.; Castellano, F. N. Thermally Activated Delayed Photoluminescence from Pyrenyl-Functionalized CdSe Quantum Dots. *Nat. Chem.* **2018**, *10* (2), 225–230.

6. Bender, J. A.; Raulerson, E. K.; Li, X.; Goldzak, T.; Xia, P.; Van Voorhis, T.; Tang, M. L.; Roberts, S. T. Surface States Mediate Triplet Energy Transfer in Nanocrystal–Acene Composite Systems. *J. Am. Chem. Soc.* **2018**, *140* (24), 7543–7553.

7. Cossairt, B. M.; Juhas, P.; Billinge, S. J. L.; Owen, J. S. Tuning the Surface Structure and Optical Properties of CdSe Clusters Using Coordination Chemistry. *J. Phys. Chem. Lett.* **2011**, *2* (24), 3075–3080.

8. Garakyaraghi, S.; Castellano, F. N. Nanocrystals for Triplet Sensitization: Molecular Behavior from Quantum-Confined Materials. *Inorg. Chem.* **2018**, *57* (5), 2351–2359.

9. Li, X.; Huang, Z.; Zavala, R.; Tang, M. L. Distance-Dependent Triplet Energy Transfer between CdSe Nanocrystals and Surface Bound Anthracene. *J. Phys. Chem. Lett.* **2016**, *7* (11), 1955–1959.

10. Huang, Z.; Tang, M. L. Designing Transmitter Ligands That Mediate Energy Transfer between Semiconductor Nanocrystals and Molecules. *J. Am. Chem. Soc.* **2017**, *139* (28), 9412–9418.

11. Huang, Z.; Xu, Z.; Mahboub, M.; Li, X.; Taylor, J. W.; Harman, W. H.; Lian, T.; Tang, M. L. PbS/CdS Core–Shell Quantum Dots Suppress Charge Transfer and Enhance Triplet Transfer. *Angew. Chem. Int. Ed.* **2017**, *56* (52), 16583–16587.

12. Huang, Z.; Li, X.; Mahboub, M.; Hanson, K. M.; Nichols, V. M.; Le, H.; Tang, M. L.; Bardeen, C. J. Hybrid Molecule–Nanocrystal Photon Upconversion Across the Visible and Near-Infrared. *Nano Lett.* **2015**, *15* (8), 5552–5557.

13. Zhang, J.; Kouno, H.; Yanai, N.; Eguchi, D.; Nakagawa, T.; Kimizuka, N.; Teranishi, T.; Sakamoto, M. Number of Surface-Attached Acceptors on a Quantum Dot Impacts Energy Transfer and Photon Upconversion Efficiencies. *ACS Photonics* **2020**.

14. La Rosa, M.; Denisov, S. A.; Jonusauskas, G.; McClenaghan, N. D.; Credi, A. Designed Long-Lived Emission from CdSe Quantum Dots through Reversible Electronic Energy Transfer with a Surface-Bound Chromophore. *Angew. Chem.* **2018**, *130* (12), 3158–3161.

15. Yanai, N.; Kimizuka, N. New Triplet Sensitization Routes for Photon Upconversion: Thermally Activated Delayed Fluorescence Molecules, Inorganic Nanocrystals, and Singlet-to-Triplet Absorption. *Acc. Chem. Res.* **2017**, *50* (10), 2487–2495.

16. Xu, Z.; Jin, T.; Huang, Y.; Mulla, K.; Evangelista, F. A.; Egap, E.; Lian, T. Direct Triplet Sensitization of Oligothiophene by Quantum Dots. *Chem. Sci.* **2019**, *10* (24), 6120–6124.

17. Luo, X.; Han, Y.; Chen, Z.; Li, Y.; Liang, G.; Liu, X.; Ding, T.; Nie, C.; Wang, M.; Castellano, F. N.; Wu, K. Mechanisms of Triplet Energy Transfer across the Inorganic Nanocrystal/Organic Molecule Interface. *Nat. Commun.* **2020**, *11* (1), 28.

18. Wang, K.; Lu, H.; Zhu, X.; Lin, Y.; Beard, M. C.; Yan, Y.; Chen, X. Ultrafast Reaction Mechanisms in Perovskite Based Photocatalytic C–C Coupling. *ACS Energy Lett.* **2020**, *5* (2), 566–571.

19. Weiss, E. A. Designing the Surfaces of Semiconductor Quantum Dots for Colloidal Photocatalysis. *ACS Energy Lett.* **2017**, *2* (5), 1005–1013.

20. Brus, L. Electronic Wave Functions in Semiconductor Clusters: Experiment and Theory. *J. Phys. Chem.* **1986**, *90* (12), 2555–2560.

21. Yu, W. W.; Qu, L.; Guo, W.; Peng, X. Experimental Determination of the Extinction Coefficient of CdTe, CdSe, and CdS Nanocrystals. *Chem. Mater.* **2003**, *15* (14), 2854–2860.

22. Schmehl, R. H. Something New in Transition Metal Complex Sensitizers: Bringing Metal Diimine Complexes and Aromatic Hydrocarbons Together. *The Spectrum 13* (2).

23. Bergmann, L.; Hedley, G. J.; Baumann, T.; Bräse, S.; Samuel, I. D. W. *Sci. Adv.* **2016**, *2* (1), e1500889.

24. Chen, X.-L.; Yu, R.; Zhang, Q.-K.; Zhou, L.-J.; Wu, X.-Y.; Zhang, Q.; Lu, C.-Z. Rational Design of Strongly Blue-Emitting Cuprous Complexes with Thermally Activated Delayed Fluorescence and Application in Solution-Processed OLEDs. *Chem. Mater.* **2013**, *25* (19), 3910–3920.

25. Czerwieniec, R.; Yu, J.; Yersin, H. Blue-Light Emission of Cu(I) Complexes and Singlet Harvesting. *Inorg. Chem.* **2011**, *50* (17), 8293–8301.

26. Dias, F. B.; Bourdakos, K. N.; Jankus, V.; Moss, K. C.; Kamtekar, K. T.; Bhalla, V.; Santos, J.; Bryce, M. R.; Monkman, A. P. Triplet Harvesting with 100% Efficiency by Way of Thermally Activated Delayed Fluorescence in Charge Transfer OLED Emitters. *Adv. Mater.* **2013**, *25* (27), 3707–3714.

27. Endo, A.; Ogasawara, M.; Takahashi, A.; Yokoyama, D.; Kato, Y.; Adachi, C. Thermally Activated Delayed Fluorescence from Sn4+–Porphyrin Complexes and Their Application to Organic Light Emitting Diodes — A Novel Mechanism for Electroluminescence. *Adv. Mater.* **2009**, *21* (47), 4802–4806.

28. Dias, F. B.; Penfold, T. J.; Monkman, A. P. Photophysics of Thermally Activated Delayed Fluorescence Molecules. *Methods Appl. Fluoresc.* **2017**, *5* (1), 012001.

29. Gibson, J.; Monkman, A. P.; Penfold, T. J. The Importance of Vibronic Coupling for Efficient Reverse Intersystem Crossing in Thermally Activated Delayed Fluorescence Molecules. *ChemPhysChem* **2016**, *17* (19), 2956–2961.

30. Leitl, M. J.; Krylova, V. A.; Djurovich, P. I.; Thompson, M. E.; Yersin, H. Phosphorescence versus Thermally Activated Delayed Fluorescence. Controlling Singlet–Triplet Splitting in Brightly Emitting and Sublimable Cu(I) Compounds. *J. Am. Chem. Soc.* **2014**, *136* (45), 16032–16038.

31. Li, G.; Nobuyasu, R. S.; Zhang, B.; Geng, Y.; Yao, B.; Xie, Z.; Zhu, D.; Shan, G.; Che, W.; Yan, L.; Su, Z.; Dias, F. B.; Bryce, M. R. Thermally Activated Delayed Fluorescence in CuI Complexes Originating from Restricted Molecular Vibrations. *Chem. Weinh. Bergstr. Ger.* **2017**, *23* (49), 11761–11766.

32. Mieno, H.; Kabe, R.; Allendorf, M. D.; Adachi, C. Thermally Activated Delayed Fluorescence of a Zr-Based Metal–Organic Framework. *Chem. Commun.* **2018**, *54* (6), 631–634.

33. Penfold, T. J.; Dias, F. B.; Monkman, A. P. The Theory of Thermally Activated Delayed Fluorescence for Organic Light Emitting Diodes. *Chem. Commun.* **2018**, *54* (32), 3926–3935.

34. Steinegger, A.; Klimant, I.; Borisov, S. M. Purely Organic Dyes with Thermally Activated Delayed Fluorescence—A Versatile Class of Indicators for Optical Temperature Sensing. *Adv. Opt. Mater.* **2017**, *5* (18), 1700372.

35. Tao, Y.; Yuan, K.; Chen, T.; Xu, P.; Li, H.; Chen, R.; Zheng, C.; Zhang, L.; Huang, W. Thermally Activated Delayed Fluorescence Materials Towards the Breakthrough of Organoelectronics. *Adv. Mater.* **2014**, *26* (47), 7931–7958.

36. Yersin, H.; Czerwieniec, R.; Shafikov, M. Z.; Suleymanova, A. F. TADF Material Design: Photophysical Background and Case Studies Focusing on Cu(I) and Ag(I) Complexesa. In *Highly Efficient OLEDs*; John Wiley & Sons, Ltd, 2018; pp 1–60.

37. Zhang, Q.; Li, B.; Huang, S.; Nomura, H.; Tanaka, H.; Adachi, C. Efficient Blue Organic Light-Emitting Diodes Employing Thermally Activated Delayed Fluorescence. *Nat. Photonics* **2014**, *8* (4), 326–332.

38. Lu, H.; Huang, Z.; Martinez, M. S.; Johnson, J. C.; Luther, J. M.; Beard, M. C. Transforming Energy Using Quantum Dots. *Energy Environ. Sci.* **2020**, *13* (5), 1347–1376.

39. Yarnell, J. E.; Deaton, J. C.; McCusker, C. E.; Castellano, F. N. Bidirectional "Ping-Pong" Energy Transfer and 3000-Fold Lifetime Enhancement in a Re(I) Charge Transfer Complex. *Inorg. Chem.* **2011**, *50* (16), 7820–7830.

40. Yarnell, J. E.; Wells, K. A.; Palmer, J. R.; Breaux, J. M.; Castellano, F. N. Excited-State Triplet Equilibria in a Series of Re(I)-Naphthalimide Bichromophores. *J. Phys. Chem. B* **2019**, *123* (35), 7611–7627.

41. Olshansky, J. H.; Harvey, S. M.; Pennel, M. L.; Krzyaniak, M. D.; Schaller, R. D.; Wasielewski, M. R. Using Photoexcited Core/Shell Quantum Dots To Spin Polarize Appended Radical Qubits. *J. Am. Chem. Soc.* **2020.**

42. Yonemoto, D. T.; Papa, C. M.; Mongin, C.; Castellano, F. N. Thermally Activated Delayed Photoluminescence: Deterministic Control of Excited-State Decay. *J. Am. Chem. Soc.* **2020**, *142* (25), 10883–10893.

43. Knauf, R. R.; Lennox, J. C.; Dempsey, J. L. Quantifying Ligand Exchange Reactions at CdSe Nanocrystal Surfaces. *Chem. Mater.* **2016**, *28* (13), 4762–4770.

44. Baleizão, C.; Berberan-Santos, M. N. Thermally Activated Delayed Fluorescence as a Cycling Process between Excited Singlet and Triplet States: Application to the Fullerenes. *J. Chem. Phys.* **2007**, *126* (20), 204510.

45. Deaton, J. C.; Switalski, S. C.; Kondakov, D. Y.; Young, R. H.; Pawlik, T. D.; Giesen, D. J.; Harkins, S. B.; Miller, A. J. M.; Mickenberg, S. F.; Peters, J. C. E-Type Delayed Fluorescence of a Phosphine-Supported Cu2(μ-NAr2)2 Diamond Core: Harvesting Singlet and Triplet Excitons in OLEDs. *J. Am. Chem. Soc.* **2010**, *132* (27), 9499–9508.

46. Kirchhoff, J. R.; Gamache, R. E.; Blaskie, M. W.; Del Paggio, A. A.; Lengel, R. K.; McMillin, D. R. Temperature Dependence of Luminescence from Cu(NN)2+ Systems in Fluid Solution. Evidence for the Participation of Two Excited States. *Inorg. Chem.* **1983**, *22* (17), 2380–2384.

47. Ravinson, D. S. M.; Thompson, M. E. Thermally Assisted Delayed Fluorescence (TADF): Fluorescence Delayed Is Fluorescence Denied. *Mater. Horiz.* **2020**, *7* (5), 1210–1217.

48. Tyson, D. S.; Henbest, K. B.; Bialecki, J.; Castellano, F. N. Excited State Processes in Ruthenium(II)/Pyrenyl Complexes Displaying Extended Lifetimes. *J. Phys. Chem. A* **2001**, *105* (35), 8154–8161.

49. McClenaghan, N. D.; Barigelletti, F.; Maubert, B.; Campagna, S. Towards Ruthenium(II) Polypyridine Complexes with Prolonged and Predetermined Excited State Lifetimes. *Chem. Commun.* **2002**, No. 6, 602–603.

50. Goze, C.; Kozlov, D. V.; Tyson, D. S.; Ziessel, R.; Castellano, F. N. Synthesis and Photophysics of Ruthenium(II) Complexes with Multiple Pyrenylethynylene Subunits. *New J. Chem.* **2003**, *27* (12), 1679–1683.

51. Finkenzeller, W. J.; Yersin, H. Emission of Ir(Ppy)3. Temperature Dependence, Decay Dynamics, and Magnetic Field Properties. *Chem. Phys. Lett.* **2003**, *377* (3), 299–305.

52. Tyson, D. S.; Bialecki, J.; Castellano, F. N. Ruthenium(II) Complex with a Notably Longexcited State Lifetime. *Chem. Commun.* **2000**, No. 23, 2355–2356.

Supporting Information for Chapter 3: Controlling Thermally Activated Delayed Photoluminescence in CdSe Quantum Dots through Triplet Acceptor Surface Coverage

General Experimental Techniques

General Techniques

Steady-state solution electronic absorption experiments were performed using a Shimadzu UV-3600. Steady-state solution photoluminescence experiments were performed using an Edinburgh FLS 980 fluorimeter. Excitation was achieved by passing a 450 W Xe arc lamp through a monochromator. Attenuated total reflectance Fourier-transform infrared (ATR-FTIR) spectroscopy experiments were performed on solid state samples using a Bruker Alpha Platinum ATR instrument.

Time Gated Emission

Suprananosecond Time-Gated Photoluminescence measurements (TGE) were executed using an Edinburgh Instruments LP920 laser flash photolysis system (Edinburgh Instruments) equipped with an iStar ICCD camera (Andor Technology) controlled with the LP920 software package. The reported TGE spectra are the average of 20 laser pulses. Sample excitation was achieved with a vibrant LD 355 II Nd:YAG/OPO laser system (OPOTEK) functioning at 1 Hz. The pulse energy of the laser was manipulated using neutral density filters to achieve the desired pulse energy of 2 mJ. Samples were prepared in toluene and degassed via standard freeze-pump-thaw technique with a minimum of three cycles in a 10 mm path length custom quartz optical cell. Samples were prepared to an optical density of 0.2 at λ_{ex} 475 nm. Unless otherwise noted, experiments were performed at room temperature.

S3.1. Synthesis of CdSe:

S3.1.1. Chemicals

Cadmium oxide (CdO, 99.995% trace metal basis, BTC), selenium powder (Se^0, 99.5% trace metal basis, Aldrich), oleic acid (OA, tech gr. 90% Alfa Aesar), octadecene (ODE, tech gr. 90% Acros) toluene (ACS gr. 99.5%), methanol (MeOH, ACS gr. 99.5%), ethanol (EtOH, 200 proof ACS gr.), acetone (ACS gr. 99.5%), 1−pyrenecarboxylic acid (PCA, >97.0% TCI), were all used as received without further purification unless otherwise noted.

S3.1.2. Synthetic Procedure for CdSe

CdSe QD's were synthesized following an adapted procedure via Dempsey et al.[1] Cadmium(II) oxide (CdO, 300 mg, 2.3 mmol), oleic acid (OA, 2 mL, 6.3 mmol) and octadecene (ODE, 10 mL, 63 mmol) are combined in a 100 mL 3-neck flask equipped with a thermometer, reflux condenser with nitrogen adapter, rubber septa and stir bar. Once added, the reaction flask is degassed for a minimum of 30 mins at 100 °C to remove water and air while stirring vigorously. The reaction flask is then subjected to a N_2 atmosphere and the temperature is slowly ramped 280 °C. The reaction slowly will turn from a dark brown color to a clear colorless solution indicating the successful conversion from CdO to cadmium(II) oleate ($Cd(OA)_2$). Note: if the reaction is not well degassed or the temperature is not well controlled and exceeds ~290 °C, the reaction will carbonize and turn a gray/brown color and must be discarded. Once $Cd(OA)_2$ is formed, the reaction mixture is cooled to ~100 °C.

In a separate 100 mL 3-neck flask − equipped with a thermometer, reflux condenser with nitrogen adapter, rubber septa and stir bar − selenium powder (Se^0, 100 mg, 1.2 mmol) and ODE (10 mL, 63 mmol) were degassed at 100 °C for a minimum of 30 mins with vigorous stirring and then placed under flowing N_2. To this flask the previously synthesized $Cd(OA)_2$ was injected and the temperature was slowly ramped to 240 °C. A stark color change is noticed at 180 °C as the

black Se^0 dispersion converts to an orange/yellow color. Once at 240 °C, the reaction temperature is maintained and the CdSe grow for various times before being quenched with 40 mL of toluene to yield the desired material size, **Figure S3.1**. These materials are then cooled to room temperature before being washed.

S3.2. Washing Procedure for CdSe:

Washing is completed using centrifugation in 4 phases at 4300 rpm. The first phase is addition of acetone to the reaction mixture in 1:1.5 ratios acetone:rxn to remove excess reactants i.e. $Cd(OA)_2$ or Se^0. The second phase is precipitation of the QDs by adding toluene to disperse the CdSe and MeOH to precipitate in a 1:10 ratio respectively. Note: the first centrifugation of this phase only adds MeOH to precipitate the QDs as the supernatant already contains the dispersed QDs. This is repeated 5 times. The third phase is flocculation of the NPs via a 1:10 mixture of toluene:EtOH. This is also repeated 5 times. The final phase is addition of toluene to disperse and acetone to precipitate in a 1:10 ratio respectively. This is repeated 5 times and upon completion a solid pellet of CdSe should form. The pellet was then dried before being stored as a powder for later use.

S3.3. Spectroscopic Screening of CdSe Materials:

In order to ensure that the synthesized materials are suitable for complex photophysical investigation, steady-state absorbance and photoluminescence measurements are conducted on the washed CdSe. These experiments verify the quality of the materials by monitoring the FWHM (± 0.07 eV), asymmetry of the PL band and checks for the observation of sub-bandgap trap states. **Figure S3.1** demonstrates examples of suitable spectra as well as unacceptable spectra of CdSe. Samples with any asymmetry in PL band which is the evidence of significant trap states, and/or loss of narrow FWHM (± 0.07 eV) were deemed unusable and discarded. This procedure ensures

that the photophysics of the end composite material were solely altered by the introduction of chromophore molecules. Established empirical equations were used to determine the diameter of these materials and their molar extinction coefficients at E_g, 2.5 nm, 71,000 M^{-1} cm^{-1} and 4.0 nm, 230,000 M^{-1} cm^{-1} for CdSe520 and CdSe585, respectively.[2]

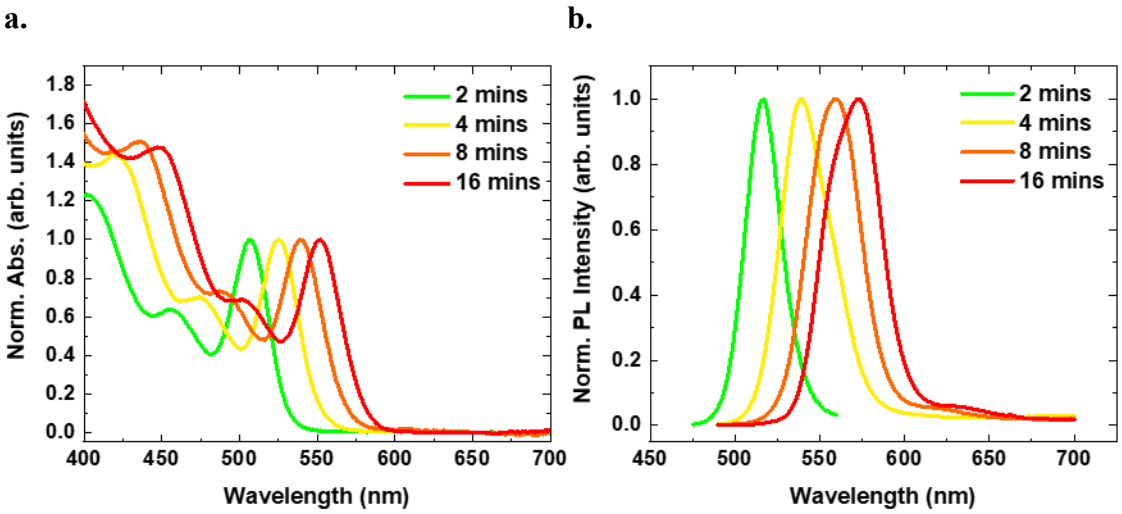

Figure S3.1. Representative spectra of different sized CdSe **a.** absorbance and **b.** photoluminescence in toluene. Examples of sub-bandgap trap states are observed in the 8 and 16 min samples and asymmetry is noted in all but the 4 min spectra. For these materials, only the 2 min sample would be deemed acceptable for further use.

S3.4. Ligand Exchange:

Ligand exchange was revised from previously reported methodologies.[3–6] A stock solution of the acceptor molecule was generated by measuring >20 mg of acceptor and dissolve ng in acetone. Aliquots corresponding to the desired mg amounts of acceptor were then added to vials and the vials were set aside to allow the solvent to slowly evaporate until gone and generate crystalline acceptor. While the crystals are being formed, a stock solution of CdSe is made by dissolving the desired E_g CdSe in toluene. This solution was examined via steady state absorbance in a 2 mm cuvet to ensure ~2 abs at E_g. This step is important to prevent destruction of the QDs, if the CdSe is not concentrated enough the addition of acceptor will cause a broadening of the CdSe

E_g and the nanoparticles will become colloidally unstable. Once the acceptor crystals form, 100 µL of acetone is added to the vials to redissolve the crystals, followed by 1 mL of the CdSe stock solution. The reaction mixtures are then sealed with parafilm, placed in a sonicator preheated to 35 °C, and sonicated for 1 hour. Once the sonication is completed, the reactions are removed and allowed to cool to room temperature before being isolated.

Isolation of the composite materials is achieved through a standard washing protocol. Step 1 is to draw the reaction solution into a syringe. Step 2 is to draw 3 mL of MeOH into the same syringe to precipitate the CdSe with surface anchored acceptor molecules (CdSe/mol). Step 4 is to pass the 3:1, MeOH:toluene, solution through a 450 µm syringe filter. As the CdSe/mol materials are insoluble in MeOH, this precipitates the CdSe/mol materials and removes excess acceptor which readily dissolve in MeOH. For step 5, 1 mL of toluene is drawn into a clean syringe and passed through the same syringe filter to extract the precipitated CdSe/mol composites via dissolution into the toluene. These materials are used without further purification and are stored in a 1 dram vial sealed with parafilm.

S3.5. TEM and ATR−IR of CdSe585/PCA:

To further characterize the effects of ligand exchange on CdSe, representative TEM and ATR−IR experiments were conducted for CdSe585/PCA samples. **Figure S3.12** demonstrates the retention of particle size post ligand exchange and ATR−IR indicates the loss of OA for the introduction of PCA to the CdSe's surface.

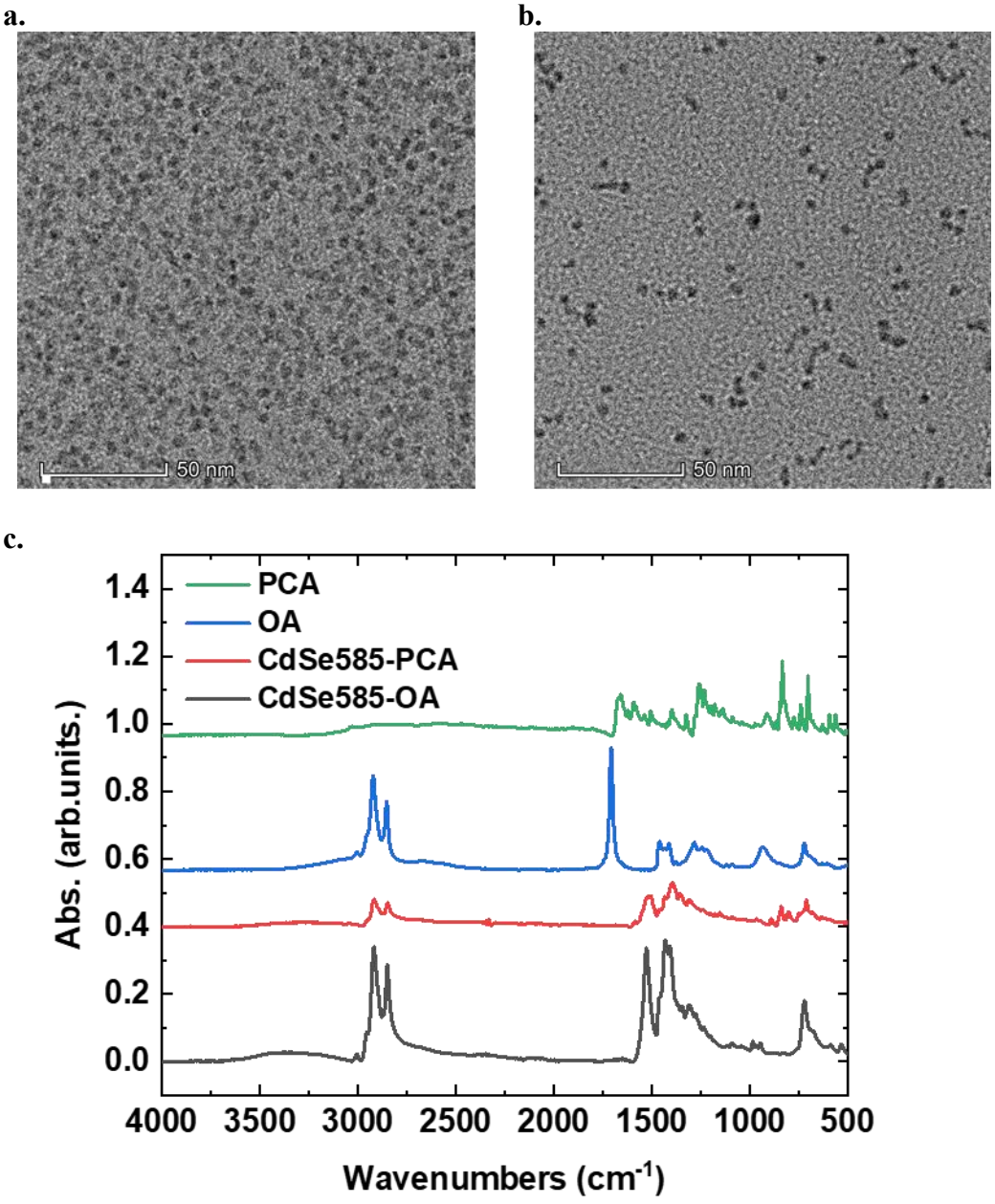

Figure S3.2. Representative TEM images of CdSe585 **a.** before and **b.** after ligand exchange with PCA and **c.** the corresponding solid-state ATR-IR spectra indicating the coordination of PCA to the QD surface via the exchange with OA.

S3.6. NCA and 5TET Control Studies:

To verify ligand exchange reactions are not destructive to the CdSe, two additional control studies were conducted with 5-tetracene carboxylic acid (5TET) and naphthoic acid (NCA). These

chromophores were chosen to directly identify the effect of ligand exchange on the quality of CdSe585 when no TADPL processes are observed. This is possible due to the triplet energies of 5TET, 1.3 eV, and NCA, 2.5 eV, being energetically outside of the acceptable energy range for TADPL to occur. As shown in **Figure S3.3a** and **Table S3.1**, no significant changes in photophysical processes are noted for NCA as expected given the high energy of the NCA triplet. CdSe585/5TET indicates quenching as expected for the low energy triplet, but no change in band shape or addition of sub-bandgap trap states are noted, **Figure S3.3b**. These results indicate that our exchange of carboxylate ligands at the CdSe interface are generating negligible surface defects. As such, surface degradation altering the intrinsic CdSe properties resultant from ligand exchange processes will also be considered negligible to the observed decay processes for the CdSe585/PCA_n species of interest.

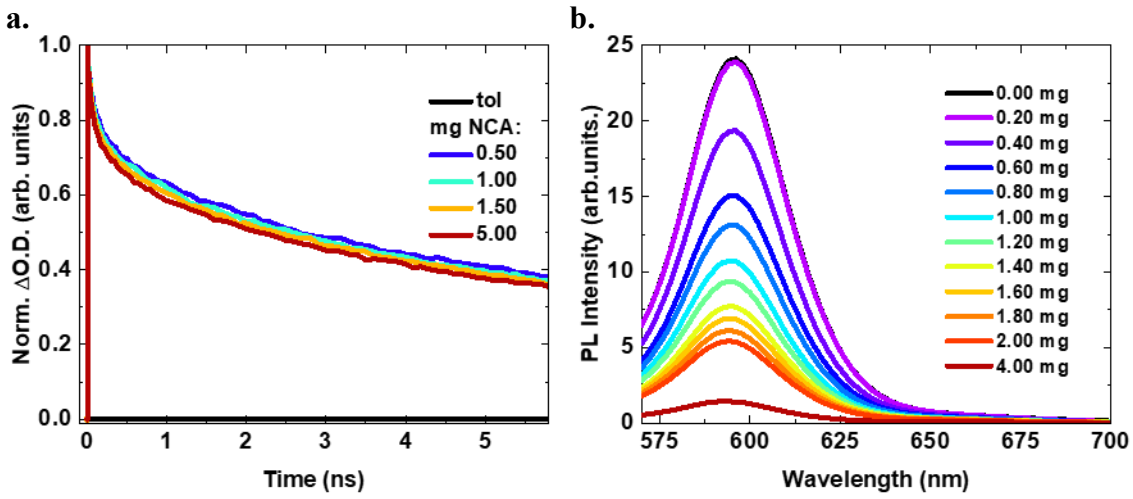

Figure S3.3. Control CdSe/mol studies of **a.** fsTA kinetic decay with NCA at 585 nm with λ_{ex} = 475 nm (0.5 μJ per pulse, 100 fs FWHM) and **b.** steady-state PL spectra with 5TET in toluene, λ_{ex} = 475. Resultant photophysics of CdSe/mols indicate retention of the CdSe intrinsic properties after ligand exchange evident by lifetime retention in CdSe585/NCA and lack of sub band gap trap states and band shape retention in CdSe585/5TET.

Table S3.1. Kinetic data for CdSe585/NCA fsTA data demonstrate stable excited state dynamics independent of additional NCA in ligand exchange reactions. Results indicate any surface degradation is negligible to the decay kinetics noted for CdSe585/PCA.

NCA Loading (mg)	τ ($s \times 10^{-9}$)	β	$\langle\tau\rangle$ ($s \times 10^{-8}$)	$\langle k\rangle$ ($s^{-1} \times 10^{7}$)
0.00	6.16	0.37	2.7	3.7
0.50	6.14	0.35	3.09	3.2
1.00	5.10	0.32	3.64	2.7
1.50	4.70	0.30	4.29	2.3
5.00	3.87	0.28	5.15	1.9

Synthesis of 5-Tetracene Carboxylic Acid (5TET):

S3.6.1. Chemicals and Instrumentation

All chemicals and solvents were analytical grade and they were used without purification. ^{1}H- and ^{13}C-NMR spectra were measured with a Bruker® Avance NEO 400 MHz NMR spectrometer. The chemical shifts (δ ppm) are referenced to the respective solvent and splitting patterns are designed as s (singlet), d (doublet), dd (doublet of doublet), ddd (doublet of doublet of doublet), dddd (doublet of doublet of doublet of doublet), t (triplet), m (multiplet). Mass-spectrometry studies were performed using an Agilent 5975B inert Series GC/MS system.

S3.6.2. Synthesis

*S3.6.2.1 Synthesis of 5-Bromotetracene (**1**).*

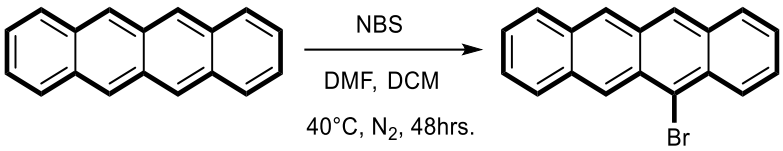

1: 85 %

5-bromotetracene **1** was prepared using a modified procedure from those described in the literature.[7] In a 25 mL round-bottom flask, tetracene (256 mg, 1.12 mmol) was suspended in 70 mL of dichloromethane (DCM) under nitrogen. The resulting suspension was sonicated for 20 minutes. An additional funnel containing a solution of N-Bromosuccinimide (NBS) (200 mg, 1.12 mmol) in 4 mL of dimethylformamide (DMF) and 18 mL of DCM under nitrogen was installed onto the flask containing the tetracene suspension. The flask was covered by aluminum foil and heated to 40°C. The solution of NBS was added slowly, over a period of 2 hours. The resulting reaction mixture was stirring in the dark, under nitrogen for 2 days. Then, the reaction mixture was

cooled to room temperature, and DCM was removed by rotary evaporation in vacuo. 10 mL of cold methanol was added to the remaining slurry and cooled to 0°C for 30 minutes. 1 mL of water was added dropwise, and the solids were collected by vacuum filtration. The resulting red solids were rinsed with cold water and methanol to give 300 mg (0.98 mmol) of 5-bromotetracene in 85% yield.

MS [GC-MS (ACN) m/z] 306.0 $[M]^+$

^{1}H NMR (400 MHz, $C_2D_2Cl_4$-d_2): δ 9.15 (s, 1H), 8.70 (d, J = 5.1 Hz, 2H), 8.52-8.47 (m, 1H), 8.14-8.10 (m, 1H), 8.03 (dd, J = 10.6, 7.9 Hz, 2H), 7.57 (ddd, J = 9.1, 6.4, 1.3 Hz, 1H), 7.48 (dddd, J = 13.0, 6.6, 3.9, 1.1 Hz, 3H) ppm.

^{13}C NMR (125 MHz, $C_2D_2Cl_4$-d_2): δ 132.26, 131.51, 131.26, 130.16, 130.04, 128.71, 128.70, 128.60, 128.16, 127.75, 127.33, 127.26, 127.04, 126.18, 125.99, 125.90, 125.21, 121.94 ppm.

6.2.2 Synthesis of 5-Tetracenecarboxylic Acid (**2**).

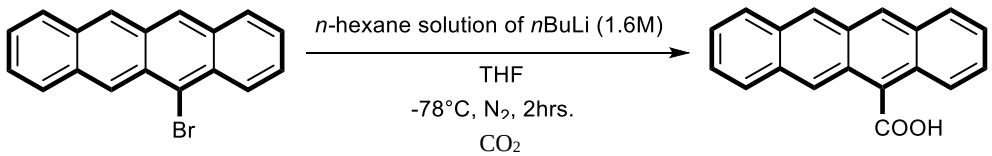

1 **2:** 58 %

5-Tetracene carboxylic Acid **2** was prepared using a modified procedure from those described in the literature.[8] In a 25 mL round-bottom flask, 5-bromotetracene **1** (190 mg, 0.62 mmol) was suspended in tetrahydrofuran (THF) (6 mL). *n*-hexane solution of *n*BuLi (1.60M, 450 µL, 0.68 mmol, 1.1 equiv) was added dropwise to the solution of 1 at -78°C. The reaction mixture

was stirring for 2 hours. Then, some pellets of dry ice were added under a stream of nitrogen. The mixture was kept at the same temperature for additional 1 hour. After this time, the reaction mixture was allowed to warm to room temperature. After that, 2 mL distilled water was added and solvents were concentrated under reduced pressure to obtain yellow-orangish solids, which were dissolved in aqueous sodium hydroxide solution (1.0 M, 42 mL). The solids were then filtered off. The filtrate solution was acidified with aqueous hydrogen chloride solution (2.0 M) to precipitate orange solids. The orange solids were filtered off and dried over phosphorus (V) oxide under reduced pressure to give 98 mg (0.36 mmol) of 5-tetracene carboxylic acid in 58% yield.

MS [GC-MS (ACN) m/z] 271.0 $[M-H]^-$

^{1}H NMR (400 MHz, DMSO-d_6): δ 13.99 (s, 1H), 8.98 (s, 1H), 8.92 (s, 1H), 8.75 (s, 1H), 8.14 (ddd, J = 13.9, 7.2, 3.7 Hz, 3H), 8.05 (d, J = 8.8 Hz, 1H), 7.61-7.56 (m, 1H), 7.35–7.48 (m, 3H) ppm.

^{13}C NMR (125 MHz, DMSO-d_6): δ 170.28, 131.67, 130.92, 130.20, 129.43, 128.91, 128.73, 128.69, 128.40, 128.01, 127.09, 127.01, 126.79, 126.18, 125.90, 125.44, 125.32, 124.84, 123.30 ppm.

S3.6.3. NMR spectra

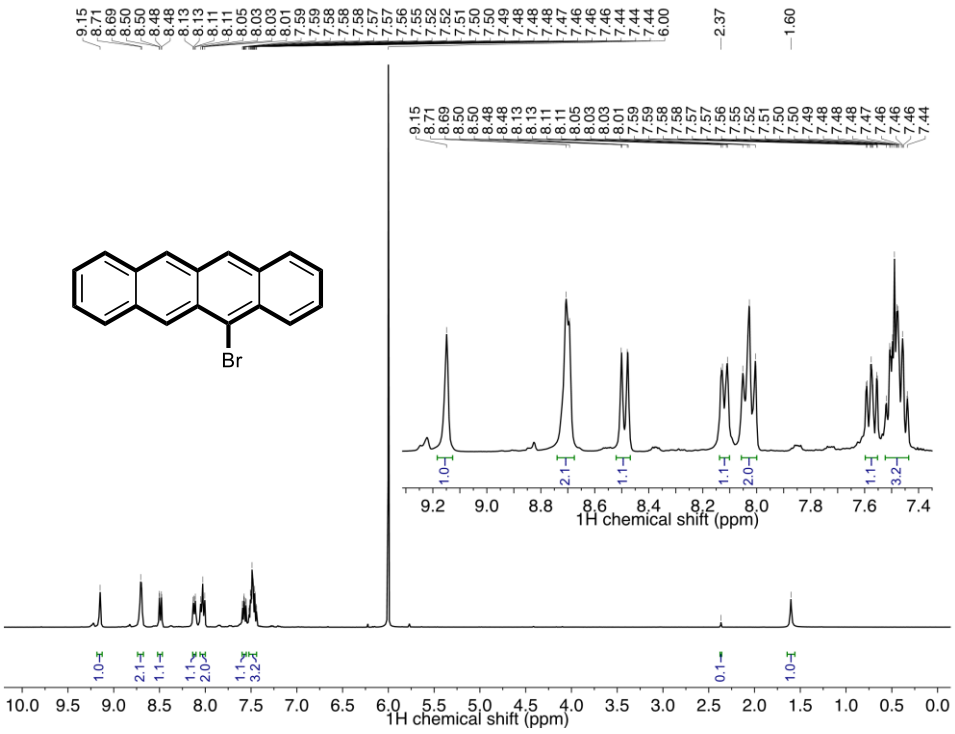

Figure S3.4. ^{1}H NMR spectrum (400 MHz) of 5-bromotetracene in $C_2D_2Cl_4$.

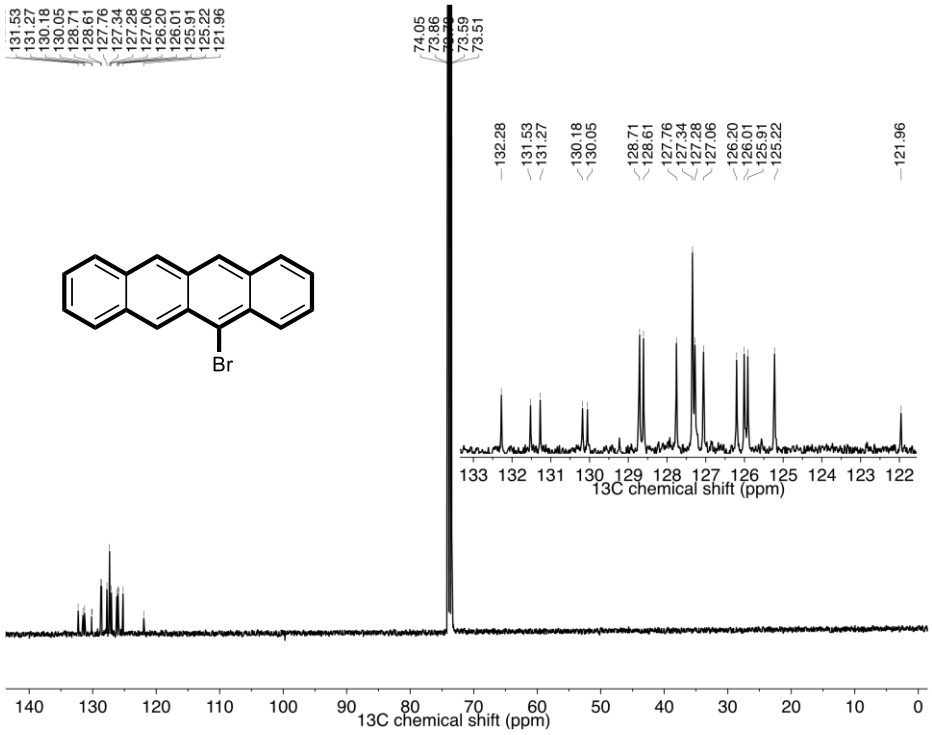

Figure S3.5. ^{13}C NMR spectrum (125 MHz) of 5-bromotetracene in $C_2D_2Cl_4$.

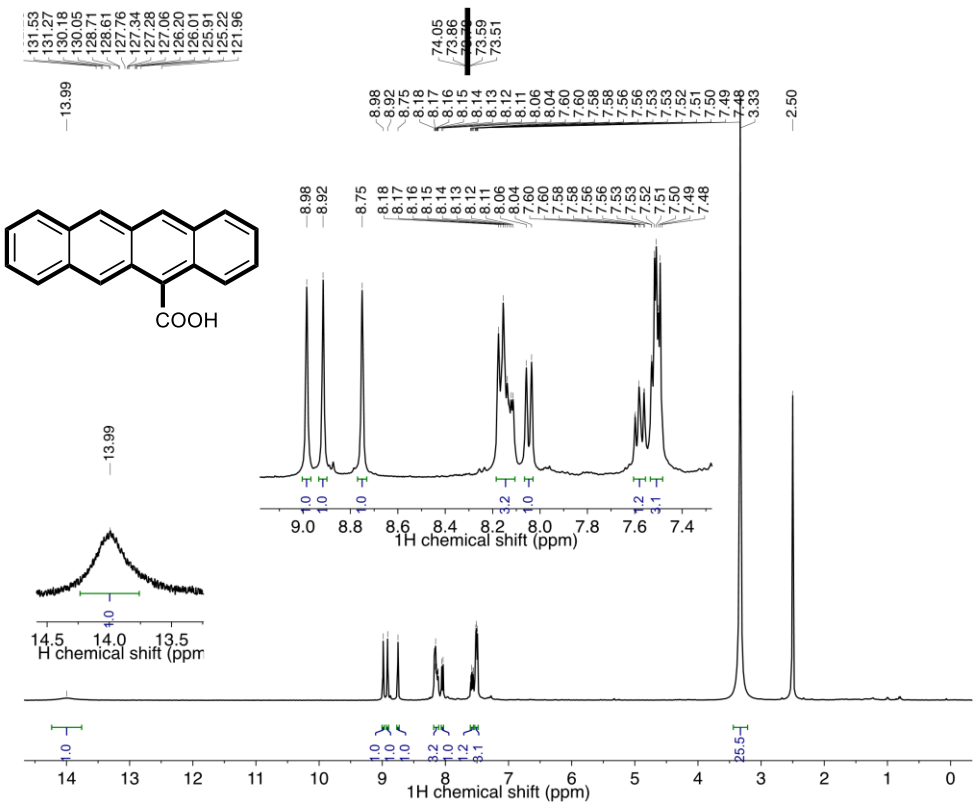

Figure S3.6. ^{1}H NMR spectrum (400 MHz) of tetracenecarboxylic acid in DMSO.

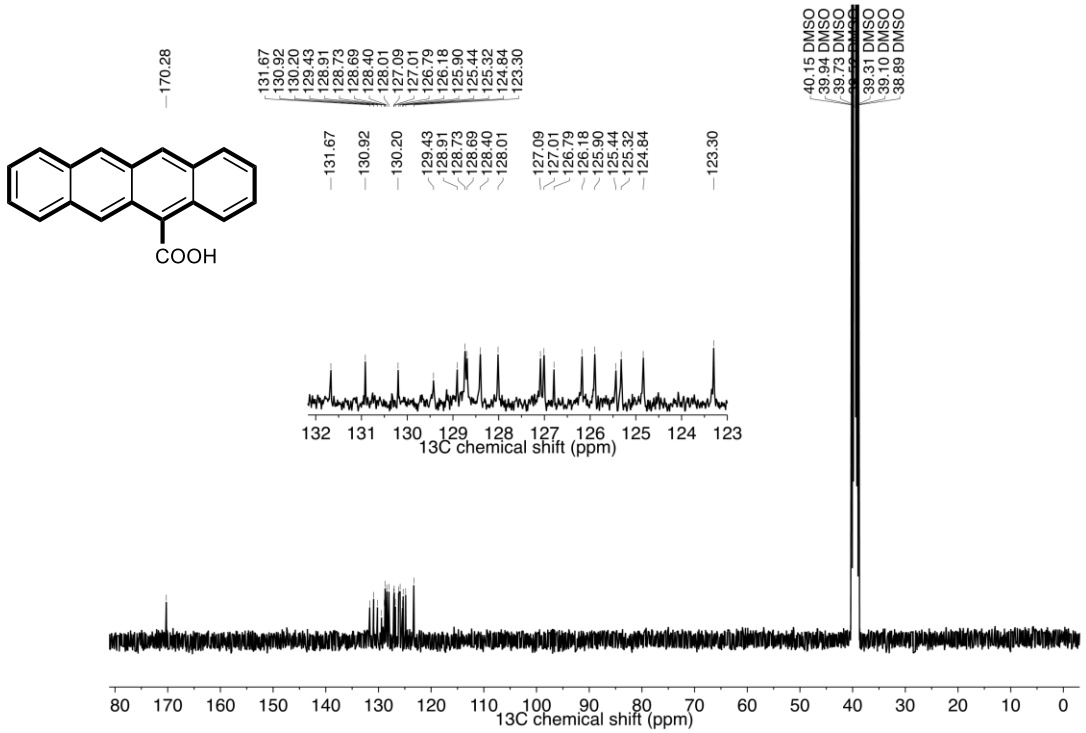

Figure S3.7. ^{13}C NMR spectrum (125 MHz) of tetracenecarboxylic acid in DMSO.

S3.6.4. Mass Spectrometry

Figure S3.8. GC-MS spectrum of 5-bromotetracene.

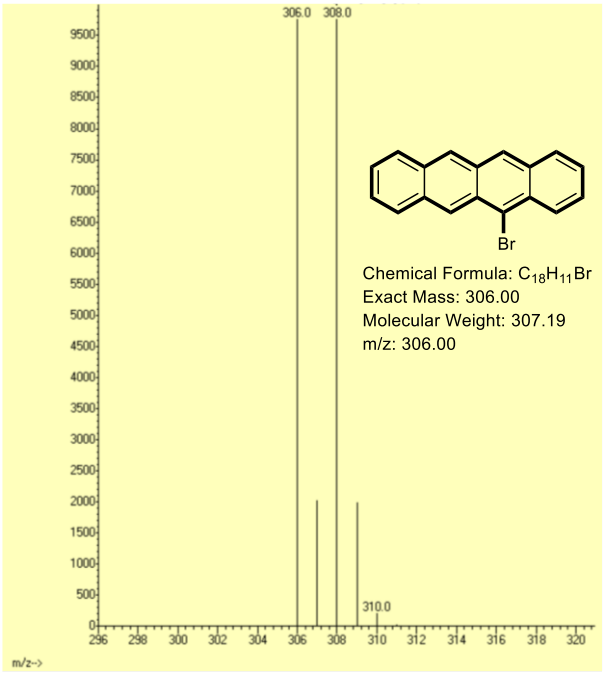

Figure S3.9. MALDI-MS spectrum of tetracenecarboxylic acid.

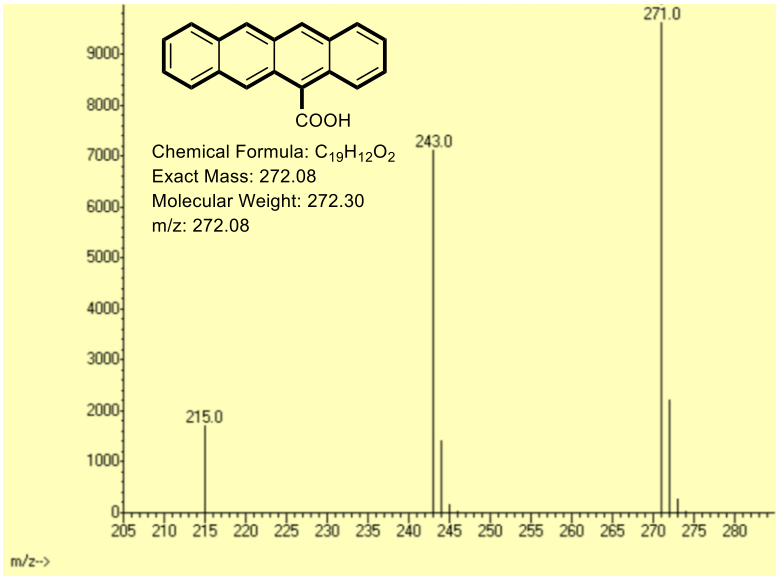

S3.6.5 NCA Femtosecond Transient Absorption Spectroscopy

Femtosecond transient absorption (fsTA) measurements were executed at the NCSU Imaging and Kinetic Spectroscopy (IMAKS) Laboratory using a mode-locked Ti:sapphire (Coherent Libra) laser system and a Helios, Ultrafast Systems transient absorption spectrometer as previously described.[9] The pump beam was fired into a parametric amplifier (coherent Opera Solo) to generate 475 nm excitation beam. White light continuum was generated between 350 and 775 nm via focusing the probe beam onto a calcium fluoride crystal. The pump (~700 μm) and probe were focused and overlapped through the sample dissolved in toluene inside a 2 mm cuvette equipped with a stir bar. All samples were selectively excited into the CdSe at 475 nm for CdSe585. The average number of excitations per pulse ($<N_{ex}>$) were kept < 0.1. At the $<N_{ex}>$ significantly < 1, multiexciton events previously reported in QDs is effectively suppressed.[3] Ground-state absorption spectra were conducted before and after each experiment to verify no photodegradation was observed in the samples. Transient kinetic data at select wavelengths was analyzed using fitting routines available in OriginPro 2020 SR1 (v 9.7). Lifetimes were extracted using stretched exponential fits, $I(t) = A\exp(-(t/\tau)^{\beta})$, following the previously established procedures in the literature, full details available in supplementary section 7. Decay Analysis Methods.[4,5,10–13]

Data Analysis Methods:

S3.7. Decay Analysis Methods:

S3.7.1 Stretch Exponential Fits:

Kinetic analysis was monitored from the CdSe bright state in photoluminescence decay measurements and the CdSe ground state bleach signal in transient absorption experiments. To appropriately model the variations in the surface organization of the CdSe/PCA and the initially

populated CdSe excited state, a stretched exponential function was used. The collected data was fit using the below equation, results from these fits are shown in **Tables 3.1, 3.2, S3.1,** & **S3.2**.

$$I(t) = A \times \exp(-(t/\tau)^{\beta})$$

Here, A is the amplitude of the decay, τ is the stretched lifetime and β is the stretching exponent of the CdSe kinetic decay. The average weighted lifetime, $\langle\tau\rangle$, is calculated using the obtained values of τ and β with the following equation:

$$\langle\tau\rangle = \tau/\beta \times \Gamma(1/\beta)$$

S3.7.2 TGE Experiments:

Suprananosecond Time-Gated Photoluminescence measurements (TGE) were executed using an Edinburgh Instruments LP920 Spectrometer equipped with an andor iccd camera. Sample excitation was achieved with an Opotek (vibrant LD 355 II) Nd:YAG/OPO laser system functioning at 1 Hz. The pulse energy of the laser was manipulated using neutral density filters to achieve the desired pulse energy. Resultant spectra are displayed in **Figure S3.10** and the extracted kinetic data is tabulated in **Table S3.2**.

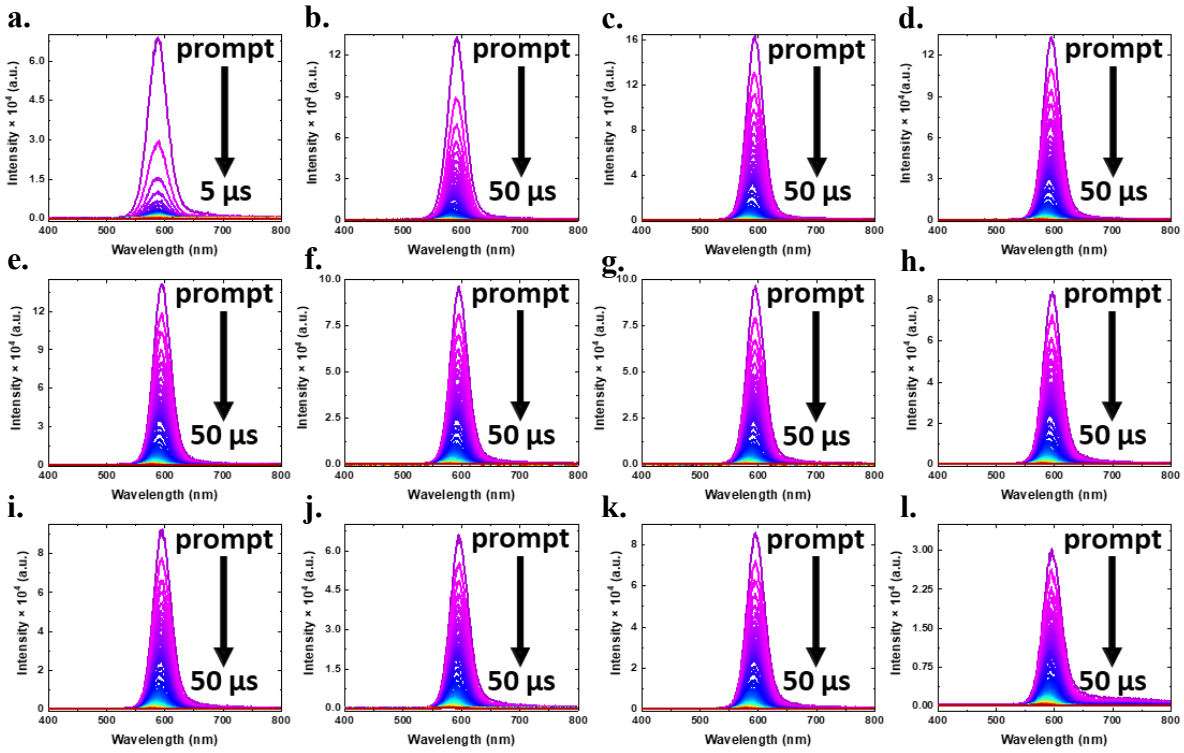

Figure S3.10. Time gated photoluminescence spectra post 475 nm laser excitation (2 mJ, 5-7 ns FWHM) for a. – l. CdSe585/PCA00 − CdSe585/PCA27 samples, respectively. All experiments were executed using an Edinburgh LP920 Flash Photolysis system and degassed toluene in a custom freeze pump thaw optical cell.

Table S3.2. Kinetic fitting parameters for CdSe585/PCA materials from TGE experiments. Derived values indicate a positive correlation between surface concentration and k_{TTET}. Lifetimes calculated using a stretch exponential fit, $I(t) = A \exp(-(t/\tau)^{\beta})$.

<n> PCA	**τ (s)**	**β**	**Exp. <t> (s)**	**k_{obs} (s^{-1})**
0	1.79×10^{-7}	1.00	1.82×10^{-7}	5.50×10^{6}
5.6	3.12×10^{-6}	0.97	2.94×10^{-6}	3.13×10^{5}
12.1	3.37×10^{-6}	0.94	3.28×10^{-6}	2.82×10^{5}
17.1	3.93×10^{-6}	0.87	4.00×10^{-6}	2.30×10^{5}
18.4	3.72×10^{-6}	0.90	3.39×10^{-6}	2.55×10^{5}
19.0	4.50×10^{-6}	0.82	4.75×10^{-6}	1.92×10^{5}
19.9	4.34×10^{-6}	0.83	4.43×10^{-6}	2.03×10^{5}
20.9	4.83×10^{-6}	0.78	5.39×10^{-6}	1.71×10^{5}
26.2	5.46×10^{-6}	0.72	6.38×10^{-6}	1.43×10^{5}

S3.8. Boltzmann Approximation Derivation

A steady−state approximation was used to determine K_{eq} from steady−state PL measurements.[14] In this model, the relative PL (rPL) of the composite materials to the pristine CdSe585 is used to determine K_{eq} via steady state PL measurements where PL is calculated by Eq. S3.1 .

$$I_{PL} = kI_{ex}\varepsilon b\Phi[A] \qquad \text{Eq. S3.1}$$

Here I_{PL} is the PL intensity, k is an instrumental constant, I_{ex} is the intensity of the excitation beam, ε is the extinction coefficient, b is the path length, Φ is the quantum yield and [A] is the excited state concentration of the sample. If Φ, and ε are assumed to be unchanged in CdSe585

upon ligand exchange, and if I_{ex} and b are fixed experimentally, the changes in I_{PL} between the pristine CdSe585 and CdSe585/PCA become directly proportional to [A]. Changes in [A] are represented by the following Eq. S3.2:

$$[A] = [A_0] \times \frac{k_{rEnT}}{k_{EnT}} \qquad \text{Eq. S3.2}$$

k_{rEnT}/k_{EnT} represents K_{eq} between the CdSe585* and ^{3}PCA*.[15–17] By substituting K_{eq} into Eq. S3.2 and rearranging we determine the value of K_{eq} in Eq. S3.3:

$$K_{eq} = \frac{[A]}{[A]_o} \qquad \text{Eq. S3.3}$$

Keeping the same assumptions used in Eq. S3.2, the relative quantum yield (Φ_{rPL}) is calculated with the PL intensity of CdSe585/PCA materials (I_{TADPL}) and the undecorated CdSe585 PL (I_{0PL}) yielding K_{eq} via Eq. S3.4:

$$\Phi_{rPL} = \frac{I_{TADPL}}{I_{0PL}} = K_{eq} \qquad \text{Eq. S3.4}$$

With K_{eq} in hand, theoretical calculations were performed to determine the expected lifetimes of τ_{TADPL}, using K_{eq} and the unaltered CdSe585 lifetime, τ_{CdSe}, via Eq. S3.5, a modified version of a previously reported equation from Ravinson et al used to model TADF materials.[17]

$$\tau_{TADPL} = \tau_{CdSe} \times K_{eq}^{-1} \qquad \text{Eq. S3.5}$$

Eq. S5 is acceptable under the assumptions $k_{CdSe} >> k_{PCA}$ and k_{rEnT}, $k_{EnT} >> k_{CdSe}$.

Chapter 3 SI References:

1. Knauf, R. R.; Lennox, J. C.; Dempsey, J. L. Quantifying Ligand Exchange Reactions at CdSe Nanocrystal Surfaces. *Chem. Mater.* **2016**, *28*, 4762–4770.

2. Yu, W. W.; Qu, L.; Guo, W.; Peng, X. Experimental Determination of the Extinction Coefficient of CdTe, CdSe, and CdS Nanocrystals. *Chem. Mater.* **2003**, *15*, 2854–2860.

3. Garakyaraghi, S.; Mongin, C.; Granger, D. B.; Anthony, J. E.; Castellano, F. N. Delayed Molecular Triplet Generation from Energized Lead Sulfide Quantum Dots. *J. Phys. Chem. Lett.* **2017**, *8*, 1458–1463.

4. Mongin, C.; Garakyaraghi, S.; Razgoniaeva, N.; Zamkov, M.; Castellano, F. N. Direct Observation of Triplet Energy Transfer from Semiconductor Nanocrystals. *Science* **2016**, *351*, 369–372.

5. Mongin, C.; Moroz, P.; Zamkov, M.; Castellano, F. N. Thermally Activated Delayed Photoluminescence from Pyrenyl-Functionalized CdSe Quantum Dots. *Nat. Chem.* **2018**, *10*, 225–230.

6. La Rosa, M.; Denisov, S. A.; Jonusauskas, G.; McClenaghan, N. D.; Credi, A. Designed Long-Lived Emission from CdSe Quantum Dots through Reversible Electronic Energy Transfer with a Surface-Bound Chromophore. *Angew. Chem.* **2018**, *130*, 3158–3161.

7. Korovina, N. V.; Joy, J.; Feng, X.; Feltenberger, C.; Krylov, A. I.; Bradforth, S. E.; Thompson, M. E. Linker-Dependent Singlet Fission in Tetracene Dimers. *J. Am. Chem. Soc.* **2018**, *140*, 10179–10190.

8. Okamoto, T.; Suzuki, T.; Tanaka, H.; Hashizume, D.; Matsuo, Y. Tetracene Dicarboxylic Imide and Its Disulfide: Synthesis of Ambipolar Organic Semiconductors for Organic Photovoltaic Cells. *Chem. – Asian J.* **2012**, *7*, 105–111.

9. Wells, K. A.; Yarnell, J. E.; Palmer, J. R.; Lee, T. S.; Papa, C. M.; Castellano, F. N. Energy Migration Processes in Re(I) MLCT Complexes Featuring a Chromophoric Ancillary Ligand. *Inorg. Chem.* **2020**, *59*, 8259–8271.

10. Dias, F. B.; Bourdakos, K. N.; Jankus, V.; Moss, K. C.; Kamtekar, K. T.; Bhalla, V.; Santos, J.; Bryce, M. R.; Monkman, A. P. Triplet Harvesting with 100% Efficiency by Way of Thermally Activated Delayed Fluorescence in Charge Transfer OLED Emitters. *Adv. Mater.* **2013**, *25*, 3707–3714.

11. Robel, I.; Kuno, M.; Kamat, P. V. Size-Dependent Electron Injection from Excited CdSe Quantum Dots into TiO2 Nanoparticles. *J. Am. Chem. Soc.* **2007**, *129*, 4136–4137.

12. Soloviev, V. N.; Eichhöfer, A.; Fenske, D.; Banin, U. Size-Dependent Optical Spectroscopy of a Homologous Series of CdSe Cluster Molecules. *J. Am. Chem. Soc.* **2001**, *123*, 2354–2364.

13. Williams, G.; Watts, D. C. Non-Symmetrical Dielectric Relaxation Behaviour Arising from a Simple Empirical Decay Function. *Trans. Faraday Soc.* **1970**, *66*, 80–85.

14. Finkenzeller, W. J.; Yersin, H. Emission of Ir(Ppy)3. Temperature Dependence, Decay Dynamics, and Magnetic Field Properties. *Chem. Phys. Lett.* **2003**, *377*, 299–305.

15. Tyson, D. S.; Henbest, K. B.; Bialecki, J.; Castellano, F. N. Excited State Processes in Ruthenium(II)/Pyrenyl Complexes Displaying Extended Lifetimes. *J. Phys. Chem. A* **2001**, *105*, 8154–8161.

16. McClenaghan, N. D.; Barigelletti, F.; Maubert, B.; Campagna, S. Towards Ruthenium(II) Polypyridine Complexes with Prolonged and Predetermined Excited State Lifetimes. *Chem. Commun.* **2002**, No. 6, 602–603.

17. Ravinson, D. S. M.; Thompson, M. E. Thermally Assisted Delayed Fluorescence (TADF): Fluorescence Delayed Is Fluorescence Denied. *Mater. Horiz.* **2020**, *7*, 1210–1217.

Chapter 4:1D, 2D, 3D, Red Dot, Green Dot, Blue Dot, All in Efforts to Exploit Morphology

Chapter 4 Preface

Understanding the effects of interfacial concentration in 0D materials obviates the next research progression: studying a variety of morphologies with different surface areas to identify the utility of entropically driven surface phenomena. Previous studies have identified a relationship between thermally activated delayed photoluminescence (TADPL) lifetime and the number of acceptors involved for both molecular systems and for quantum-dot/molecule composites (QD/mol) materials.[1–6] In the case of QD/mol species, unlike purely molecular systems, simple changes in the morphology of the quantum confined material allow for dramatic changes in the available surface area providing substantial increases in the number of surface bound acceptors. By implementing non-0D materials, the theoretical limit of lifetime extension becomes accessible via a shift in excited state equilibrium from the quantum confined material to the molecular acceptor.[7,8] Understanding the dynamics of such a system requires additional troubleshooting to develop the appropriate starting materials and fully characterizing them to determine the number of absorbed molecules. Unfortunately, the results that were desired, an extension of the nanorod (NR) lifetime via TADPL, were not achieved. Instead, the results indicate a surface healing effect similar to other QD/mol systems and suggest further efforts are necessary to achieve strong TADPL character from materials of this type.[9–12] Preliminary results of CdSe rods with appended PCA are discussed below.

Abstract: Nanocrystal semiconductors have demonstrated useful photochemical properties for many applications, with quantum-dot/molecule composites (QD/mol) demonstrating very useful optoelectronic and photonic properties. The leading research in QD/mol has led to the interest in anisotropic materials such as nanocrystal-rod/molecule composites (NR/mol) due to their similar properties but increased surface area allowing for increased surface anchored acceptors. Triplet-triplet energy transfer (TTET) at QD/mol interface has been reported, however a comprehensive understanding of the NR/mol materials remains elusive. The current work also includes a series of cadmium(II) selenide/1-pyrenecarboxylic acid (CdSe/PCA) nanomaterials featuring variable PCA surface coverage in CdSe577 (coded by the peak of the first exciton absorption band) to gain insight into the design parameters necessary to achieve predictable NR/mol photophysical behavior. By tailoring the energy gap between the CdSe577 first exciton band (2.17 eV) and the lowest PCA triplet level (T_1 = 2.00 eV) to be nearly isoenergetic, strong thermally activated delayed photoluminescence (TADPL) was expected with a resultant lifetime increase in the materials bright state. The lifetimes observed for these materials however showed negligible changes with additional PCA loadings indicating a more complex ligand exchange than previously denoted for 0D composite materials of the same family. Thus, more experiments are necessary to identify the systematic exchange of the NRs surface ligands to fully elucidate the photophysical characteristics of these materials in a controlled way.

Introduction

The scientific community has invested considerable efforts to develop a new class of nanocrystals with bound acceptors, specifically quantum dot-molecule composites (QD/mol) and nanocrystal rod-molecule composites (NR/mol) .[2,5,6,13–28] These photophysical constructs meld the highly tunable, strongly absorbing, and synthetically facile nature of QDs and NRs with well-

established molecular chromophores to exploit interfacial photo-induced energy transfer (EnT) reactions.[5,6,14–20] This is carried out through the specific characteristics of both the molecule of interest and the nanocrystals. Modifications of QD/mols and NR/mols are reported for a variety of photophysical applications with extensive research in photocatalysis and excited state lifetime extension.[14–20,25–30] The change in observed photophysical properties is a direct result of EnT reactions in the composite materials. Many of the constructs studying these interactions focus mainly on 0D QD/mols for fundamental studies. More recent efforts have expanded to work on anisotropic materials to exploit the nanomaterial's structural properties.[22–24,31,32] For example, the NRs long axis provides potential continuous transport of electrons bypassing the need for electron hopping which in QDs is required.[22,29–32] These studies suggest anisotropic materials offer enhanced material capability in real world applications when compared to their 0D counterparts. Additionally, recent reports have begun to analyze the effects of anchored acceptor number (n) in 0D QD/mol materials demonstrating that simple changes in n yield altered observed photophysics.[1,3–6,33] Relative to 0D materials like QDs, NRs and other anisotropic materials have substantial surface area increases allowing for increased maximum values of n as demonstrated in **Figure 4.1**.[22,31,34] Despite these changes the available research on the subject leaves much to be discovered. As such, NR/mols, with their versatile photochemically-active systems, are prepped for a variety of exploratory research efforts across numerous application-specific demands.[22,31,34,35]

The potential for NR/mol materials is great, but there is a lack of understanding of their excited state reaction dynamics which remain particularly elusive in comparison to QD/mols and purely molecular counterparts that display similar energy transfer reactions.[15,25,29–31,33] One of the questions that has gone unanswered for NR/mol systems is the effect of molecular acceptor concentration/surface coverage on the resultant photophysical properties. Some recent studies with

QD/mols have demonstrated an interfacial acceptor concentration dependence on observed photophysical behavior which is otherwise ignored in previous QD/mol reports.[2,5,6,13,14,16,18–21,36] Likewise, NRs possess a notable change in surface area as a function of size, however, a systematic study monitoring the effects of surface concentration has yet to be performed. This is interesting because recent studies have elucidated a clear impact in surface concentration for QD/mol systems as an effective means to tune energy transfer dynamics.[5,6] Given that the available surface area of anisotropic materials is substantially larger than that observed for dots, **Figure 4.1**, it seems obvious to explore these changes in interfacial concentration in non-0D morphologies.

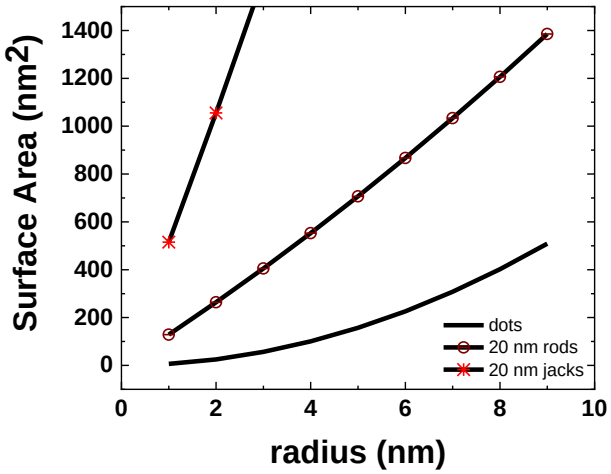

Figure 4.1. Relative surface area variation of quantum-jacks, nanocrystal-rods, and quantum-dots with the same basal radius. The surface area trends demonstrate a significant increase as the morphology becomes increasingly less 0D.

To ensure that observed photophysical changes are a result of solely surface acceptor number, it is important in each instance of synthesizing these anisotropic nanocrystals to have reproducible materials for a comprehensive and cohesive study. Here, we specifically aim to monitor thermally activated delayed photoluminescence (TADPL) to build on our previous work in QD/mols and expand our understanding of surface effects in TADPL active composite materials.[5,8] The current study addresses this question regarding the influence of molecular

acceptor surface concentration by monitoring the photophysical behavior of NR/mol materials that are energetically thermally accessible to achieve TADPL. This is achieved by using a series of cadmium(II) selenide/1-pyrenecarboxylic acid (CdSe/PCA) nanomaterials featuring variable PCA surface coverage in CdSe577 NRs (coded by the peak of the first exciton absorption band). These materials were chosen to elucidate the observed photophysical properties of these materials between the CdSe577 bright state and the bound PCA molecular triplet when their energies, 2.17eV and 2.00 eV respectively, are nearly isoenergetic and theoretically thermally accessible allowing for TADPL.[2,5,8,18]

Results

The CdSe577 NRs were synthesized using an adapted literature procedure described in the experimental section. TEM experiments were performed on pristine NRs and on NR/mol with the maximum acceptor loading, 4 mg of PCA and are shown in **Figure 4.2**. These experiments are critical for anisotropic materials to verify their non 0D nature. The CdSe NRs shown in **Figure 4.2a**, were determined to have an average surface area of 72 nm^2 (18 nm x 4 nm, length x diameter), as previously reported by Mokari and Banin.[37] If TEM experiments do not demonstrate a well-defined rod structure, a new batch of rods must be prepared before continuing to further experiments.

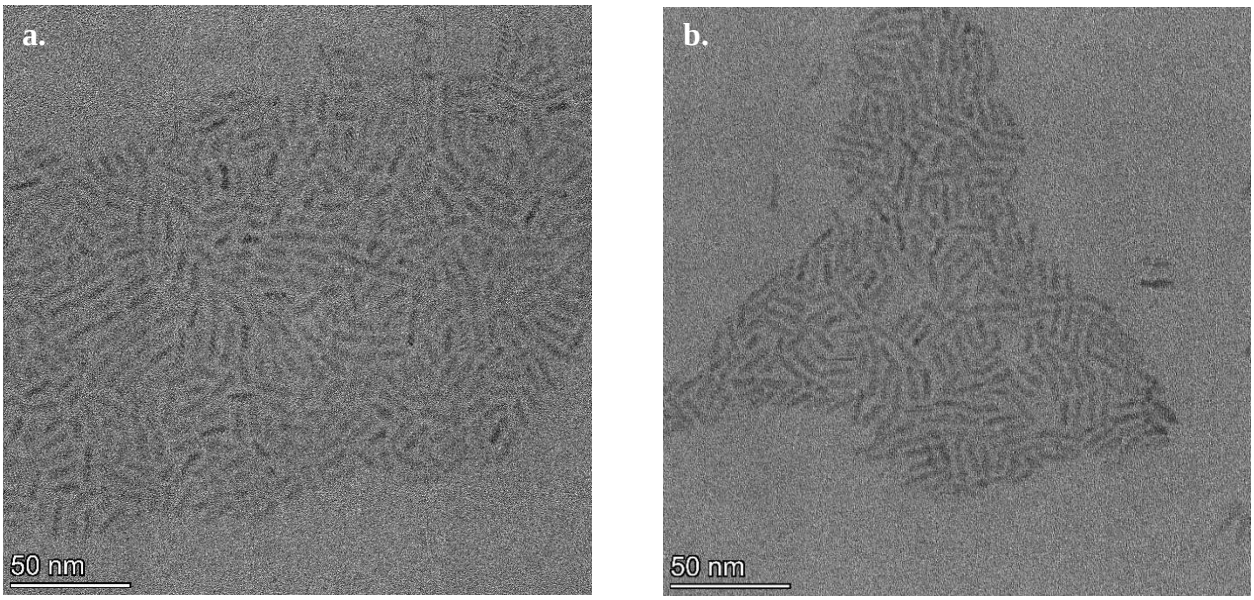

Figure 4.2. a. Representative TEM image of CdSe577 NRs before ligand exchange. b. Representative TEM image of CdSe577/PCA after addition of the maximum acceptor loading, 4 mg PCA. No changes are noted in morphology between a. and b. suggesting retention of the pristine material's properties post ligand exchange.

To ensure that the synthesized materials were suitable for complex photophysical investigation, the NRs were further screened for selected photophysical properties via steady-state absorbance and photoluminescence spectroscopy. These measurements, shown in **Figures 4.3** and **4.4**, verify the quality of the materials by identifying the extent of quantum confinement, monitoring the full width at half max (FWHM) (± 0.029 eV), asymmetry of the PL band to verify the monodispersity seen in TEM images, and check for the observation of sub-bandgap trap states. In the case of absorbance (**Figure 4.3**), the pristine NR materials have a first exciton band centered at 577 nm (2.14 eV), making them theoretically energetically accessible for TADPL.[8]

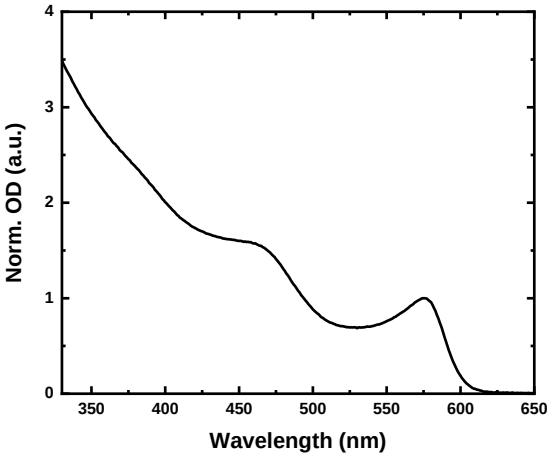

Figure 4.3. Representative absorption spectra of CdSe577 NRs used for NR/mol composite materials confirming first exciton band at an acceptable wavelength of 577 nm with reasonable quantum confinement.

Upon verification of the energy of the materials via absorbance measurements, PL spectra were collected to determine the material's monodispersity and presence of sub-bandgap trap states. If the material is polydisperse or has significant trap states, the PL spectra will have significant asymmetry or potentially multiple peaks and/or shoulders. **Figure 4.4** illustrates suitable PL spectra of CdSe NRs with a symmetric PL band, no signs of trap states, and narrow FWHM (± 0.029 eV) indicating these materials are suitable for ligand exchange reactions. Once successful screening is completed, NRs are subjected to ligand exchange as detailed in the experimental section. The successful screening ensures that the changes in observed photophysics of the end NR/mol material are solely altered through the introduction of interfacial acceptors.

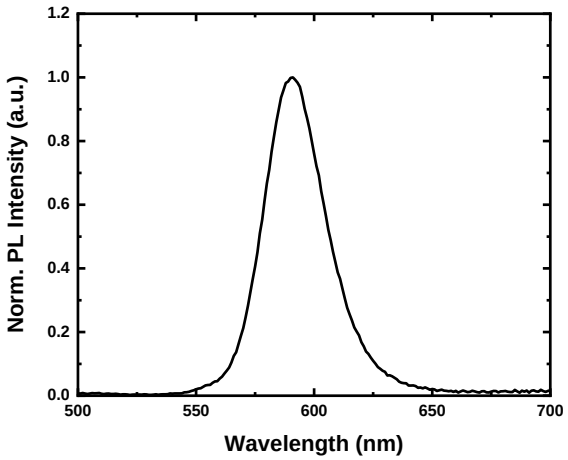

Figure 4.4. Representative photoluminescence spectra of CdSe577 NRs. There are no sub-bandgap trap states observed and symmetry in the spectra is noted for the NRs. Sample would be deemed acceptable for further use.

To show retention of the pristine CdSe577 NRs morphology post ligand exchange, representative TEM was performed on the CdSe577/PCA sample with the highest loading of PCA (4 mg) (**Figure 4.2b**). The CdSe577 NR/mol materials shown in **Figure 4.2b**, retain their aspect ratio of 18 nm x 4 nm (length x diameter) upon ligand exchange. Therefore, these representative TEM experiments give insight that the NR structure is retained through the exchange process as the addition of chromophore at the highest loading is not destructive to the initial material. By logical deduction, this also suggests the exchange reactions utilizing less PCA also retain their intrinsic properties as observed previously in 0D materials.[2,5,17,18,20,36] Still, spectroscopic comparison of the pristine, as-synthesized CdSe577 to surface-exchanged CdSe577/PCA_n is important to ensure the ligand exchange has occurred and to verify that the NR/mol's material photophysical integrity has not been compromised. Previously, the absorbance spectra of the various CdSe/PCA_n materials indicate the systematic increase of the PCA band at ~350 nm with increased acceptor loading n (See chapter 3) .[5] As such, absorbance measurements were conducted to determine if the same trend observed in 0D materials is observed in this NR/PCA series. **Figure**

4.5a shows the absorbance spectra overlay of the pristine NR material and the surface-exchanged NR/mol composite materials.

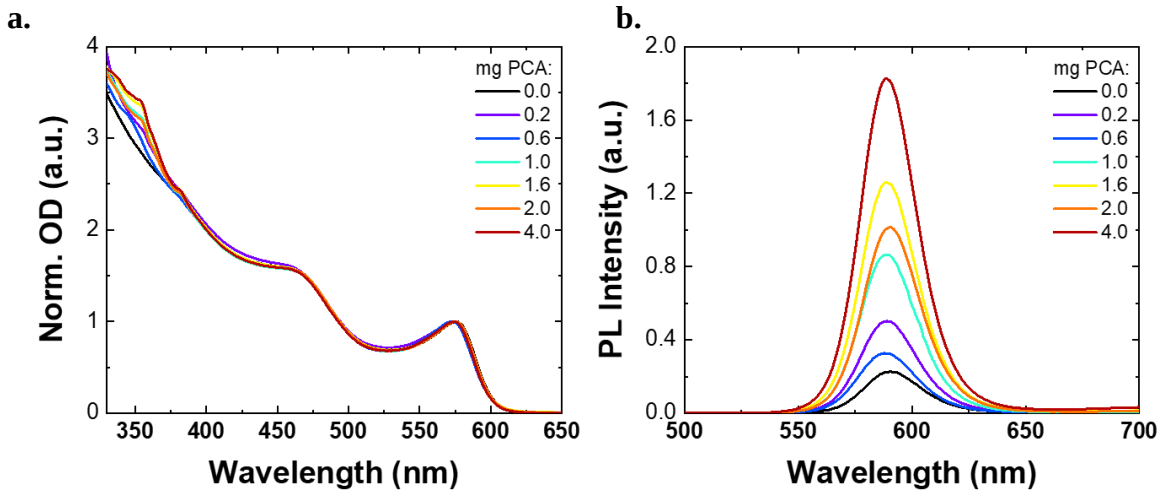

Figure 4.5. a. UV-Vis spectra of CdSe/PCA_n composites measured in toluene indicating an increase in the PCA band at ~350 nm with increased loading. **b.** Photoluminescence spectra of CdSe577/PCA_n composites measured in toluene measured at room temperature with 475 nm excitation. Curiously, the PL intensity appears to be arbitrary relative to PCA loading.

In the case of the CdSe577 NRs, as additional chromophores are added to the surface, no spectral changes were noted in the absorbance spectra for the CdSe577/PCA NR's first exciton band when compared to the pristine material, **Figure 4.5a**. This suggests that the materials retain both their size and quantum confinement properties upon ligand exchange.[34] In **Figure 4.5a**, the peak increasing at ~350 nm shows indication of additional PCA bound to the NRs. When compared to CdSe QD/mols, CdSe NR/mols show a less profound increase of the PCA band with the same loading of chromophore and indicates a less efficient adsorption of chromophore onto the NRs surface. This result indicates a more complex surface chemistry than previously observed for the 0D counterparts of the same material family.

In addition to absorbance measurements, previous studies have elucidated a systematic quenching of the PL intensity of 0D materials as a function of surface bound PCA (See chapter

3).[5] To determine if the same trend is noted for the NR/PCA materials, PL measurements were performed and their spectra are reported in **Figure 4.5b**. The steady-state PL data shown in **Figure 4.5b** indicates no evidence of any red-shifted PL features present in the CdSe/PCA_n materials when compared to the pristine CdSe577 materials. This result suggests there is no generation of trap states during the ligand exchange process. However, **Figure 4.5b** also shows a capricious *increase* in PL intensity with increasing PCA loading. This data suggests that the surface chemistry for these materials is more nuanced than previously expected and will require more troubleshooting as the results are the opposite of what is observed previously for CdSe/PCA QD/mol materials where an increase in the amount of PCA results in steady-state photoluminescence quenching.

For further clarification, information regarding the role of interfacial concentration on CdSe577/PCA_n's dynamics is necessary. Therefore, more intricate time-resolved spectroscopic techniques were conducted to determine the underlying photophysics of the CdSe577/PCA_n materials. Supra-nanosecond time gated emission (TGE) experiments were performed to extract k_{obs} for the various CdSe577/PCA_n materials and determine if a systematic trend is observed based on PCA adsorption. Due to the thermodynamics of the system, an equilibrium between CdSe577 and ^{3}PCA* was expected. This equilibrium was expected to allow the ^{3}PCA* to act as a reservoir that would thermally resupply the CdSe577 bright state resulting in TADPL.[5,18,20,38,39] By introducing additional PCA molecules to the surface of the CdSe577, the equilibrium between the two states is previously reported to entropically shift toward the long lived ^{3}PCA* resulting in systematic lifetime extension as a function of n.[2,5,18,38] Similar results were expected to occur in the CdSe577/PCA_n materials.

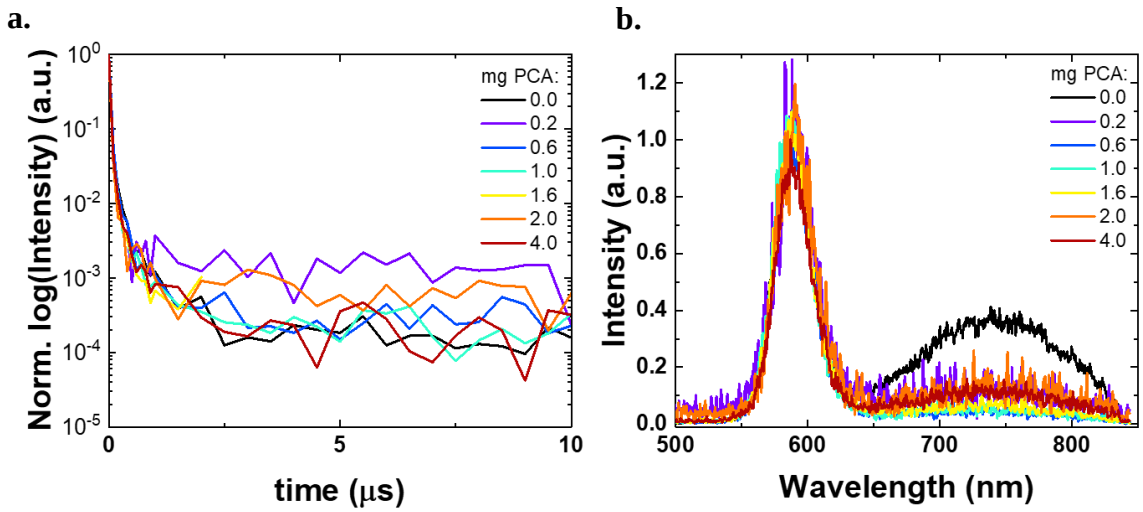

Figure 4.6. a. Representative single wavelength kinetic trace of the TGE signal of CdSe/PCA$_n$ series measured in degassed tol at room temperature following selective excitation (475 nm, 2.0 mJ/pulse) of CdSe. Average lifetimes calculated using a stretch exponential fit, $I(t) = A \exp(-t/\tau)^{\beta}$), further explanation is listed below. **b.** Representative prompt TGE spectra of CdSe/PCA$_n$ series measured in degassed Tol at room temperature following selective excitation (2.0 mJ/pulse) of CdSe at 475 nm.

To verify whether these materials demonstrate a lifetime dependence as a function of bound PCA, the pristine TGE kinetics were compared to the NR/mol materials. In **Figure 4.6a**, the kinetic trace of the CdSe577/PCA$_n$ NR/mols is shown and qualitatively demonstrates that the observed lifetime changes appear to be trivial. Fitting of the kinetic traces further suggests that the lifetime changes observed in the CdSe577/PCA$_n$ NR/mols materials is negligible. Average lifetime values ($<\tau>$) for these materials, displayed in **Table 4.1**, quantify this result demonstrating no significant change in the lifetime of these materials. This is an interesting result as previous reports indicate orders of magnitude lifetime increases with the addition of PCA.[2,5,18] In **Figure 4.6b**, the spectral TGE of the CdSe577/PCA materials is shown indicating the presence of trap emission centered at ~750 nm previously undetected in ssPL measurements. For the NR/PCA composite materials, substantial changes are observed in the low energy trap emission. This suggests the PCA is passivating the surface of the NRs, as there is a reduction of trap emission centered at ~750 nm in the TGE spectra, and increased ssPL intensity in **Figure 4.5b**, of the NR/PCA materials relative

to the pristine CdSe577. This is not entirely surprising and suggests that the initial surfactants used in the pristine materials play a sophisticated and layered role in not just the material's intrinsic properties, as commonly reported for quantum confined materials, but also in the ligand exchange processes that we employ to develop these composite materials.[2,5,18,20,40,41] As observed time constants for the CdSe577/PCA_n materials do not change in a meaningful way, more experiments are necessary to understand the chemistry taking place for the CdSe577/PCA_n NR/mol composite materials.

Table 4.1. Kinetic fitting parameters for CdSe/PCA materials from TGE experiments. Lifetimes calculated using a stretch exponential fit $I(t) = Aexp(-(t/\tau)^{\beta})$. $<\tau>$ was extracted using the derived experimental values β and τ and the following equation: $< \tau> = (\tau/ \beta) \times \Gamma(1/ \beta)$

mg PCA	τ (s)	β	<t> (s)	k_{obs} (s^{-1})
0.0	5.81×10^{-9}	0.40	1.98×10^{-8}	5.04×10^{7}
0.2	1.33×10^{-8}	0.55	2.29×10^{-8}	4.37×10^{7}
0.6	1.18×10^{-8}	0.50	2.39×10^{-8}	4.20×10^{7}
1.0	7.61×10^{-9}	0.45	1.88×10^{-8}	5.33×10^{7}
1.6	9.04×10^{-9}	0.48	1.92×10^{-8}	5.20×10^{7}
2.0	6.40×10^{-9}	0.45	1.59×10^{-8}	6.27×10^{7}
4.0	7.10×10^{-9}	0.44	1.84×10^{-8}	5.43×10^{7}

Conclusion

Overall, the preliminary data in this report illustrates the complex nature of the photophysical properties of NR/mol composites. The τ_{obs} values should increase with the addition of n PCA on CdSe577 due to TADPL being enabled, however, the trends previously reported for 0D materials of the same type are not observed in these materials. These results suggest that the

surface environment in the pristine NR materials plays a crucial role in the development of TADPL active materials. Further exploration is necessary to fully uncover the role of surface chemistry in these materials. Still, the retention of the pristine CdSe NR's morphological characteristics by TEM post ligand exchange is encouraging as it suggests the surface treatments retain the material's initial characteristics. This is an important quality for performing meaningful photophysical experiments in these materials. Further, understanding the variance in post-synthetic processing of NR/mol relative to QD/mols is critical to pursuing composite materials with deterministic photophysical properties, including the barriers to achieving bespoke properties between systems.

Experimental Section

Cadmium Oxide (CdO, 99.995% trace metal basis, BTC), Selenium powder (Se^0, 99.5% trace metal basis, Aldrich), Tri-n-butylphosphine (TBP, 99% trace metal basis), Trioctylphosphine oxide (TOPO, 99% trace metal basis), Tetradecylphosphonic acid (TDPA, 98% trace metal basis), Toluene (ACS gr. 99.5%), Methanol (MeOH, ACS gr. 99.5%), Acetone (ACS gr. 99.5%), 1-pyrenecarboxylic acid (PCA, >97% TCI), were all used as received without further purification unless otherwise noted.

The CdSe570 NRs were synthesized using an adapted literature procedure via Sitt, A. et al.[24] Cadmium(II) oxide (CdO, 145.2 mg, 1.13 mmol), Trioctylphosphine oxide (TOPO, 4 g, 10 mmol), Tetradecylphosphonic acid (TDPA, 629 mg, 2.26 mmol) were combined in a 250 mL 3-neck flask equipped with a thermometer, dry-ice reflux condenser with nitrogen adapter, rubber septa and stir bar. Once added, the reaction was degassed via vacuum for 30 mins at 100 °C to remove water and air while stirring vigorously. The reaction flask was then subjected to a nitrogen (N_2) atmosphere and the temperature was slowly raised to 280 °C to avoid overheating. The reaction slowly turned from a dark copper brown color to a clear, colorless solution indicating the

successful conversion from CdO to cadmium(II) tetradecylphosphate ($Cd(TDPA)_2$). Note that if the reaction were not well degassed or the temperature was not well controlled and exceeds ~290 $^{\circ}C$, the reaction would not fully convert and will be a clear, pale yellow color, and will result in lower yields. Once $Cd(TDPA)_2$ formed, tri-n-butylphosphine (TBP, 404.9 mg, 2 mmol) was added dropwise to the reaction mixture with a N_2 conditioned syringe. The reaction mixture was then heated slowly to 360 $^{\circ}C$. During this process a cloudy gas forms, but quickly dissipates if slowly heated. While the reaction was heating, a solution of selenium powder (Se^0, 64 mg, 8.11 mmol) and tri-n-butylphosphine (TBP, 1.721 g, 8.51 mmol) was prepared by mixing the Se^0 with TBP in a vial in the glovebox. Once at 360 $^{\circ}C$, the temperature was lowered to 290 $^{\circ}C$ and the TBPSe solution was injected using a N_2 conditioned syringe all at once, the reaction mixture then turned to a dark red color. The temperature was maintained at 290 $^{\circ}C$ for 10 mins. After 10 mins, the solution was quenched with 40 mL of cold toluene to yield the desired material size and the resultant solution was a strawberry kool aid red. The materials were then left to cool to room temperature before being washed. Under a handheld blacklight with 365 nm excitation, the reaction solution, before washing, emitted a yellow/orange color.

Washing was completed using centrifugation at 4300 rpm. This was done by the addition of methanol to the reaction mixture in a 5:1 ratio to remove excess reactants. This was repeated 3 times with spectral grade toluene (tol) used sparingly (~1 mL) to redissolve the precipitate between washes. Upon completion, a solid pellet of CdSe NRs should form. The pellet was then dried completely using Schlenk line techniques and stored in 2 mL of tol.

To ensure synthesized materials are suitable for complex photophysical investigation, steady-state absorbance and photoluminescence measurements were conducted on the washed CdSe NRs. Once the NRs are verified as adequate candidates, the ligand exchange was done using

a revised synthesis from previously reported methodologies.[2,5,15,18,20] A stock solution of the acceptor molecule was generated by measuring >20 mg of acceptor and dissolving in spectral grade acetone (ACE). Aliquots corresponding to the desired mg amounts of acceptor were then added to vials and the vials were set aside to allow the solvent to slowly evaporate until gone and generate crystalline acceptor. While the crystals formed, a stock solution of CdSe was made by dissolving the CdSe NRs in tol. This solution was examined via steady state absorbance in a 2 mm cuvette to ensure ~2 abs at the materials first exciton band (Eg). This step has proven important in preceding composite studies to prevent destruction of the material during ligand exchange; previously, if the CdSe QD was not concentrated enough the addition of acceptor would cause a broadening of the CdSe Eg and the nanoparticles would become colloidally unstable.[2,5,14,34,35] As such, the same techniques were used with the NRs to avoid possible destruction of the materials. Once the acceptor crystals formed, 100 μL of ace was added to the vials to redissolve the crystals, followed by 1 mL of the CdSe NR stock solution. The reaction mixtures were then sealed with parafilm, placed in a sonicator preheated to 35 °C, and sonicated for 1 hour in the dark. Once the sonication was completed, the reactions were removed and allowed to cool to room temperature before being isolated.

To isolate the composite materials from excess acceptor in solution, washing steps were performed. The solution was drawn into a syringe along with 3 mL of MeOH to precipitate the CdSe/mol. The syringe was inverted three times to perturb the precipitate and to ensure adequate washing of the materials. The solution was passed through a 0.450 μm syringe filter. As the CdSe/mol materials are insoluble in MeOH, this precipitates the CdSe/mol materials and removes excess unbound acceptor which readily dissolve in MeOH. In a clean syringe 2 mL of tol was drawn and passed through the same syringe filter to extract the precipitated CdSe/mol composites

via dissolution into tol. The materials are used without further purification and stored in a 1-dram vial sealed with parafilm.

Optical Experimental Methods

Steady state electronic absorption experiments (UV-vis) were performed using a Shimadzu UV-3600 and Agilent 8453 UV-visible spectrometer. Steady-state photoluminescence experiments (PL) were performed using an Edinburgh FLS 980 fluorimeter. Samples were excited at 475 nm with an OD at excitation of 0.1 at room temperature.

Time-Gated Photoluminescence measurements (TGE) were executed using an Edinburgh Instruments LP920 laser flash photolysis system (Edinburgh Instruments) equipped with an iStar ICCD camera (Andor Technology) controlled by the L900 software package. The reported TGE spectra are the average of 10 laser pulses. Sample excitation was achieved with a vibrant LD 355 II Nd:YAG/OPO laser system (OPOTEK) functioning at 1 Hz. The pulse energy of the laser was manipulated using neutral density filters to achieve the desired pulse energy of 2.0 mJ/pulse. Samples were prepared in spectrophotometric grade toluene and degassed via standard freeze-pump-thaw technique with a minimum of three cycles in a 10 mm path length custom quartz optical cell. Samples were prepared to an optical density of 0.4 at the excitation wavelength (λ_{ex} = 475 nm). Experiments were performed at room temperature.

Chapter 4 Acknowledgments

We thank Margaret H. Hudson and Christopher M. Papa at NC State University for their fruitful discussions and suggestions. This work was supported by the Organic Materials Chemistry Program in the Air Force Office of Scientific Research (FA9550-18-1-0331). I'd also like to thank my coauthors Megan E. Griffin, and Felix N. Castellano for their contributions.

Chapter 4 References

1. Goze, C.; Kozlov, D. V.; Tyson, D. S.; Ziessel, R.; Castellano, F. N. Synthesis and Photophysics of Ruthenium(II) Complexes with Multiple Pyrenylethynylene Subunits. *New J. Chem.* **2003**, *27* (12), 1679–1683.

2. Mongin, C.; Moroz, P.; Zamkov, M.; Castellano, F. N. Thermally Activated Delayed Photoluminescence from Pyrenyl-Functionalized CdSe Quantum Dots. *Nat. Chem.* **2018**, *10* (2), 225–230.

3. Tyson, D. S.; Henbest, K. B.; Bialecki, J.; Castellano, F. N. Excited State Processes in Ruthenium(II)/Pyrenyl Complexes Displaying Extended Lifetimes. *J. Phys. Chem. A* **2001**, *105* (35), 8154–8161.

4. McClenaghan, N. D.; Barigelletti, F.; Maubert, B.; Campagna, S. Towards Ruthenium(II) Polypyridine Complexes with Prolonged and Predetermined Excited State Lifetimes. *Chem. Commun.* **2002**, No. 6, 602–603.

5. Yonemoto, D. T.; Papa, C. M.; Sheykhi, S.; Castellano, F. N. Controlling Thermally Activated Delayed Photoluminescence in CdSe Quantum Dots through Triplet Acceptor Surface Coverage. *J. Phys. Chem. Lett.* **2021**, 3718–3723.

6. Zhang, J.; Kouno, H.; Yanai, N.; Eguchi, D.; Nakagawa, T.; Kimizuka, N.; Teranishi, T.; Sakamoto, M. Number of Surface-Attached Acceptors on a Quantum Dot Impacts Energy Transfer and Photon Upconversion Efficiencies. *ACS Photonics* **2020**.

7. Schmehl, R. H. Something New in Transition Metal Complex Sensitizers: Bringing Metal Diimine Complexes and Aromatic Hydrocarbons Together. *The Spectrum* **2000**, *13* (2), 17–21.

8. Yonemoto, D. T.; Papa, C. M.; Mongin, C.; Castellano, F. N. Thermally Activated Delayed Photoluminescence: Deterministic Control of Excited-State Decay. *J. Am. Chem. Soc.* **2020**, *142* (25), 10883–10893.

9. Zhang, X.; Hudson, M. H.; Castellano, F. N. Passivation of Electron Trap States in InP Quantum Dots with Benzoic Acid Ligands. *J. Phys. Chem. C* **2021**.

10. Houtepen, A. J.; Hens, Z.; Owen, J. S.; Infante, I. On the Origin of Surface Traps in Colloidal II–VI Semiconductor Nanocrystals. *Chem. Mater.* **2017**, *29* (2), 752–761.

11. Kim, T.-G.; Zherebetskyy, D.; Bekenstein, Y.; Oh, M. H.; Wang, L.-W.; Jang, E.; Alivisatos, A. P. Trap Passivation in Indium-Based Quantum Dots through Surface Fluorination: Mechanism and Applications. *ACS Nano* **2018**, *12* (11), 11529–11540.

12. Hughes, K. E.; Stein, J. L.; Friedfeld, M. R.; Cossairt, B. M.; Gamelin, D. R. Effects of Surface Chemistry on the Photophysics of Colloidal InP Nanocrystals. *ACS Nano* **2019**, *13* (12), 14198–14207.

13. Cossairt, B. M.; Juhas, P.; Billinge, S. J. L.; Owen, J. S. Tuning the Surface Structure and Optical Properties of CdSe Clusters Using Coordination Chemistry. *J. Phys. Chem. Lett.* **2011**, *2* (24), 3075–3080.

14. Garakyaraghi, S.; Castellano, F. N. Nanocrystals for Triplet Sensitization: Molecular Behavior from Quantum-Confined Materials. *Inorg. Chem.* **2018**, *57* (5), 2351–2359.

15. Garakyaraghi, S.; Mongin, C.; Granger, D. B.; Anthony, J. E.; Castellano, F. N. Delayed Molecular Triplet Generation from Energized Lead Sulfide Quantum Dots. *J. Phys. Chem. Lett.* **2017**, *8* (7), 1458–1463.

16. Huang, Z.; Tang, M. L. Designing Transmitter Ligands That Mediate Energy Transfer between Semiconductor Nanocrystals and Molecules. *J. Am. Chem. Soc.* **2017**, *139* (28), 9412–9418.

17. Jiang, Y.; Wang, C.; Rogers, C. R.; Kodaimati, M. S.; Weiss, E. A. Regio- and Diastereoselective Intermolecular [2+2] Cycloadditions Photocatalysed by Quantum Dots. *Nat. Chem.* **2019**, *11* (11), 1034–1040.

18. La Rosa, M.; Denisov, S. A.; Jonusauskas, G.; McClenaghan, N. D.; Credi, A. Designed Long-Lived Emission from CdSe Quantum Dots through Reversible Electronic Energy Transfer with a Surface-Bound Chromophore. *Angew. Chem.* **2018**, *130* (12), 3158–3161.

19. Li, X.; Huang, Z.; Zavala, R.; Tang, M. L. Distance-Dependent Triplet Energy Transfer between CdSe Nanocrystals and Surface Bound Anthracene. *J. Phys. Chem. Lett.* **2016**, *7* (11), 1955–1959.

20. Mongin, C.; Garakyaraghi, S.; Razgoniaeva, N.; Zamkov, M.; Castellano, F. N. Direct Observation of Triplet Energy Transfer from Semiconductor Nanocrystals. *Science* **2016**, *351* (6271), 369–372.

21. Moroz, P.; Romero, L. R.; Zamkov, M. Colloidal Semiconductor Nanocrystals in Energy Transfer Reactions. *Chem. Commun.* **2019**, *55* (21), 3033–3048.

22. Rastogi, P.; Palazon, F.; Prato, M.; Di Stasio, F.; Krahne, R. Enhancing the Performance of CdSe/CdS Dot-in-Rod Light-Emitting Diodes via Surface Ligand Modification. *ACS Appl. Mater. Interfaces* **2018**, *10* (6), 5665–5672.

23. Cunningham, P. D.; Souza, J. B.; Fedin, I.; She, C.; Lee, B.; Talapin, D. V. Assessment of Anisotropic Semiconductor Nanorod and Nanoplatelet Heterostructures with Polarized Emission for Liquid Crystal Display Technology. *ACS Nano* **2016**, *10* (6), 5769–5781.

24. Sitt, A.; Salant, A.; Menagen, G.; Banin, U. Highly Emissive Nano Rod-in-Rod Heterostructures with Strong Linear Polarization. *Nano Lett.* **2011**, *11* (5), 2054–2060.

25. Zhao, L.; Pang, X.; Adhikary, R.; Petrich, J. W.; Jeffries-EL, M.; Lin, Z. Organic−Inorganic Nanocomposites by Placing Conjugated Polymers in Intimate Contact with Quantum Rods. *Adv. Mater.* **2011**, *23* (25), 2844–2849.

26. Wang, W.; Kong, Y.; Jiang, J.; Tian, X.; Li, S.; Akshath, U. S.; Tiede, C.; Hondow, N.; Yu, A.; Guo, Y.; Zhou, D. Photon Induced Quantum Yield Regeneration of Cap-Exchanged CdSe/CdS Quantum Rods for Ratiometric Biosensing and Cellular Imaging. *Nanoscale* **2020**, *12* (16), 8647–8655.

27. Rothenberg, E.; Kazes, M.; Shaviv, E.; Banin, U. Electric Field Induced Switching of the Fluorescence of Single Semiconductor Quantum Rods. *Nano Lett.* **2005**, *5* (8), 1581–1586.

28. Koole, R.; Schapotschnikow, P.; de Mello Donegá, C.; Vlugt, T. J. H.; Meijerink, A. Time-Dependent Photoluminescence Spectroscopy as a Tool to Measure the Ligand Exchange Kinetics on a Quantum Dot Surface. *ACS Nano* **2008**, *2* (8), 1703–1714.

29. Gur, I.; Fromer, N. A.; Geier, M. L.; Alivisatos, A. P. Air-Stable All-Inorganic Nanocrystal Solar Cells Processed from Solution. *Science* **2005**, *310* (5747), 462–465.

30. Huynh, W. U.; Dittmer, J. J.; Alivisatos, A. P. Hybrid Nanorod-Polymer Solar Cells. *Science* **2002**, *295* (5564), 2425–2427.

31. Zhu, H.; Lian, T. Enhanced Multiple Exciton Dissociation from CdSe Quantum Rods: The Effect of Nanocrystal Shape. *J. Am. Chem. Soc.* **2012**, *134* (27), 11289–11297.

32. Zhao, L.; Pang, X.; Adhikary, R.; Petrich, J. W.; Lin, Z. Semiconductor Anisotropic Nanocomposites Obtained by Directly Coupling Conjugated Polymers with Quantum Rods. *Angew. Chem.* **2011**, *123* (17), 4044–4048.

33. Castellano, F. N. Altering Molecular Photophysics by Merging Organic and Inorganic Chromophores. *Acc. Chem. Res.* **2015**, *48* (3), 828–839.

34. Yu, W. W.; Qu, L.; Guo, W.; Peng, X. Experimental Determination of the Extinction Coefficient of CdTe, CdSe, and CdS Nanocrystals. *Chem. Mater.* **2003**, *15* (14), 2854–2860.

35. Brus, L. Electronic Wave Functions in Semiconductor Clusters: Experiment and Theory. *J. Phys. Chem.* **1986**, *90* (12), 2555–2560.

36. Olshansky, J. H.; Harvey, S. M.; Pennel, M. L.; Krzyaniak, M. D.; Schaller, R. D.; Wasielewski, M. R. Using Photoexcited Core/Shell Quantum Dots To Spin Polarize Appended Radical Qubits. *J. Am. Chem. Soc.* **2020**.

37. Mokari, T.; Banin, U. Synthesis and Properties of CdSe/ZnS Core/Shell Nanorods. *Chem. Mater.* **2003**, *15* (20), 3955–3960.

38. Yarnell, J. E.; Wells, K. A.; Palmer, J. R.; Breaux, J. M.; Castellano, F. N. Excited-State Triplet Equilibria in a Series of Re(I)-Naphthalimide Bichromophores. *J. Phys. Chem. B* **2019**, *123* (35), 7611–7627.

39. Yarnell, J. E.; Deaton, J. C.; McCusker, C. E.; Castellano, F. N. Bidirectional "Ping-Pong" Energy Transfer and 3000-Fold Lifetime Enhancement in a Re(I) Charge Transfer Complex. *Inorg. Chem.* **2011**, *50* (16), 7820–7830.

40. Gao, Y.; Peng, X. Photogenerated Excitons in Plain Core CdSe Nanocrystals with Unity Radiative Decay in Single Channel: The Effects of Surface and Ligands. *J. Am. Chem. Soc.* **2015**, *137* (12), 4230–4235.

41. Kirkwood, N.; Monchen, J. O. V.; Crisp, R. W.; Grimaldi, G.; Bergstein, H. A. C.; du Fossé, I.; van der Stam, W.; Infante, I.; Houtepen, A. J. Finding and Fixing Traps in II–VI and III–V Colloidal Quantum Dots: The Importance of Z-Type Ligand Passivation. *J. Am. Chem. Soc.* **2018**, *140* (46), 15712–15723.

Chapter 5: Boulevard of Broken Dreams and Incomplete Things

Introduction

The previous chapters have discussed altering excited state dynamics in a deterministic fashion by manipulating the number of interfacial acceptor species. This chapter is a forward-looking discussion on dictating the desired photophysical properties via other interfacial changes. Several methods for manipulating quantum confined materials in the absence of an interfacial acceptor exist in the literature. These methods include photoluminescence quantum yield (PLQY) enhancements, photon charging/multi-exciton generation (MEG) and integration of these materials into larger more complicated photochemical and photophysical systems.[1–7] In general, the use of quantum confined materials in these various application spaces is comparable or outperforms their molecular competitors.[3,8,9]

With respect to quantum confined materials with surface anchored acceptors, the adolescence of the field provides a unique opportunity to explore these materials as incipient researchers. Many have recognized this opportunity and have begun research developing photocatalytic systems, core shell materials, expansion into perovskite and additional classes of semiconductor nanocrystals as well as research monitoring the fundamental interactions of the base materials.[10–20] In the case of cadmium selenide (CdSe), the understanding of these materials and their interactions is simplified due to their expansive research on the base material in the absence of an acceptor. Similarly, the use of a well-studied acceptor such as 1-pyrenecarboxylic acid (PCA) limits the variables presented in these studies. As such the direction for these future projects focuses on using the same system previously studied, however, it is important to

acknowledge that the use of various acceptors and nanomaterials will be critical in identifying the complete characteristics of these materials necessitating the need for high throughput systems. Section 1.3.3 discusses this topic more broadly and identifies a possible high throughput system that would be useful to identify new interfacial chromophores.

Utilizing non-TADPL Active Materials

Previously the near unity Dexter-like energy transfer process has been demonstrated in quantum dot/molecular (QD/mol) materials.[21] The work herein largely builds off this phenomenon exploiting the properties of both the quantum dots and the surface bound molecular chromophores in a synergistic platform designed for efficient thermally activated delayed photoluminescence (See Chapters 2 and 3). Equally important is understanding the utility of QD/mol materials in the absence of TADPL and the effects of interfacial acceptor concentration within these systems.

To reveal information on the operation of QD/mol systems that operate in the absence of TADPL, experiments were conducted using CdSe520 (coded by the peak position of the first exciton) and PCA. A series of materials that were capable of attenuating energy transfer (EnT) from the CdSe520 to the PCA molecular triplet state were synthesized in the same manner reported for the TADPL active materials discussed in Chapter 3 but instead using the higher energy material, CdSe520. Additionally, steady-state absorbance and photoluminescence measurements were performed to identify the concentration of PCA adsorbed and the changes in PL intensity, respectively, as well as the overall effect on the material's intrinsic properties. These results are shown in **Figure 5.1** demonstrating similar steady state changes as noted for TADPL active composite materials. However, due to the change in size associated with the higher energy CdSe520 materials, the maximum PCA loading (n = 8) is significantly lower than for the larger materials reported in Chapter 3 as noted in **Figure 5.1a**. Further, the PL intensity is quenched much

more efficiently for these materials as indicated by **Figure 5.1b** wherein quantitative quenching is achieved at n ≈ 6, **Figure 5.1c**.

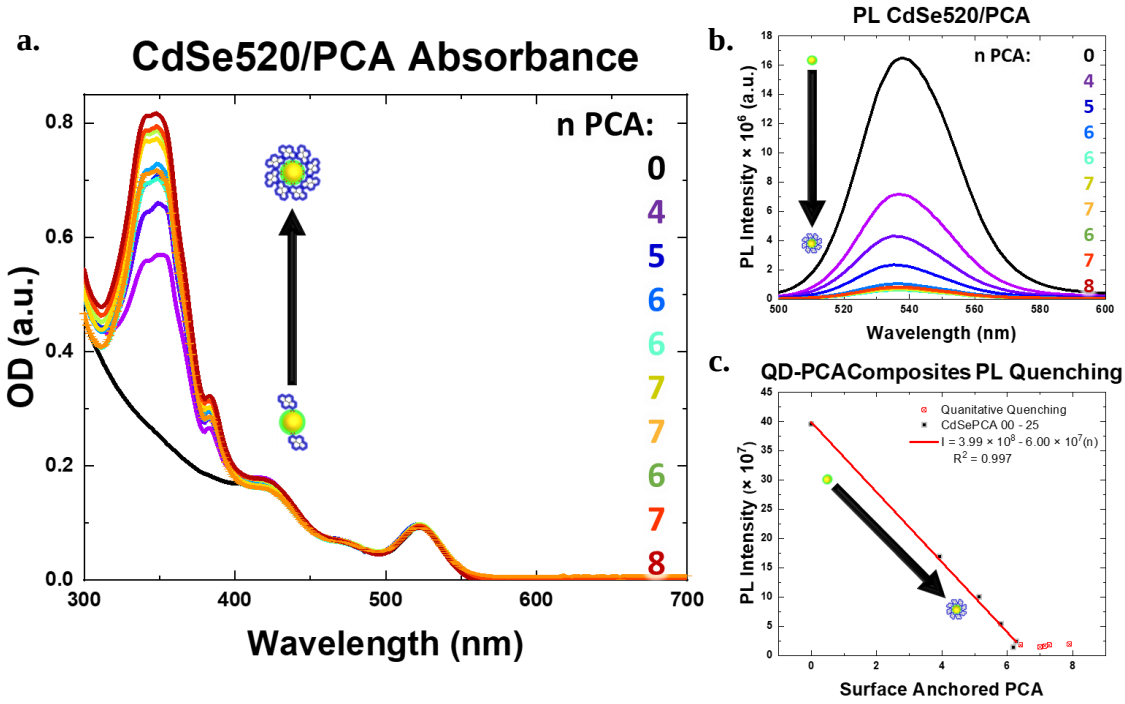

Figure 5.1 CdSe520/PCAn steady state **(a)** absorbance and **(b)** photoluminescence spectra, arrows indicate increasing PCA concentration. **(c)**.PL quenching as a function of adsorbed PCA, fit line indicates quenching rate constant per PCA.

While static PL measurements suggest the concentration of the appended chromophore in CdSe520/PCAn materials plays a noticeable role in the photophysical properties, transient measurements are necessary to gain a full picture of the excited state dynamics involved in these systems. As such, ultrafast transient absorption (UFTA) measurements were conducted to monitor the change in the rate of energy transfer from the CdSe520 to the PCA in these materials. Single wavelength kinetic traces from these experiments demonstrate the change in the EnT rate as a function of PCA concentration and are displayed in **Figure 5.2a**. As noted in PL measurements, when n ≈ 6 the changes in EnT rate stop, suggesting the "speed limit" for this process has been achieved. By calculating k_{EnT} using a previously reported methodology, it is observed that these

simple changes in surface concentration result in an order of magnitude increase in k_{EnT}, complete fitting results are available in **Table 5.1**.[21] Time gated emission (TGE) experiments were also conducted to monitor qualitatively the increase in k_{EnT} as a function of PCA by monitoring the prompt TGE signal. **Figure 5.2b** displays an overlay of the prompt TGE spectra indicating the decrease in signal as a function of surface PCA acceptor number.

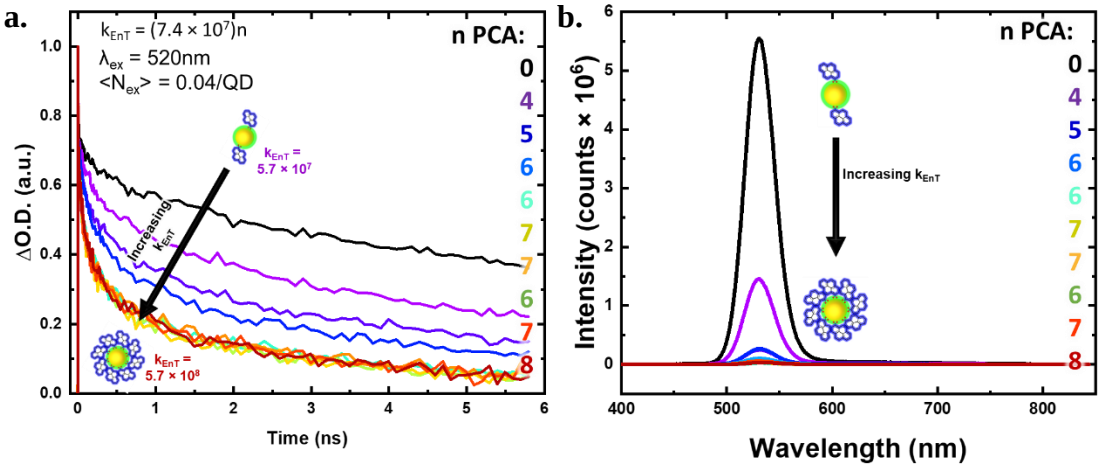

Figure 5.2 CdSe520/PCAn **(a)** UFTA single wavelength kinetics at 473 nm with λ_{ex} = 520 nm (0.5 μJ per pulse, 100 fs FWHM) **(b)** time gated emission spectra post 475 nm laser excitation (2 mJ per pulse, 7 ns FWHM), arrows indicate increasing PCA concentration and the subsequent increase in k_{EnT}.

Results from these experiments suggest that the dynamics of these materials is controlled via the interfacial concentration and suggests similar outcomes to that of other reports of materials where surface concentration is monitored.[22,23] On its own, these materials are well poised as efficient photosensitizer materials, however, the complete understanding of these materials has yet to be illuminated. One of the hallmark qualities of QDs is their ability to undergo multi-exciton generation (MEG) and photon charging.[1,2] As such, conducting incident light power dependent studies to monitor the changes in triplet quantum yield become particularly interesting for these materials as it may provide a way to populate multiple molecular triplets on a single quantum dot.

As this chapter is designed as a discussion, this project would be potentially interesting for a young graduate student's research focus.

Table 5.1. Fitting results from UFTA experiments. Single wavelength kinetics were monitored at 473 nm with λ_{ex} = 520 nm (0.5 μJ per pulse, 100 fs FWHM).

<n> (PCA/QD)	τ (s)	β	$\langle\tau_{obs}\rangle^a$ (s)	$\langle k_{obs}\rangle$ (s^{-1})	$\langle k_{EnT}\rangle^b$ (s^{-1})
0	1.32×10^{-8}	0.297	1.46×10^{-7}	7.9×10^{6}	-----
4	2.60×10^{-9}	0.337	1.51×10^{-8}	6.8×10^{7}	6.0×10^{7}
5	1.06×10^{-9}	0.314	8.06×10^{-9}	1.3×10^{8}	1.2×10^{8}
6	6.26×10^{-10}	0.328	4.03×10^{-9}	2.6×10^{8}	2.5×10^{8}
6	2.35×10^{-10}	0.320	1.72×10^{-9}	6.4×10^{8}	6.3×10^{8}
7	1.74×10^{-10}	0.308	1.51×10^{-9}	7.4×10^{8}	7.4×10^{8}
7	1.64×10^{-10}	0.314	1.30×10^{-9}	8.6×10^{8}	8.5×10^{8}
6	1.97×10^{-10}	0.294	2.09×10^{-9}	5.3×10^{8}	5.2×10^{8}
7	2.03×10^{-10}	0.310	1.69×10^{-9}	6.5×10^{8}	6.4×10^{8}
8	2.29×10^{-10}	0.328	1.51×10^{-9}	7.2×10^{8}	7.1×10^{8}

a. $\langle\tau\rangle$ derived using a stretch exponential fit, $I(t) = A\exp(-(t/\tau)^{\beta})$. b. values extracted from $\langle k_{EnT}\rangle = \langle k_{obs}\rangle - \langle k_0\rangle$, where $\langle k_0\rangle$ represents the initial PCA free CdSe520 rate constant.

High Quantum Yield Materials

Many have heard the phrase, "you get out what you put in" often from a parent or a coach regarding the effort they put into a task being comparable to the outcome they will achieve as a result. In the case of TADPL active QD/mol composite materials, the same concept may be applied, specifically, to the starting PLQY of the QD. Chapter 3 indicates that the intrinsic properties of the starting QD material are unperturbed by ligand exchange. As such, a material that begins with a high PLQY will be beneficial for applications that require long-lived, highly photoluminescent materials. Many techniques are available in the literature to enhance the PLQY of CdSe materials.[4,5,24] The Castellano lab is uniquely poised to interrogate these types of materials with rigorous spectroscopic studies to determine their utility in QD/mol composite systems and

identify areas for improvement. This is another research space that would be readily accessible to a dedicated graduate student which could easily be integrated into collaborative efforts developing devices based on these materials. These materials could be also integrated into photocatalytic processes, providing a means to cheap and high yielding exciton sources as previously noted.[10,11]

Concluding Remarks

NCSU often advertises itself as a scientific research haven where researchers are provided the opportunity to *think and do*, and provided these different possibilities, there is plenty of room to explore in the space of QD/mol science. It is my hope that a few capable researchers will perhaps not undertake these studies, but rather undertake new studies based off these studies that were previously unimagined. That's what scientific discovery is all about, and that's what the culmination of fundamental studies is supposed to lead to. The lack of understanding in QD/mols provides the opportunity for discovery of just such the type, beyond what we could imagine.

Chapter 5 Acknowledgments

This work was supported by the Organic Materials Chemistry Program in the Air Force Office of Scientific Research (FA9550-18-1-0331). I'd also like to thank Margaret H. Hudson, Tia S. Lee, Christopher M. Papa, Sofia Garakyaraghi, Megan E. Griffin and Felix N. Castellano at NC State University for their fruitful discussions, suggestions, and contributions.

Chapter 5 References

1. Beard, M. C. Multiple Exciton Generation in Semiconductor Quantum Dots. *J. Phys. Chem. Lett.* **2011**, *2* (11), 1282–1288.

2. Beard, M. C.; Luther, J. M.; Semonin, O. E.; Nozik, A. J. Third Generation Photovoltaics Based on Multiple Exciton Generation in Quantum Confined Semiconductors. *Acc. Chem. Res.* **2013**, *46* (6), 1252–1260.

3. Lu, H.; Huang, Z.; Martinez, M. S.; Johnson, J. C.; Luther, J. M.; Beard, M. C. Transforming Energy Using Quantum Dots. *Energy Environ. Sci.* **2020**, *13* (5), 1347–1376.

4. Zhou, J.; Zhu, M.; Meng, R.; Qin, H.; Peng, X. Ideal CdSe/CdS Core/Shell Nanocrystals Enabled by Entropic Ligands and Their Core Size-, Shell Thickness-, and Ligand-Dependent Photoluminescence Properties. *J. Am. Chem. Soc.* **2017**, *139* (46), 16556–16567.

5. Gao, Y.; Peng, X. Photogenerated Excitons in Plain Core CdSe Nanocrystals with Unity Radiative Decay in Single Channel: The Effects of Surface and Ligands. *J. Am. Chem. Soc.* **2015**, *137* (12), 4230–4235.

6. Kirkwood, N.; Monchen, J. O. V.; Crisp, R. W.; Grimaldi, G.; Bergstein, H. A. C.; du Fossé, I.; van der Stam, W.; Infante, I.; Houtepen, A. J. Finding and Fixing Traps in II–VI and III–V Colloidal Quantum Dots: The Importance of Z-Type Ligand Passivation. *J. Am. Chem. Soc.* **2018**, *140* (46), 15712–15723.

7. Chen, Q.; Liu, Y.; Guo, X.; Peng, J.; Garakyaraghi, S.; Papa, C. M.; Castellano, F. N.; Zhao, D.; Ma, Y. Energy Transfer Dynamics in Triplet–Triplet Annihilation Upconversion Using a Bichromophoric Heavy-Atom-Free Sensitizer. *J. Phys. Chem. A* **2018**, *122*, 6673–6682.

8. Garakyaraghi, S.; Castellano, F. N. Nanocrystals for Triplet Sensitization: Molecular Behavior from Quantum-Confined Materials. *Inorg. Chem.* **2018**, *57* (5), 2351–2359.

9. Kholmicheva, N.; Moroz, P.; Eckard, H.; Jensen, G.; Zamkov, M. Energy Transfer in Quantum Dot Solids. *ACS Energy Lett.* **2017**, *2* (1), 154–160.

10. Weiss, E. A. Designing the Surfaces of Semiconductor Quantum Dots for Colloidal Photocatalysis. *ACS Energy Lett.* **2017**, *2* (5), 1005–1013.

11. Jiang, Y.; Wang, C.; Rogers, C. R.; Kodaimati, M. S.; Weiss, E. A. Regio- and Diastereoselective Intermolecular [2+2] Cycloadditions Photocatalysed by Quantum Dots. *Nat. Chem.* **2019**, *11* (11), 1034–1040.

12. Huang, Z.; Xu, Z.; Mahboub, M.; Li, X.; Taylor, J. W.; Harman, W. H.; Lian, T.; Tang, M. L. PbS/CdS Core–Shell Quantum Dots Suppress Charge Transfer and Enhance Triplet Transfer. *Angew. Chem. Int. Ed.* **2017**, *56* (52), 16583–16587.

13. Okumura, K.; Mase, K.; Yanai, N.; Kimizuka, N. Employing Core-Shell Quantum Dots as Triplet Sensitizers for Photon Upconversion. *Chem.- Eur. J.* **2016**, *22* (23), 7721–7726.

14. Abdel-Latif, K.; Bateni, F.; Crouse, S.; Abolhasani, M. Flow Synthesis of Metal Halide Perovskite Quantum Dots: From Rapid Parameter Space Mapping to AI-Guided Modular Manufacturing. *Matter* **2020**, *3* (4), 1053–1086.

15. Abdel-Latif, K.; Epps, R. W.; Kerr, C. B.; Papa, C. M.; Castellano, F. N.; Abolhasani, M. Facile Room-Temperature Anion Exchange Reactions of Inorganic Perovskite Quantum Dots Enabled by a Modular Microfluidic Platform. *Adv. Funct. Mater.* **2019**, *29* (23), 1900712.

16. Bieber, A. S.; VanOrman, Z. A.; Wieghold, S.; Nienhaus, L. Perovskite-Sensitized Upconversion Bingo: Stoichiometry, Composition, Solvent, or Temperature? *J. Chem. Phys.* **2020**, *153* (8), 084703.

17. de Weerd, C.; Gomez, L.; Zhang, H.; Buma, W. J.; Nedelcu, G.; Kovalenko, M. V.; Gregorkiewicz, T. Energy Transfer between Inorganic Perovskite Nanocrystals. *J. Phys. Chem. C* **2016**, *120* (24), 13310–13315.

18. Shyamal, S.; Pradhan, N. Halide Perovskite Nanocrystal Photocatalysts for CO2 Reduction: Successes and Challenges. *J. Phys. Chem. Lett.* **2020**, *11* (16), 6921–6934.

19. Lai, R.; Liu, Y.; Luo, X.; Chen, L.; Han, Y.; Lv, M.; Liang, G.; Chen, J.; Zhang, C.; Di, D.; Scholes, G. D.; Castellano, F. N.; Wu, K. Shallow Distance-Dependent Triplet Energy Migration Mediated by Endothermic Charge-Transfer. *Nat. Commun.* **2021**, *12* (1), 1532.

20. Luo, X.; Han, Y.; Chen, Z.; Li, Y.; Liang, G.; Liu, X.; Ding, T.; Nie, C.; Wang, M.; Castellano, F. N.; Wu, K. Mechanisms of Triplet Energy Transfer across the Inorganic Nanocrystal/Organic Molecule Interface. *Nat. Commun.* **2020**, *11* (1), 28.

21. Mongin, C.; Garakyaraghi, S.; Razgoniaeva, N.; Zamkov, M.; Castellano, F. N. Direct Observation of Triplet Energy Transfer from Semiconductor Nanocrystals. *Science* **2016**, *351* (6271), 369–372.

22. Yonemoto, D. T.; Papa, C. M.; Sheykhi, S.; Castellano, F. N. Controlling Thermally Activated Delayed Photoluminescence in CdSe Quantum Dots through Triplet Acceptor Surface Coverage. *J. Phys. Chem. Lett.* **2021**, 3718–3723.

23. Zhang, J.; Kouno, H.; Yanai, N.; Eguchi, D.; Nakagawa, T.; Kimizuka, N.; Teranishi, T.; Sakamoto, M. Number of Surface-Attached Acceptors on a Quantum Dot Impacts Energy Transfer and Photon Upconversion Efficiencies. *ACS Photonics* **2020**.

24. Zhou, J.; Pu, C.; Jiao, T.; Hou, X.; Peng, X. A Two-Step Synthetic Strategy toward Monodisperse Colloidal CdSe and CdSe/CdS Core/Shell Nanocrystals. *J. Am. Chem. Soc.* **2016**, *138*, 6475–6483.